NEAR-INFRARED SPECTROSCOPY OF LOW-GRADE METAMORPHIC VOLCANIC ROCKS OF THE EAST PILBARA GRANITE-GREENSTONE TERRANE-AUSTRALIA

MOHAMMAD S. ABWENY

March, 2012

SUPERVISORS:
Dr. F.J.A. (Frank) van Ruitenbeek
Drs. J.B. (Boudewijn) de Smeth

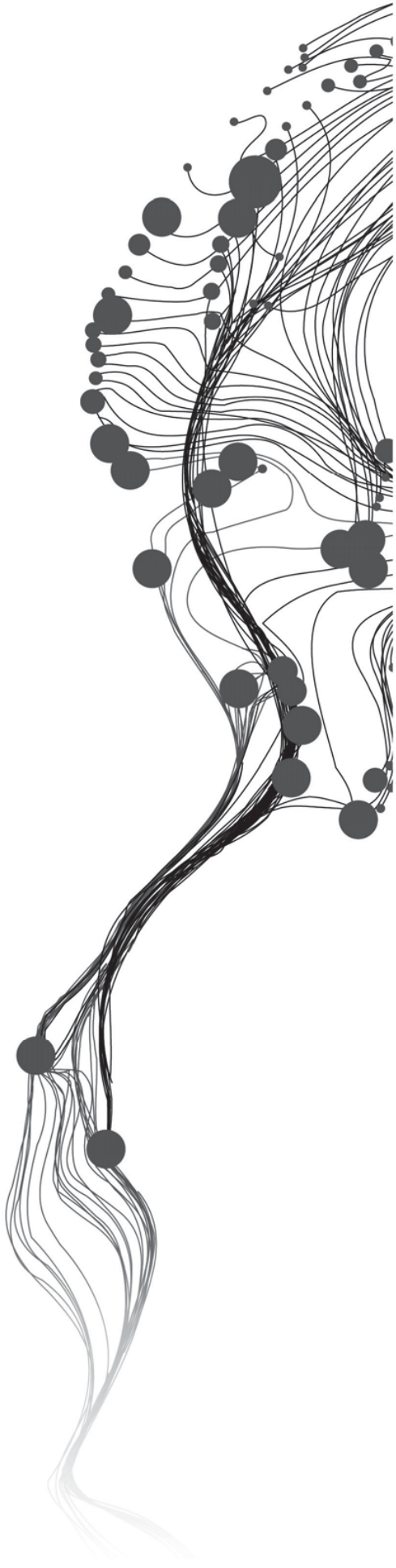

NEAR-INFRARED SPECTROSCOPY OF LOW-GRADE METAMORPHIC VOLCANIC ROCKS OF THE EAST PILBARA GRANITE-GREENSTONE TERRANE-AUSTRALIA

MOHAMMAD S. ABWENY

Enschede, The Netherlands, March, 2012

Thesis submitted to the Faculty of Geo-Information Science and Earth Observation of the University of Twente in partial fulfilment of the requirements for the degree of Master of Science in Geo-information Science and Earth Observation.
Specialization: Earth Resources Exploration

SUPERVISORS:
Dr. F.J.A. (Frank) Van Ruitenbeek
Drs. J.B. (Boudewijn) de Smeth

THESIS ASSESSMENT BOARD:
Prof. Dr. F.D. (Freek) van der Meer (Chair)
Dr. Mike Buxton (External Examiner, University of Delft – Dept. of Geotechnology - Civil Engineering & Geosciences)

ABSTRACT

Near-infrared spectroscopy has for many years been used to characterize different hydrothermal alteration styles and more recently also metapelitic rocks. This study aims at using near-infrared spectroscopy to characterize lithological composition, metamorphic grades and alteration intensities of Archean volcanic rocks in the East Pilbara Granite-Greenstone Terrane (EP). Results are useful for the interpretation of near-infrared spectral data sets of similar terrestrial and planetary terranes.

Reflectance spectra in the range of 350nm to 2500nm of the 215 rock samples (209 rock slabs made by Smithies et al. (2007) and 16 rock hand specimens collected by Thuss (2005)) were measured in the ITC spectroscopy laboratory using ASD Fieldspec Pro spectrometer. Complementary geochemical and geological dataset were obtained from published studies. The spectral position parameter of the Mg-OH (2310-2360nm) absorption feature was used to characterize the different metamorphic grades while the 2200nm Al-OH absorption feature was used to identify and characterise the intensely altered rocks where sericite and pyrophyllite are the main abundant spectral minerals. The spectral depth parameters of the Fe-OH (at ~2250nm) and Mg-OH (at ~2390nm) absorption features were used to estimate the relative alteration intensity, as well as, the metamorphic grades for Mg-OH containing minerals. The spectral depth parameters of the 2200nm Al-OH and the H_2O/OH (at ~1400nm) absorption features were used to estimate the relative alteration intensity for Al-OH containing minerals. Major elements lithogeochemistry was used to characterise the lithology and alteration type/intensity and to compare with the spectroscopic results.

The minerals that were identified from the different volcanic rocks with near-infrared spectroscopy are chlorite (Fe-chlorite, intermediate and Mg-chlorite), amphiboles (hornblende and actinolite), white mica (illite, muscovite and phengite) and pyrophyllite. Three metamorphic subfacies within the greenschist facies could be determined based on the Mg-OH (2310-2360nm) absorption feature 1) a zone containing Fe-chlorite; 2) a zone containing intermediate chlorite + epidote; and 3) a zone containing intermediate chlorite + actinolite and hornblende, in addition to the amphibolite facies. In previous studies where non-spectral methods were used, only greenschist and amphibolite facies were identified. From the near-infrared study it appears that boundaries between the greenschist subfacies are sharp due to appearance of new spectral minerals such as epidote and actinolite whereas the boundary between greenschist and amphibolite facies is transitional due to the increase of spectrally detected hornblende abundances. Prehnite-pumpellyite metamorphic facies, as well as the carbonates, couldn't be detected based on the Mg-OH (2310-2360nm) absorption feature. Volcanic rocks of basaltic composition were found to contain any of these spectral minerals. Therefore basalts are the most suitable in the characterization of the different metamorphic grades. The spectral depth parameters of the 2250nm Fe-OH and 2390nm Mg-OH absorption features respectively, as well as the 2200nm Al-OH and the H_2O/OH (at ~1400nm) absorption features were found useful in estimating the relative alteration intensity of the rocks containing abundant Mg-OH and Al-OH spectrally detectable minerals respectively. Based on the latter depth parameter, background alteration (diagenetic and metamorphic isochemical alteration) could be distinguished from the intense hydrothermal (metasomatic) alteration of rhyolitic rocks. Major elements lithogeochemistry was found useful in determining lithology, relative alteration intensity and metasomatism but not in estimation of metamorphic grade. Also the background and hydrothermal alterations could be differentiated in rhyolitic rocks.

The integration of the near-infrared spectroscopy and major elements lithogeochemistry is a useful tool to characterize low-grade metamorphosed volcanic rocks in the East Pilbara Granite-Greenstone Terrane (EP).

ACKNOWLEDGMENT

First of all, praise be to Allah (God) almighty, without his mercy and support, this study could never have been achieved. Many thanks to the Joint Japan/World Bank Graduate Scholarship Program (JJ/WBGSP), sponsored by the Government of Japan for the financial support required to complete this M.Sc. degree.

I'm heartily thankful to my supervisors Frank van Ruitenbeek and Boudewijn de Smeth whose invaluable encouragement, assistance, fruitful discussion and guidance enabled me to shape my ideas and to think in a scientific way. I owe them more than they know.

Deep gratitude is also due to Hugh Smithies who made the rock slabs collected from the study area available to this study. Special thanks also to Mr. Cudahy for providing the PIMA spectral analysis dataset.

Thanks are also extended to Barbara Thuss and her supervisors Jan-Cees Blom, Tanja Zegers (project coordinator), Freek van der Meer and Frank van Ruitenbeek for making the rocks hand specimens they collected from the study area available to this study.

I also wish to thank Henk Wilbrink, without him, microscopic photos for thin sections could never have been taken.

A special thanks to Sami El-Raghy (the Chairman of Nordana Pty Limited) for his generous encouragement and his support to my family.

Lastly, it's a pleasure to thank David Rossiter for his continuous encouragement and boost our morale, all the staff members of the Applied Earth Sciences for their generous help, all my classmates for sharing ideas and for the hard and sweet times that we spent together, and to any of those who made this thesis possible.

TABLE OF CONTENTS

LIST OF FIGURES

LIST OF TABLES

1. INTRODUCTION

1.1. Research Background

Conventional chemical and mineralogical methods (i.e. XRF, XRD, petrography and etc.) using a variety of instruments have long been used to study different varieties of rocks, alterations and metamorphism. The use of these methods requires a well-prepared field expedition and sampling program. Representative samples must be carefully collected, transported, stored, prepared and analysed. This is both time and cost consuming.

In well exposed areas; it's been proven that hyperspectral remote sensing can be used for mapping different alteration facies and metamorphic pelitic rocks which in turn reduces time and cost factors and requires less sampling (Van Ruitenbeek et al., 2005, 2006 and Doublier, 2010).

The East Pilbara Granite-Greenstone Terrane (EP) is a good example of well exposed, preserved and little deformed rocks (Brauhart et al., 1998). Low-grade metamorphism (green schist) is a major signature of the synclinal greenstone belts intervened by a domical granitoid complexes (Hickman, 2004).

1.2. Problem Definition

The abundance of the East Pilbara Granite-Greenstone Terrane (especially the greenstone belts) in different base metal resources (associated with volcanogenic massive sulphides (VMS) deposits) has made it a proper research environment to geologists and explorationists (Barley, 1998). As a consequence, different lithological units, metamorphic facies and alteration styles have been intensively studied in detail using the conventional petrological and geochemical methods. Spectroscopic remote sensing technique, so far, has been focused only on studying the different alteration styles rather than lithologies or metamorphism.

Therefore, this study will focus on using spectroscopic remote sensing technique to discriminate between different rock types and metamorphic facies.

1.3. Motivation

The presence of a range of fractionated mafic to felsic volcanic rocks gives a rare chance to investigate the spectral characteristics among the whole composition series and the effect of metamorphic process.

1.4. Research Objectives

The main objective of this research is to study the near-infrared spectral response to varying lithological composition of the low-grade metamorphosed volcanic rocks in the East Pilbara Granite-Greenstone terrane, and to determine the influence of metamorphic processes on spectra. Whole-rock major elements lithogeochemistry will be used to evaluate the spectroscopic results.

Specific objectives:

1) To determine the spectral characteristics of the lithological compositions of the low-grade metamorphosed volcanic rocks.

2) To determine whether spectroscopic method can be used to differentiate between different metamorphic facies.

3) To determine if the spectroscopic method can estimate the relative alteration intensity.

4) To compare and evaluate the spectroscopic results with the whole-rock major elements lithogeochemistry.

1.5. Research Questions

1) Can varying volcanic rocks compositions at low-grade metamorphism be spectrally determined?
2) Is it possible to differentiate between different metamorphic facies?
3) Can the relative alteration intensity be estimated by the spectroscopic method?
4) What is the comparison between the spectroscopic method and the conventional whole-rock major elements geochemistry?

1.6. Hypothesis

Spectrally, detectable mineralogy of the East Pilbara Granite-Greenstone terrane varies systematically with the variation in lithological composition, metamorphic grade and hydrothermal alteration.

1.7. Datasets

206 rock slabs of representative rock samples that were collected by Smithies et al. (2007) along 14 traverses perpendicular to the strikes will be used in this research. The samples are part of the geological studies within the region carried out by the Geological Survey of Western Australia (GSWA) to identify the geochemical characteristics of the full-range 3.52-2.93 Ga volcanic rocks sequences and to obtain additional evidence on tectonic settings (Figure 1.1). Additional nine rock hand specimens, part of samples collected by Thuss (2005) to study the spectroscopic characteristics of the different volcanic rocks and to compare with the spectra of Mars rocks, will be used in this research.
Legacy geological maps (100,000; 250,000; 500,000; and 2,500,000 scale) with reports are the backbone for lithological interpretation.

1.8. Thesis Structure

CHAPTER 1: includes the background, problem definition, objectives and questions about this research.
CHAPTER 2: describes the geology of the study area and any other studies that were carried out such as geochemical and spectroscopic studies.
CHAPTER 3: explains briefly the spectroscopic and geochemical methods to be used in this research.
CHAPTER 4: shows the spectroscopic and geochemical outputs and the discussion that took place on them.
CHAPTER 5: includes summary, conclusions and recommendations.

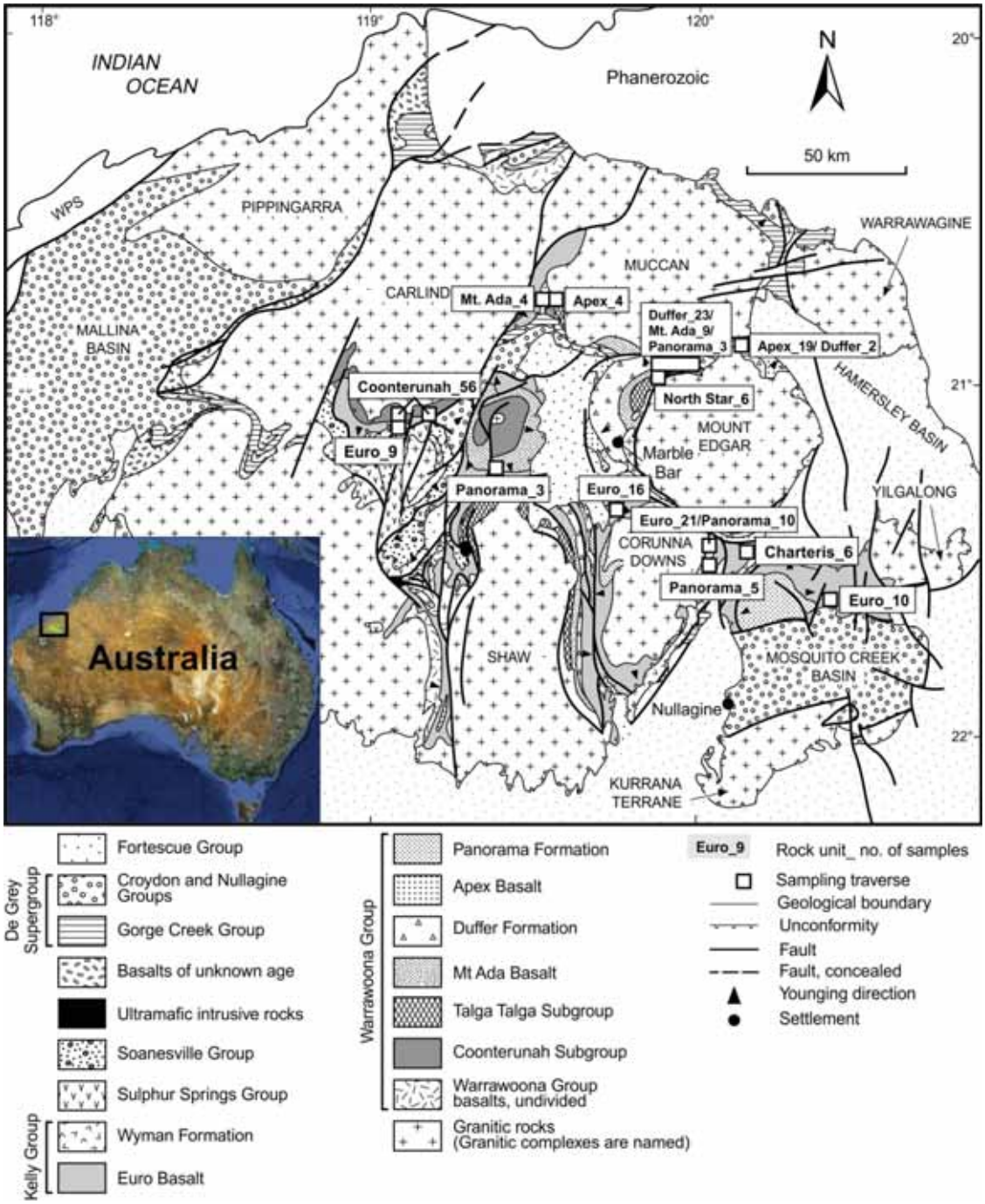

Figure 1.1: Location map of the samples collected along transacts (modified after Smithies et al., 2007).

2. LITERATURE REVIEW

2.1. Regional Geology

Generally the Archean Pilbara Craton comprises of the Archean (3.52-2.93 Ga) granite-greenstone terranes, which is believed to have formed under fundamentally different tectonic regimes in the Phanerozoic; and unconformably overlying succession of volcanic and sedimentary rocks (2.77-2.40 Ga) (Hickman, 2004). It's divided into the 3.65-3.17 Ga East Pilbara Granite-Greenstone Terrane, the 3.27-3.17 Ga West Pilbara Superterrane, the 3.2-3.18 Ga Kurrana Terrane, Sholl Terrane and Karratha Terrane. These terranes are separated by deformed clastic sedimentary basins and unconformably overlain by the 3.02-2.93 Ga De Grey Supergroup of mainly clastic sedimentary rocks (Van Kranendonk & Pirajno, 2004, Van Kranendonk et al., 2007).

Each terrane is characterized by unique lithostratigraphy, structures, geochemistry and tectonic history (Van Kranendonk et al., 2002, 2006). The East Pilbara amalgamated the West Pilbara Superterrane at about 3.07 Ga (Smithies et al., 2007).

Controversial vertical and horizontal tectonic history concepts regarding the origin of the Pilbara Craton were proposed. Many workers believe that the dome and keel pattern of the East Pilbara Granite-Greenstone Terrane is an evidence of the vertical tectonic where the upper and middle crust sunk and overturned due to the upwelling of mantle plumes (granitic diapirism) i.e. inverse of density. Other workers proved the horizontal tectonic and revealed the periods of thrusting and extensional episodes after the formation of the dome and keel pattern. Briefly, in the early stages, vertical tectonic processes dominated over horizontal tectonic processes whereas after 3.2 Ga, horizontal tectonic processes dominated (Van Kranendonk et al., 2007).

2.2. Geologic Setting of the East Pilbara Granite-Greenstone Terrane (EP)

The East Pilbara Granite-Greenstone Terrane (EP) contains the oldest rocks in the Pilbara Craton of about 3.65-3.17 Ga. (Van Kranendonk et al., 2007). It contains an ancient 3.72-3.6 Ga sialic basement; 3.525-3.165 Ga greenstone belts (the Pilbara Supergroup); and five 3.500-3.165 Ga granitic supersuites (Figure 2.1) (Van Kranendonk et al., 2006).

The Pilbara Supergroup, which is our research interest, includes four groups; Warrawoona; Kelly; Sulphur Spring; and Soanesville (Figure 2.2). The maximum cumulative thickness reaches about 22 km (maximum 12 km in any one belt). The Supergroup's preserved volcanic and sedimentary rocks are mainly of low- to medium-grade metamorphism (Van Kranendonk et al., 2006).

2.3. Low-Grade Hydrothermal Metamorphism in the Archean Greenstone Belts

The low-pressure metamorphism of the greenstone rocks in the Pilbara Craton is comparable to the seafloor metamorphism where basaltic rocks, undergoing low-grade metamorphism, are the most widespread as the upper oceanic crust and are extensively recrystallized under low-grade metamorphism conditions. Low-grade metamorphism, as well as diagenesis, occurs regionally and results in weakly altered rocks (mineralogy changes but chemical composition remains approximately the same) with preserved primary textures (or sometimes only as relics) and this is what so called isochemical alteration, in contrast, hydrothermal alteration occurs locally and results in significant changes in rock mineralogy, composition and texture hence the term metasomatic alteration. In many cases, different alteration processes in submarine volcanic successions are contemporaneous and can result in similar mineral assemblages, thus they are difficult to distinguish (Gifkins et al., 2005).

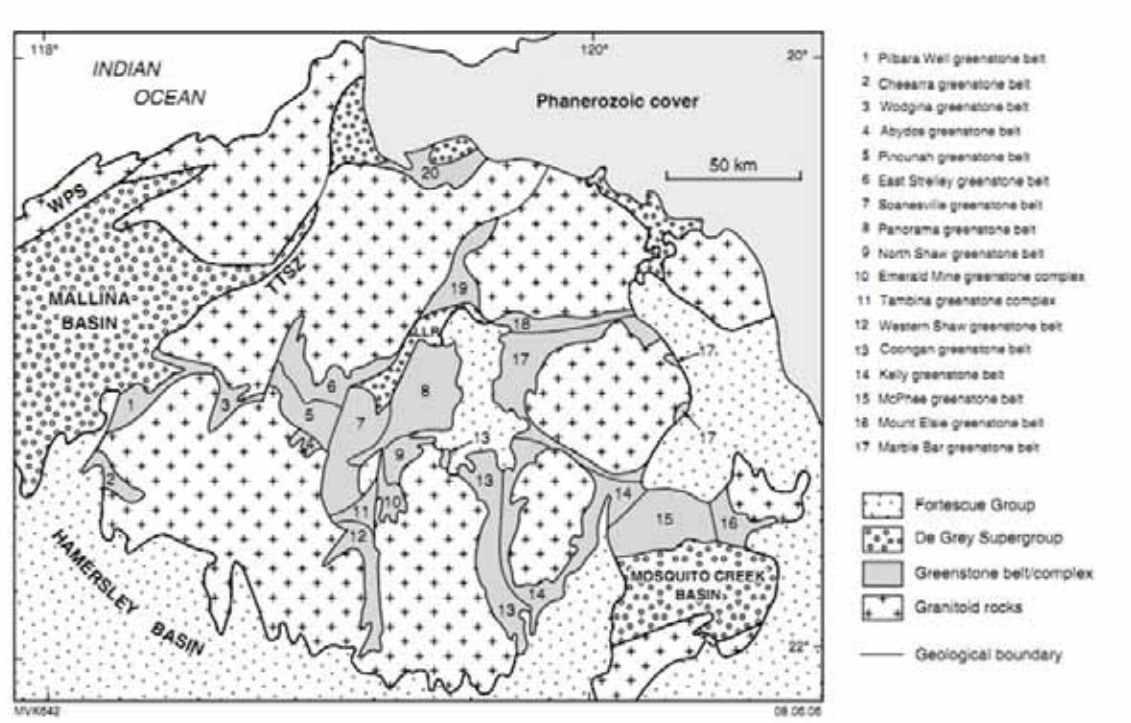

Figure 2.1: Greenstone belts (Pilbara Supergroup), granitic complexes and the sedimentary Supergroups of the East Pilbara Granite-Greenstone Terrane. LLR: Lalla Rookh Synclinorium; TTSZ: Tabba Tabba Shear Zone; WPS: West Pilbara Superterrane (after Van Kranendonk et al., 2006).

Since the oceanic process of heated fluids convection is large-scale hence, it's considered as hydrothermal metamorphism rather than diagenetic (Terabayashi et al., 2003; Frey and Robinson, 1999).

Lister (1982) proposed the terms active and passive regimes of the submarine geothermal systems. Active geothermal regimes are restricted to the spreading axes (axial convection) where the heat source is a magma chamber or cooling and cracking plutonic rocks (>350^{0}C). This regime gives rise to black smokers, hydrothermal vents and massive sulphide deposits, and extends to few kilometres from the spreading axis. High metamorphic grade can be formed such as amphibolite facies. 8-20% of the hydrothermal heat flux belongs to this regime whereas the rest belongs to the passive regime. Passive geothermal regime (2^{0}C to <150^{0}C), which is called ridge flank or off-axis systems, occurs over much larger areas (100s to 1000s of kilometres from the ridge) and over several tens of million years. Thus rocks of high alteration intensity are thought to be close to the active system whereas less altered rocks belong to the passive system.

The greenschist/greenstone facies cover the temperature 300^{0}C-500^{0}C at low to intermediate pressures. Metamorphic mineral assemblages are dependent on the original rock (protolith), physical conditions (P&T) and chemical conditions (P_{H2O}, P_{CO2} & fluid composition). The main protoliths in the study area are ultramafic, mafic, intermediate and felsic rocks. Ultramafic rocks metamorphism yields hydrous and non-hydrous Mg-silicate minerals. Metamorphism of mafic and intermediate igneous rocks gives rise to epidote, chlorite, amphiboles, garnet, quartz and plagioclase (±phengite & biotite). In rhyolitic rocks, and as in the basic volcanic rocks; temperature is the main control on secondary mineralogy with the influence of rock composition, texture and permeability, and fluid chemistry. Generally, montmorillonite and mordenite (a zeolite mineral) form at 100^0-120^{0}C and at increasing temperature; illite/smectite occurs until only illite is present at 230^{0}C. (Bucher & Grapes, 2011).

Low-grade greenschist facies (low temperature and moderate pressure) are common in non-equilibrated systems due to partial recrystallization with relict protolith features. In spite of the variation in rocks composition, greenschist facies assemblages overlap in the derived pressure and temperature space. The physical properties of rocks, as well as their composition, strongly affect the response to hydrothermal or

metamorphic processes and thus affect the nature of the final mineral assemblages e.g. within a unit, permeable rocks give rise to different mineral assemblages of higher grade than the massive less permeable rocks. This compositional variation occurs not only at units scale but also at thin section scale, hence the term meta-domains i.e. glass and pillow margins interact with the sea water to form meta-domains of predominantly mafic layer silicates. Secondary minerals are dependent on the primary rock composition i.e. olivine or orthopyroxene give Mg-smectite, serpentine and talc; plagioclase is replaced by Na- & Ca-Al silicates (zeolites, albite, prehnite, pumpellyite and epidote); and clinopyroxenes is replaced by actinolite (Uralization) that indicates the onset of greenschist conditions. According to the GMEX_Booklets, Fe-chlorite and Mg-chlorite indicate hydrothermal alteration of low and high grades respectively. Mg-chlorite could occur at seawater discharge zones whereas Fe-chlorite occurs at recharge zones. Intermediate chlorite occupies the zone between the Mg- & Fe-chlorite rich zones. Zane and Sassi (1998) indicated that in metabasic rocks, chlorites are mostly Mg-dominant whereas those in acidic rocks are mostly Fe-dominant (a compositional-based) whereas in terms of metamorphism, as metamorphic grade increases, Mg/Fe increases. Thus, due to the effect of both metamorphic process and bulk rock composition, regional scale mapping of mineral zones is possible in the low-grade metamorphic rocks (Frey & Robinson, 1999).

Transition from greenschist facies to amphibolite facies is rather gradual (>450^{0}C) as epidote and chlorite react to form hornblende in place of actinolite. Plagioclase tends to be calcic rather than sodic (Bucher & Grapes, 2011).

Terabayashi et al. (2003) studied the North Pole greenstone belts and observed that primary textures and minerals were preserved particularly in coarse-grained textures whilst in fine-grained textures, the groundmass was completely replaced by secondary minerals including chlorite, epidote, quartz and calcite. The metamorphic grade in the North Pole greenstone belt increases from south (stratigraphically top) to north (stratigraphically bottom). Three prograde metamorphic zones were defined as: prehnite-pumpellyite (epidote + prehnite + pumpellyite + chlorite + quartz + calcite); tranzitional zone (epidote ± prehnite ± pumpellyite ± actinolite + chlorite + quartz ± calcite); and greenschist facies (epidote + actinolite/hornblende + chlorite + quartz ± calcite), in addition to, highly altered zones just below chert beds as rocks near the sea floor have suffered hydrothermal alteration through interaction with circulating hot seawater. Chlorite is very common in the study area and tends to be more Mg/(Mg+Fe) ratio in the presence of hornblende and actinolite comparing to lower-grade greenschist zone thus more Mg-chlorite indicates higher grade and the vice versa. Thermobarometric estimation for the North Pole greenstones was suggested to be less than 400^{0}C. Three samples (collected by Smithies et al., 2007) from the intensely altered zones (sample nos. 179897, 179898 & 179899) were used in this research.

Inoue and Utada (1991) studied a volcaniclastics sequence, Kamikita in Japan, of about 6km thick of variable volcanic rocks that have been metamorphosed due to the intrusion of hornblende-quartz diorite body. Five mineralogical zones were defined, based on 22 secondary minerals from the drill cores, starting from the lowest to highest thermal metamorphic grade: smectite (Zone I), smectite + heulandite + stilbite (Zone II), corrensite + laumontite (Zone III), chlorite + epidote (Zone IV) and biotite + actinolite (Zone V). Pyrophyllite, dickite, alunite and other minerals are thought to be resulted by acidic hydrothermal solution (advanced argillic alteration).

According to Terabayashi et al. (2003) and Inoue and Utada (1991), the change in the metamorphic grade (mainly P, T & fluids) resulted in different mineral assemblages. A good example is the transition from actinolite to hornblende with the increase of metamorphic grade (Grapes and Graham, 1978).

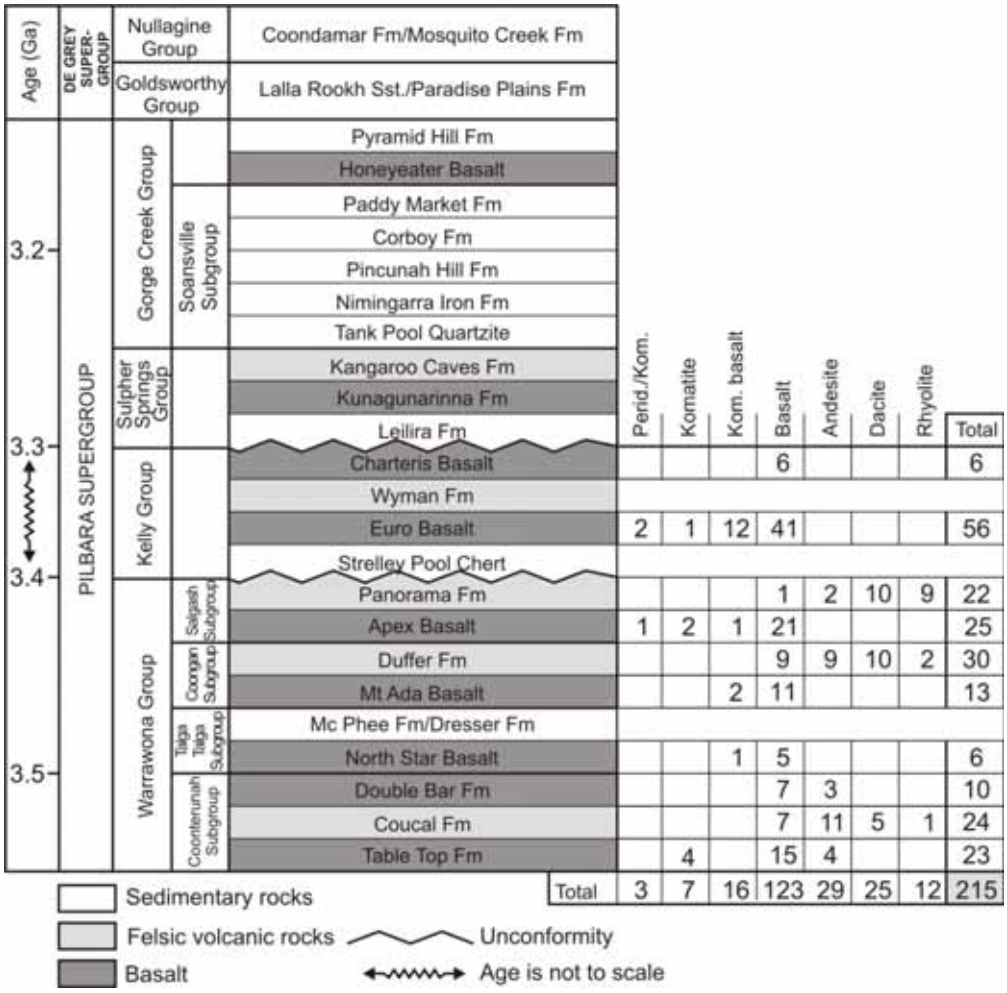

	Perid./Kom.	Komatiite	Kom. basalt	Basalt	Andesite	Dacite	Rhyolite	Total
Charteris Basalt				6				6
Euro Basalt	2	1	12	41				56
Panorama Fm				1	2	10	9	22
Apex Basalt	1	2	1	21				25
Duffer Fm				9	9	10	2	30
Mt Ada Basalt			2	11				13
North Star Basalt			1	5				6
Double Bar Fm				7	3			10
Coucal Fm				7	11	5	1	24
Table Top Fm		4		15	4			23
Total	3	7	16	123	29	25	12	215

Figure 2.2: Lithostratigraphy of the East Pilbara Granite-Greenstone Terrane with the samples (modified after Van Kranendonk et al., 2006).

2.4. Rock Units Description

In this study, only the sampled units will be described in detail and the lithological symbols described here will be explained in the chapter of results and discussion (Appendix 4) (Van Kranendonk, 2000, 2010; Smithies et al., 2007; Williams, 1999; Bagas, 2005; Williams & Bagas, 2007; Farrell, 2006 & Brown et al., 2006).

2.4.1. Coonterunah Subgroup

The bimodal mafic and felsic volcanic Coonterunah Subgroup is the oldest rock unit in the study area of about 3515 Ma and approximately 5km thick (Figure 2.2). It was intruded by the Carlindi Granitoid Batholith and is located to the southern margin of this Batholith within the East Strelley Greenstone Belt. Fine to coarse-grained amphibolite rocks surrounding the Batholith reflects a contact metamorphism associated with the emplacement of this body. The subgroup is unconformably overlain by the De Grey Group. It contains three formations (from oldest): Table Top Formation, Coucal Formation and Double Bar Formation.

Generally, the Table Top Formation (AOt) is composed from fine-grained doleritic tholeiitic basalts where the base, which is in contact with the Carlindi Granitoid Complex, exhibits metamorphic recrystallization within about 100m wide hornfelsic metamorphic aureole resulted from contact

metamorphism. Metabaslts are fine to medium-grained intergrowth of actinolite, plagioclase and opaque minerals. The felsic volcanic Coucal Formation, conformably overlying the Table Top Formation, is marked at the base by the presence of thick beds of banded cherty iron-formation (AOci). Up to 1km thick of fine-grained doleritic andesite and basalt (AOcbi) is located along the southern margin of the Carlindi Granitoid Complex and considered as transition zone between the Table Top and Coucal Formations. Felsic volcanic rocks (AOcf) of dacite and rhyolite were affected by metamorphic recrystallization and carbonate-sericite alteration as amygdales in dacite rocks were filled by carbonate and epidote. Plagioclase laths are interlocking within a fine-grained actinolite mat and opaque minerals, and altered to actinolite, carbonate and epidote (zoisite). The Double Bar Formation (AOd) is mainly composed of fine-grained tholeiitic basalt and basaltic volcanic clastic rocks where all mafic minerals were recrystallized to a metamorphic mineral assemblage of chlorite or actinolite-chlorite-epidote (zoisite)-opaque minerals.

2.4.2. North Star Basalt Formation

The North Star Basalt (up to 2000m thick and about 3490 ±15 Ma) comprises mainly of tholeiitic, massive and pillowed metabasalt, metakomatitic basalt, serpentinized peridotite, thin sedimentary chert layers and numerous dolerite and gabbro sills. The lower contact is intruded by granitic rocks (Muccan and Mount Edgar Granitoid complexes in Warralong and Marble Bar greenstone belts respectively) and the upper contact is conformably overlain by the McPhee Formation (in both Marble Bar and Warralong Greenstone Belts) and Dresser Formation (Panorama Greenstone Belt). The formation is metamorphosed at greenschist facies whereas the lower part adjacent to the granite intrusion is metamorphosed to lower amphibolite facies. The pillowed to massive tholeiitic basalt at greenschist facies unit (A-WAn-bb or Awn) is the major rock unit of the formation of about 800m thick and consists of chlorite-epidote-carbonate with accessory quartz and opaque minerals.

2.4.3. Mount Ada Basalt Formation

The Mount Ada Basalt Formation (2460m thick and about 3469 ±3 Ma) consists mainly of low-grade pillowed and massive, basalt and komatitic basalt with pyroxene spinifex texture, felsic and mafic metavolcaniclastics and thin chert rocks. The formation is conformably overlies either the McPhee Formation or the Dresser Formation in different greenstone belts and is conformably overlain by felsic volcanic rocks of the Duffer formation. Weakly metamorphosed basalt (AWmb) at greenschist facies is pillowed and interpillow hyaloclastite. The komatitic basalt unit (AWmbk) which is characterized by orange weathering appearance is weakly metamorphosed at greenschist facies. The upper part (in the Marble Bar greenstone belt) is marked by mafic with lesser felsic volcaniclastics (AWmbt) intercalated with milky grey chert.

2.4.4. Duffer Formation

The Duffer Formation, which is up to 4750m thick in the Marble Bar Greenstone Belt and of about 3.474-3.463 Ga, consists of predominantly metamorphosed volcaniclastics and flow of dacitic to rhyolitic (AWdfx) rocks, especially in the lower half of the formation, in addition to pillowed-tholeiitic basalt and layered sedimentary metachert (Marble Bar and Chinaman Pool Chert Members). The formation conformably overlies the Mount Ada Basalt Formation and is unconformably overlain by the younger formations. Feldspar-porphyritic subvolcanic intrusions are common. The base of the formation is marked by thinly-bedded, fine-grained felsic volcaniclastic rocks (AWdft) and coarse-grained phyric dacite-andesite sills (AWdfdp). Pillowed andesitic basaltic rocks (AWdb) are metamorphosed at greenschist facies.

2.4.5. Apex Basalt Formation

The Apex Basalt Formation (which is located in two greenstone belts, the Marble Bar and Warralong, and forms the lower part of the Salgash Subgroup of about 2.5km thick) disconformably overlies the Duffer Formation and conformably overlain by the Panorama Formation or Euro Basalt Formation in case of the absence of the Panorama Formation. In the Marble Bar Greenstone Belt, the formation is discordantly intruded and contact metamorphosed by the Mount Edgar Granitoid Complex. The pillowed amygdaloidal and fine-grained tholeiitic and high-Mg basalt (AWa) is about 2km thick and interlayered with metasedimentary rocks. The rocks are commonly actinolite-plagioclase-quartz assemblages with minor chlorite and epidote, and become darker with schistose amphibole-plagioclase assemblage at the contact with the granitoid complex. The formation was affected by a low-grade regional metamorphism except adjacent to the granitoid complex where it is of low amphibolite facies.
In the Warralong Greenstone Belt, the Apex Basalt Formation consists mainly of greenschist facies metamorphosed pillowed komatitic basalt (AWabk) and characterized by pyroxene spinifex texture.

2.4.6. Panorama Formation

The Panorama Formation (about 2000m thick and 3456 Ma) which forms the base of the Kelly greenstone belt is intruded by the Corunna Downs Granitoid Complex. The formation structurally overlies the Apex Basalt and is overlain by the Strelley Pool Chert or unconformably by the Euro Basalt. The formation consist of a succession of metamorphosed felsic volcaniclastic rocks with agglomerate, silicified tuffaceous volcaniclastic rocks and minor volcanic breccia. At the top of the formation, the tuffaceous unit (AWpft) is crosscut by hydrothermal veins and dykes of black chert which is thought to be feeders for the overlying Strelley Pool Chert. In the Marble Bar greenstone belt, the formation is about 800m thick and rapidly thins eastwards to less than 100m, and is remarked by discontinuous lenses. The rocks of the felsic unit (AWp) are altered, siliceous, porphyritic and fine-grained rhyolite to dacite and tuffaceous rocks. Quartz and altered feldspar are the phenocrysts whereas rutile, zircon, chlorite and leucoxene are accessories. In the McFee greenstone belt, the formation consists of 3433-3426 Ma felsic volcaniclastic rocks with subordinate felsic lava and chert, and interbedded with andesitic basalt (AWpfa). Sericite, carbonate, epidote and chlorite (after hornblende) are the main secondary minerals. In the Panorama greenstone belt, the base of the formation consists of massive, orange-weathering rhyolite unit (AWpr) where the matrix (under microscope) is finely recrystallized quartz and feldspar with sericite-altered plagioclase laths. In the North Pole Dome, the Monzogranite laccolith is found syn-volcanic to the Panorama Formation and is thought to be the feeder. During the deposition of the Panorama formation, a high-temperature alteration (300^0C) due to intense hydrothermal activity began and led to the formation of highly schistose and pyrophyllite-rich horizon. Fine-grained felsic tuff and agglomerate rocks (AWpt) is located in the northeast and southwest of the Panorama greenstone belt and are characterized by shards of clear crystalline quartz and devitrified felsic glass. Fuchsite mineral (variety of chromium-rich muscovite) is found in rounded agglomerate rhyolite clasts in a rhyolite matrix.

2.4.7. Euro Basalt Formation

The Euro Basalt Formation (about 9.4km thick and 3350-3325 Ma) conformably overlies above the Strelley Pool Chert in the east Strelley, Panorama and North Shaw greenstone belts and unconformably overlies the Panorama Formation in the Kelly greenstone belt. It's structurally overlain by the younger Duffer, Apex and Charteris formations. In the McPhee greenstone belt, the Gorge Creek and Fortescue Groups unconformably overlie the formation. The formation consists predominantly of pillowed basalt of interbedded tholeiitic unit and high Mg-basalt (AWebm) in addition to basaltic komatite and thin beds of chert intercalated with felsic volcaniclastics. At the base of the formation, the rocks are of high-Mg komatitic basalt. In the Kelly and McPhee greenstone belts, the formation is the dominated by metamorphosed pillowed tholeiitic basalt, komatitic basalt and metadolerite (A-KEe-bbo). The basal unit (A-KEe-bk) is mostly komatitic with some tholeiitic basalt and consists of tremolite, albite, chlorite,

epidote, quartz and titanite with clinopyroxenes that may be altered to chlorite and epidote. In the Mount Elsie greenstone belt, the Euro Basalt is the oldest rock unit and consists mainly of basalt, mafic schist, subordinate gabbro, chert, ultramafic rocks and clastic sedimentary rocks. The formation is intruded by the Yilgalong Granitoid Complex. The metamorphosed komatitic basalt unit (AWebk) is the dominant rock unit and variously foliated. Mafic schist unit (AWbs) is common. The pillowed basalt contains various proportions of chlorite, actinolite, epidote, albite and carbonates. Tholeiitic basalt (AWeb) is dark blue-green to grey-green and weakly foliated with local zones of quartz veining.

2.4.8. Charteris Basalt Formation

The Charteris Basalt Formation, which is located within the Kelly Greenstone Belt and restricted to the Charteris Creek area, is the youngest rock unit in this study. It belongs to the Kelly Group. It conformably overlies the Wyman Formation (felsic volcanic rocks) and unconformably overlain by the Budjan Creek Formation. The formation consists of metamorphosed tholeiitic basalt (AWcbk) interlayered with thin dolerite and minor komatitic basalt that contains chlorite after pyroxene.

2.5. Geochemical Studies

Many geochemical studies on the East Pilbara Granite-Greenstone Terrane were carried out. Smithies et al. (2007) studied the geochemistry in detail and new geochemical data that cover the full (3.52-2.93 Ga) depositional range of the greenstone belts and volcanic sequences were provided. He studied the different volcanic rocks of the greenstones of the East Pilbara Granite-Greenstone Terrane and the West Pilbara Superterrane, and compared between them based on the trace elements geochemistry. Thus this study provides relevant information about the volcanic rocks that can be used reliably for other studies i.e. in this study. The dataset, of both major oxides and trace elements, is available and can be obtained from the website of the Geological Survey of Western Australia (GSWA).

2.6. Spectroscopic Studies

For many years, spectroscopy technique has been used to obtain information of the Earth surface by investigating the reflectance spectra (measured as the ratio of the reflected light to the incident light) of its different compositional material (Van der Meer and Jong, 2006).

All spectroscopic remote sensing techniques, applied in the East Pilbara Granite-Greenstone Terrane, were meant to study different alteration facies i.e. Van Ruitenbeek et al. (2005, 2006) and Brown et al. (2006) used spectroscopic remote sensing to study the hydrothermal alteration styles in the Panorama-VMS district-East Pilbara Granite-Greenstone Terrane in different locations. Both studies resulted in the usefulness of the spectroscopic remote sensing technique for mapping the Earth mineral composition. Van Ruitenbeek et al. (2005, 2006) used the near-infrared spectroscopy to detect and reconstruct the fluid pathways in fossil hydrothermal systems. He could discriminate between different hydrothermal alteration facies by studying the abundance of white mica based on its Al content. Brown et al. (2006) identified and mapped the hydrothermal minerals based on the OH^- anion absorption features between 2.2-2.35μm Based on this study he concluded the spatial relationship between the subvertical pyrophyllite veins connected to a pyrophyllite-rich paleohorizontal layer.

3. METHODOLOGY

3.1. Introduction

In this research project, spectroscopic methods were used mainly to study the mineralogy of volcanic rocks in the study area while whole rock lithogeochemistry, petrographic study and the geological information provided with the geological maps and reports were used to compare, evaluate and validate the spectroscopic results (Figure 3.1).

Samples that were used in this study are 206 slabs (also their major and trace elements chemical analyses were provided) that were collected by Smithies et al. (2007) and 9 rock hand specimens that were collected by Thuss (2005) from the same locations of the Smithies et al. (2007) samples and brought to the ITC. The slabs and rock hand specimens were analysed by an ASD Fieldspec Pro spectrometer for the spectroscopic study, in addition, the nine rock hand specimens were used for petrographic study. More detail about how samples were collected can be obtained from Smithies et al. (2007) and Thuss (2005).

The samplers tried carefully to collect samples from fresh unweathered rocks to avoid any visible veins or alteration although some low degree of carbonate and silicification alteration was evident in some mafic and ultramafic rocks. All rocks in the study area have been metamorphosed to a lower-green schist facies and this is considered typical for Archean supracrustal rocks (Smithies et al., 2007).

Smithies (2007) in his report described the preparation and the analytical methods in detail. XRF spectrometry was used to analyse major elements on fused disks similar to Norrish and Hutton (1969) methods with ±1% precision; and trace elements Ba, Cr, Cu, Ni, Sc, V, Zn, and Zr on a pressed pellet similar to Norrish and Chappell (1977). Cs, Ga, Nb, Pb, Rb, Sr, Ta, Th, U, Y, and the REE were analysed by ICP–MS (Perkin Elmer ELAN 6000) similar to Eggins et al. (1997) method but on solutions obtained by dissolution of fused glass disks (Pyke, 2000). The precision of the trace elements is 10%. LOI and Fe abundances were determined by gravimetry (after combustion at 1100°C by digestion) and electrochemical titration (using a modified methodology based on Shapiro and Brannock (1962)) respectively. The standards of major and trace element analysis are given in Morris and Pirajno (2005).

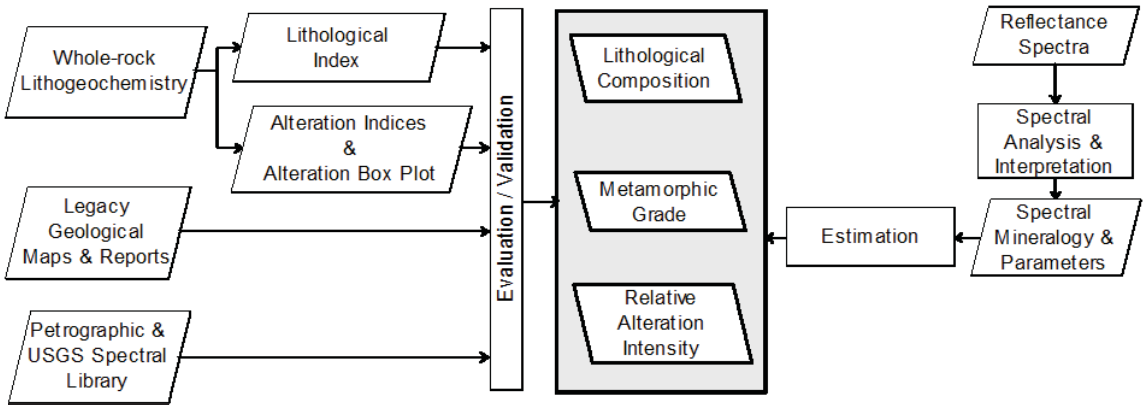

Figure 3.1: Research methodology flowchart.

3.2. Spectroscopic Method

Three measurements were taken from each rock sample using an ASD Fieldspec Pro spectrometer within the range 350-2500nm. Specifications of the instrument are shown in Table 3.1. The ASD raw spectra files were corrected using the ViewSpecPro software (Splice Correction) and then converted to ASCII format

file where they can be imported by ENVI software to create spectral library. The spectrum of each rock sample was carefully studied (using the Spectral Geologist and ENVI softwares) and interpreted (mainly based on the GMEX_Booklets) then compared with the geology and geochemistry of these rocks.

Table 3.1: ASD Fieldspec Pro instrument specifications.

Spectral Range	350-2500 nm
Spectral Resolution	3 nm @700 nm 10 nm @1400 -2100 nm
Sampling Interval	1.4 nm @ 350-1050 nm 2 nm @ 1000-2500 nm
Scanning Time	100 milliseconds
Detectors	One 512 element Si photodiode array 350-1000nm Two separate, graded index InGaAs photodiodes 1000-2500 nm
Input	2 m. fiber optic (25° field of view) Optional foreoptics available
Weight	7.2 kg. (excluding batteries, notebook and optional accessories)

3.2.1. Detectable Mineralogy in the VIS-SWIR

Reflectance spectra in the VIS-SWIR region provide a rapid and inexpensive means for determining mineralogy and hence; the chemical composition. Light interaction with the surfaces of different terrestrial materials results in preferential absorption of portion of the electromagnetic spectrum at certain wavelengths while at other wavelengths it's transmitted in the substance or reflected. Absorption features due to electronic or vibrational processes (i.e. transition metals ions Fe, Ti, Cr and Ni; and H_2O, $OH^{\neg}$, SO_4^{2-}, NH_4 and CO_3^{2-} fundamentals respectively) are diagnostic features for many minerals in the VIS-NIR and mid- to SWIR regions respectively. The position, depth, shape and width of the absorption features can be directly related to the structure (mineralogy) and chemistry of the minerals (Clark, 1999; and Van der Meer, 2004).

The absence or presence of transition metals and H_2O, $OH^{\neg}$, SO_4^{2-}, NH_4 and CO_3^{2-} fundamentals determine the absorption features in the VIS-SWIR region. Thus, minerals such as phyllosilicates, hydrated/hydroxyl silicates, sulphates, carbonates and iron-containing minerals can be spectrally detected. Minerals without diagnostic features in VIS-SWIR region (such as quartz and feldspars) are difficult to recognize.

Each volcanic rock has a certain lithological composition in which the dominant mineral(s) may either spectrally detectable (in the VIS-SWIR region) or not, as a consequence, the reflectance spectra of different volcanic rocks are varying correspondingly. Thus, a relationship between reflectance spectra and the different volcanic rocks can be established based on lithological composition.

In case of altered or metamorphosed volcanic rocks; alteration minerals are highly dependent on the original lithological composition and thus they can be used as indicators to infer the parent rock. So, by studying the spectral absorption features of these alteration minerals; a bridge between the reflectance spectra and the different volcanic rock types can be established.

3.2.2. Spectral Analysis and Interpretation

The analysis of spectra is mainly based on the waveform analysis method that's using a linear interpolation technique for the hull-quotient reflectance spectrum derived by taking the ratio of the band reflectance spectrum to the enveloping upper convex Hull (Green & Graig, 1985, after Van der Meer, 2004). This technique is useful to quantify the spectral absorption features that are related to a certain mineral, in terms of wavelength position, width, depth, asymmetry and slope of the upper convex hull. These spectral

parameters are controlled by the crystal structure and chemical composition of the minerals thus; they can be used to infer the different volcanic rock types (Van der Meer, 2004).

Okada & Iwashita (1992) performed a waveform parameterization for the spectral absorption features in order to map the surface materials from the GER AIS hyper-multispectral image data in the Cuprite mining area. They proposed the absorption position, depth, symmetry factor, and slope of upper convex hull parameters to produce five parameter images showing the surface materials in terms of their spectral characteristics.

Herrmann et al. (2001) analysed the SWIR spectra for VHMS-related alteration zones in Mount Read volcanics and used the depth parameter to estimate semi quantitatively the relative amounts of the main component minerals. He used the depth ratio of Al-OH/Fe-OH (for white mica and chlorite respectively) to avoid the influence of albedo (brightness), secondary Al-OH and CO_3^{2-} absorption features coincident with chlorite Mg-OH absorption feature at about 2340nm.

Van der Meer (2004) proposed a simple linear interpolation technique to characterize the spectral absorption features in terms of position, depth and asymmetry. He applied this technique to derive information from hyperspectral image data in the Cuprite mining area and concluded that the estimated depth and position can be related to the chemistry of the samples.

In this study, the spectral absorption position parameter will be used to characterize the different volcanic rocks lithology and metamorphism in terms of mineralogy whereas the spectral depth parameter will be used to estimate the metamorphic grade and relative alteration intensity in terms of spectral minerals abundance.

3.3. Lithogeochemistry and Petrographic Study for Evaluation Spectroscopic Results

Different rock units in the study area have been extensively studied and their original parent rocks have been determined in previous studies (e.g. Van Kranendonk et al., 2006; and Smithies et al., 2007). Rock samples being used in this research project were originally collected by Smithies et al. (2007) to characterize the different rock units so they are considered as representative. Samples that were collected by Thuss (2005) were mainly used for petrographic study. Thus, the main purpose of using the whole-rock lithogeochemistry, in addition to the petrographic study, is to compare with and evaluate the spectroscopic results.

3.3.1. Major Elements Lithogeochemistry

Sabine et al. (1985) found that TAS (total alkalis diagram based on major elements oxides SiO_2 vs. Na_2O+K_2O) can be satisfactory applied to many low-grade metavolcanic rocks based on the fact that in very low to low-grade metamorphism; elements mobility is limited. Ghataka et al. (2011) also concluded the limited mobility of elements in subduction metamorphic rocks of the Franciscan Complex and the Feather River ultramafic belt in California. Therefore, major elements are useful in the classification of the low-grade metamorphosed volcanic rocks and thus can be used to represent the different rock lithologies in order to evaluate the spectroscopic results.

Since the Archean Pilbara Supergroup rocks underwent low-grade hydrothermal metamorphism, it's difficult to ascertain the absence of any intensely altered rocks especially in case of post-consolidation metasomatic alteration where the gain and loss of elements occur especially the major elements, in this case an immobile trace elements geochemistry must be used such as Ti, Zr, Nb, Y, Ce, Ga, and Sc (Winchester & Floyd, 1977).

3.3.2. Alteration Indices and the Alteration Box Plot

Alteration indices are a multivariable numerical expressions that calculate the relative proportion between altered and unaltered components using major elements, expressed as oxides, to highlight alteration halos

around ore bodies and to determine the intensity of the hydrothermal alteration (Piche & Jebrak, 2004). The enriched components are represented in the numerator while the depleted ones in the denominator.
As the East Pilbara Granite-Greenstone Terrane hosts VMS-type deposits; it can make use of several proposed alteration indices that are relevant to determine the intensity in case of hydrothermally altered rocks. Some alteration indices were listed in Table 3.2.

Table 3.2: Alteration indices applied in VMS-related hydrothermal alteration (modified after Franklin, 1997 & Brauhart et al., 1998).

Alteration Index	Element Ratios	Alteration Process	Reference	
Ishikawa (AI)	$(MgO+K_2O)/(MgO+K_2O+CaO+Na_2O)$	Addition of Mg & K as chlorite and sericite – loss of CaO and Na_2O by destruction feldspar.	Ishikawa et al. (1976)	(1)
CCPI	$(FeO+MgO)/(FeO+MgO+K_2O+Na_2O)$	Addition of Fe and Mg as chlorite – loss of K_2O and Na_2O.	Large et al. (2001)	(2)
Modified Hashimoto	$(FeO+MgO+K_2O)/(MgO+K_2O+CaO+Na_2O)$	As above with addition of FeO.	Coad (1985)	(3)
Chlorite	$(Fe_2O_3+MgO)/(Fe_2O_3+MgO+2CaO+2Na_2O)$	Addition of Fe and Mg as chlorite – loss of CaO and Na_2O by destruction feldspar.	Saeki & Date (1980)	(4)
Alkali	$(CaO+Na_2O)/(CaO+Na_2O+K_2O)$	Loss of CaO and Na_2O by destruction feldspar.	Saeki & Date (1980)	(5)
Hashiguchi	$(Fe_2O_3)/(Fe_2O_3+MgO)$	Addition of Fe as Fe_2O_3.	Hashiguchi & Usui (1975)	(6)
Sericite	$(K_2O)/(K_2O+Na_2O)$	Replacement of feldspar by sericite.	Saeki & Date (1980)	(7)
Spitz	$(Al_2O_3)/(Na_2O)$	Sodium depletion (Al_2O_3 conserved).	Spitz & Darling (1978)	(8)

Altered or unaltered rocks, as well as the alteration intensity, will be determined based on the alteration indices and then to compare with the spectroscopy results. In case of intensely altered rocks; it's useful to identify the style of alteration as this makes the spectroscopic interpretation easier, and for this purpose; alteration box plot method is a useful tool.
The alteration box plot (proposed by Large et al., 2001) is a scatterplot of the Ishikawa alteration index (AI) versus the chlorite-carbonate-pyrite-index (CCPI) (equations (1) & (2) respectively from Table 3.2). The alteration index (proposed by Ishikawa, 1976) measures the intensity of chlorite and sericite alterations in Kuroko-type VMS deposits whereas; the chlorite-carbonate-pyrite-index (which is also proposed by Large et al., 2001) measures the intensity of chlorite, carbonate and pyrite alterations.
Both indices were designed for areas where the primary minerals that involved in the original reactions were highly preserved and not for highly deformed and high-grade facies metamorphosed areas (Theart et al., 2011).

4. RESULTS AND DISCUSSION

4.1. Spectroscopy

The analysis of the reflectance spectra (hull-corrected reflectance spectra between 350nm and 2500nm) was done using two softwares: the spectral geologist TSG and ENVI whilst the interpretation was mainly based on the GMEX_Booklets that are associated with the TSG software. The TSG software and the booklets are appropriate for this study because different geological environments were taken into consideration during the interpretation of the short wave infrared reflectance spectra and creating the spectral library i.e. volcanogenic massive sulphides (VMS) or Archean greenstones or etc. In addition, problems of the interpretation of mixed spectra were dealt and handled. Therefore, the TSG spectral library was the main reference for this study in addition to the ENVI spectral library that's mainly used for validation.

4.1.1. Spectrally Detectable Minerals

As a result of the spectroscopic interpretation, chlorites, hornblende, actinolite, epidote, sericite (illite, paragonite, muscovite and phengite), pyrophyllite and prehnite minerals have been identified according to the spectral absorption features that are considered as diagnostic. Fe-OH and Mg-OH absorption features were basically used to identify mafic minerals whereas Al-OH absorption feature was used for felsic minerals.

Chlorites

The chlorites are a group of phyllosilicate minerals containing Al, Mg and Fe endmembers. Spectrally, Mg and Fe varieties (as a result of Fe and Mg substitution) can be identified as Mg-OH and Fe-OH absorption features. The spectral positions of the Mg-OH and Fe-OH features depend mainly on the iron content, as a consequence, more or less iron content leads to the displacement of the absorption features positions to longer or shorter wavelengths respectively. The main diagnostic spectral positions of the Mg-OH and Fe-OH absorption features are 2325nm and 2245nm for Mg-chlorite respectively; and 2355nm and 2261nm for Fe-chlorite respectively. Intermediate chlorite composition has Mg-OH and Fe-OH absorption features close to 2347nm and 2254nm respectively. In normal conditions under sea, glass transforms to hydrated alteration products, i.e. palagonite (palagonitization), but at higher metamorphic grades it recrystallizes into mafic silicates such as chlorite and smectite. The ratio of Fe/(Fe+Mg) decreases with the increase in metamorphic or hydrothermal grade (Frey & Robinson, 1999). As a consequence, Fe-rich chlorite tends to be stable in low temperature conditions and in terms of mineralization it increases outward. Chlorite type is controlled by the composition of the original rock in case of fresh or least altered and controlled by the fluid phase in case of hydrothermal alteration. The mean chlorite temperature for sub-greenschist and greenschist facies are 263^0C and 311^0C respectively (Figure 4.1 A, B & C) (Shikazono & Kawahata, 1987; and Frey & Robinson, 1999).

Amphiboles

Hornblende is a ferromagnesian mineral of the amphibole group that can be found in a wide variety of igneous rocks. In case of metamorphism, it's common in transitional greenschist/amphibolite and amphibolite facies. Spectrally it has two main diagnostic absorption features due to Mg-OH from 2324-2350nm and from 2390-2410nm. The variation in the features positions is related to the iron content as hornblende can be either ferro-hornblende or magnesio-hornblende but this compositional variation cannot be recognised if other Mg-OH minerals are present (Figure 4.1 D). Actinolite is a ferromagnesian mineral of the amphibole group. It's a common mineral in upper greenschist metamorphic rocks as fibrous or asbestiform. Like hornblende and chlorite, actinolite is an intermediate variety between

magnesium-rich tremolite and iron-rich ferro-actinolite. Spectrally, two Mg-OH absorption features are the main diagnostic features and vary between 2314-2324nm and 2380-2390nm depending on the iron content (Figure 4.1 E).

Carbonates

Carbonates are a group of minerals containing the carbonate ion CO_3^{2-} as a basic structural and compositional unit. Carbonate minerals are abundant and can be found as primary, e.g. in limestone and carbonatite rocks, or as secondary i.e. after the alteration of other minerals. In volcanogenic massive sulphide environments, carbonates related to deposits tend to be more Fe, Mg and Mn in content i.e. ankerite, siderite, rhodochrosite, and magnesite whereas carbonates related to background diagenetic or metamorphism are mostly calcic i.e. calcite and dolomite. This compositional variation, i.e. Ca substitution by Fe and Mg, can be spectrally determined by the diagnostic CO_3^{2-} absorption feature within 2300-2340nm. Pure calcite has long absorption feature wavelength (around 2345nm) followed by Fe- and Mg-carbonates absorption features at nearly 2335nm and 2302nm respectively. The presence of sericite and chlorite minerals affect strongly the carbonates spectra and mask their absorption features, as a consequence, the absorption feature close to 2340nm becomes deeper than in the background phase (Figure 4.1 F) (Gifkins et al., 2005).

White Micas

Sericite is a common fine-grained phyllosilicate mineral that refers to white mica (illite, paragonite, muscovite and phengite). It is found in a wide variety of rocks, i.e. sedimentary, igneous and metamorphic, and environments due to weathering or alteration of feldspars. Illite is a K-deficient muscovite and can be formed by the alteration of K-feldspar, muscovite and phengite minerals or due to smectite-to-illite transition in low-grade metamorphic rocks. Paragonite-muscovite series is formed due to Na-K substitutions whereas phengite is Fe-Mg sericite. The progressive transition from illite to phengite indicates higher-grade alteration (Meunier, 2005). Spectrally, all the sericite minerals are characterized by a prominent Al-OH absorption feature around 2180-2228nm and two secondary diagnostic Al-OH absorption features close to 2344nm and 2440nm. Illite is difficult to distinguish from muscovite, however, illite has deeper water absorption feature close to 1900nm and shallower Al-OH absorption feature at nearly 2200nm (refers to illite-to-muscovite crystallinity) whereas the identification of compositional variation from paragonite (2180nm) through muscovite (2200nm) to phengite (2228nm) based on the main Al-OH absorption feature is possible (Figure 4.2 A, B & C). Al-content in sericite (Al-rich at shorter wavelength and Al-poor at longer wavelength) can be related to the indirect influence by the Na/K ratio and to the direct Fe-Mg substitution to the octahedral Al sites which in turn indicates the metamorphic grade since less Al-content means higher grade (Duke, 1994). The depth of the absorption feature close to 2344nm can be used to indicate the presence of carbonates (in the absence of Mg-OH minerals) as it is increased. The Mg-OH minerals also influence the same absorption feature but, alternatively, it can be better identified by another secondary absorption features, i.e. chlorite results in an absorption feature around 2240nm, and as a consequence the coexistence of sericite, carbonates and Mg-OH minerals leads to overprinting the spectral features, and thus misinterpreting any presence, of carbonates (Guidotti, 1984; Nieto et al., 1994; Frey and Robinson, 1999; Meunier, 2005; and Velde and Meunier, 2008).

Pyrophyllite

Pyrophyllite is a common hydrothermal alteration phyllosilicate mineral (advanced argillic alteration) and is occurred as a metamorphic mineral in phyllic and schistose rocks. The formation of pyrophyllite (stable at 2 kbar and between 275^0-350^0C) indicates active leaching process to the parent rocks leading to high alumina and silica rocks. Metamorphic pyrophyllite mineral is reported to be associated mainly with felsic volcanic and tuffaceous rocks (Sykes & Moody, 1978; Condie, 1981; and Bozkaya et al., 2007). The main spectral absorption features are due to the Al-OH absorption at 2166nm and nearly 2319nm. These absorption features persist in mixtures (Bierwirth, 2002; and Freek, 2004). Another sharp and deep

absorption feature due to H_2O/OH^- is close to 1396nm and less important secondary absorption feature that disappears in mixtures is close to 2066-2078nm (Figure 4.2 D). Samples that contain pyrophyllite, in this study, were collected from a known intensely altered zones in the Panorama Formation due to active hydrothermal alteration associated with the emplacement of the Euro Baslt Formation (Brown et al., 2006).

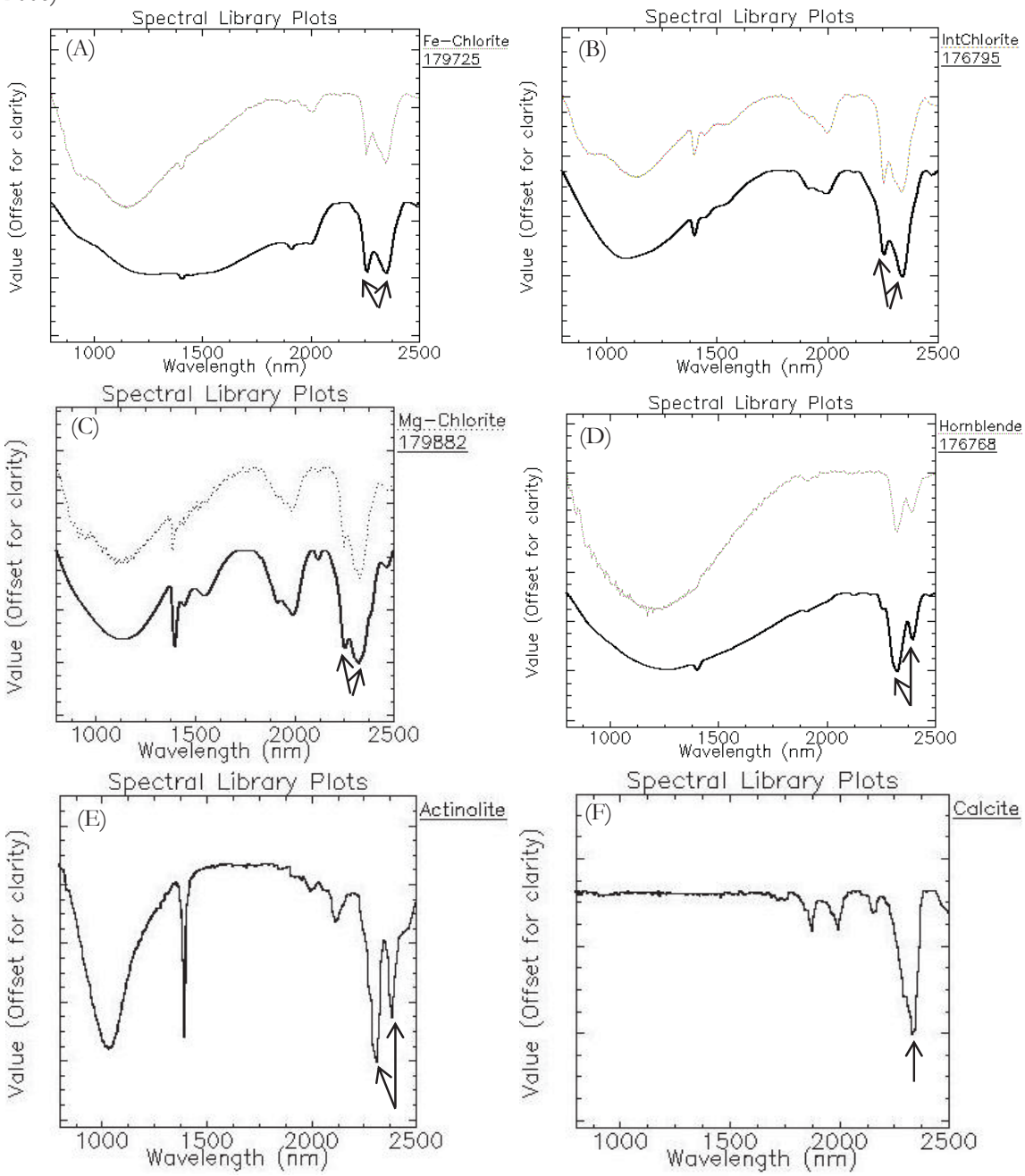

Figure 4.1: The main spectral diagnostic features of chlorites (A, B & C), hornblende (D), actinolite (E) and calcite (F). Spectra were compared with the USGS spectral library (Fe-chlorites: cchlore2.spc Clinochlore_Fe GDS157; IntChlorite: cchlore3.spc Clinochlore GDS158 Flagst; Mg-chlorite: chlorit3.spc Chlorite SMR-13.b 60-104u; Hornblende: hornble3.spc Hornblende HS16.3B; Actinolite: actinol3.spc Actinolite HS315.4B; and Calcite: calcite1.spc Calcite WS272). Arrows indicate the main diagnostic absorption features that were referred in the text.

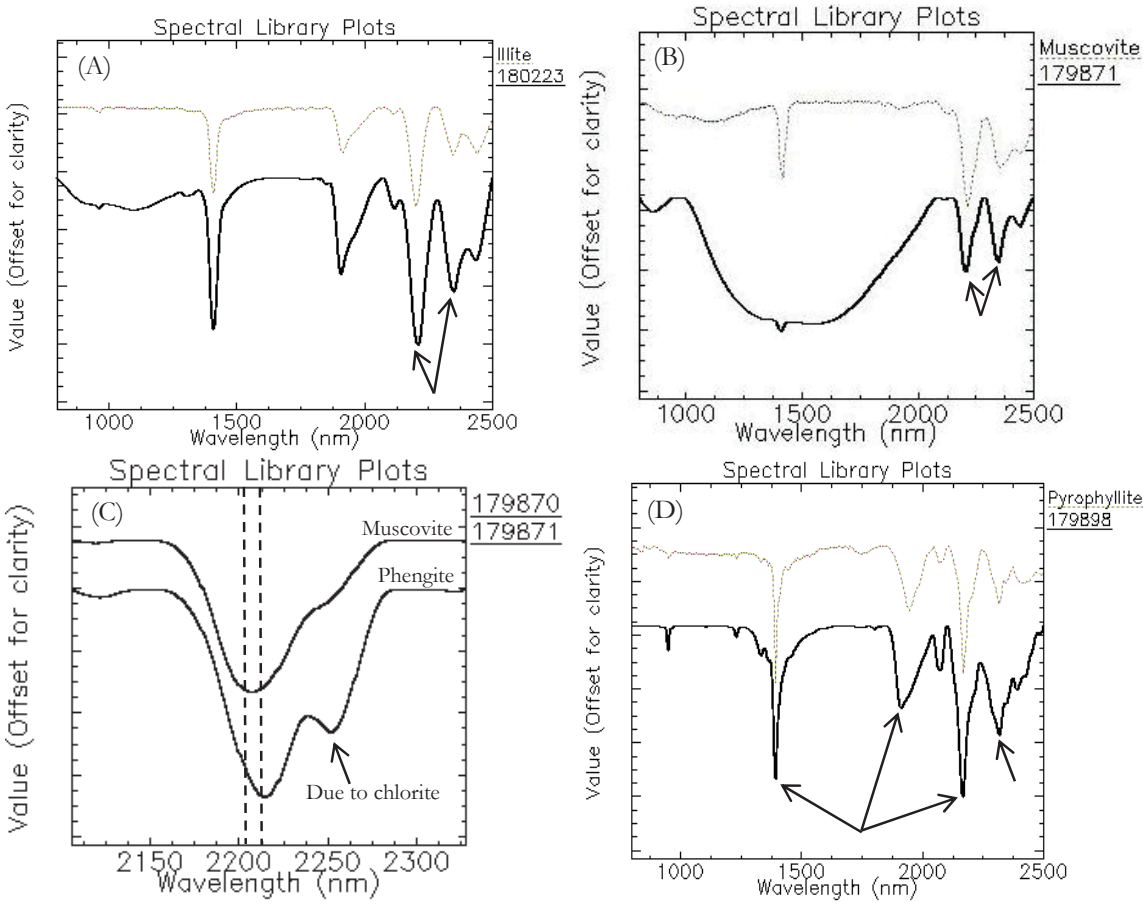

Figure 4.2: The main spectral diagnostic features of sericite (A, B & C) and pyrophyllite (D). Spectra were compared with the USGS spectral library except in (C) where sample no. 179870 (phengite) was compared with the sample no. 179871 (muscovite) (Illite: illite1.spc Illite GDS4 (Marblehead); Muscovite: muscovi6.spc Muscovite GDS116 Tanzania; and Pyrophyllite: pyrophy3.spc Pyrophyllite SU1421). Arrows indicate the main diagnostic absorption features that were referred in the text.

Epidote

Epidote group is a common Ca-Al-Fe^{3+} silicate minerals in altered mafic to intermediate igneous rocks due to hydrothermal and metamorphic processes, and is formed after various minerals i.e. feldspars, amphiboles, pyroxenes, micas and etc. Iron to aluminum ratio (due to Fe^{3+}-Al exchange) that leads to different epidote minerals depends on the bulk composition and the pressure-temperature-fluid-redox conditions. Thus the iron content refers to both rock composition and the conditions of the formation i.e. in metabasites epidote tends to be more Fe-rich whilst in metasediments it is poor in Fe (rich in Al), on the other hand, Fe-rich epidote indicates lower grade than Fe-poor epidote. The main spectral absorption features are due to Fe-OH and Mg-OH absorptions and located at nearly 2240nm and 2335-2342nm respectively. Other important secondary absorption features due to OH^- bond are at nearly 1540nm and 1835nm. The main absorption features strongly overlap the chlorite spectral features (Figure 4.3 A) (Grapes & Hoskin, 2004).

Prehnite

Although prehnite mineral hasn't been reported in the previous studies that were done on the study area, it was spectrally detected in several samples. It has less been discussed in this study because it was found irregularly distributed along the stratigraphic sequence (mainly as meta-domains due to textural variations) may be as relics due to prograde metamorphism or as newly formed due to retrograde metamorphism. Prehnite is a secondary Ca-Al phyllosilicate mineral usually found in mafic volcanic and very low-grade

metamorphic rocks. It's considered as an indicator to very low-grade prehnite-pumpellyite metamorphic facies. The main spectral absorption features are around 1470nm and 2340nm which overlaps with the Mg-OH minerals. Prehnite typically coexists with pumpellyite mineral (Ca-Al phyllosilicate) but the latter couldn't be spectrally detected because its spectral features strongly overlap the chlorite spectral features (Figure 4.3 B) (Yuasa et al., 1992).

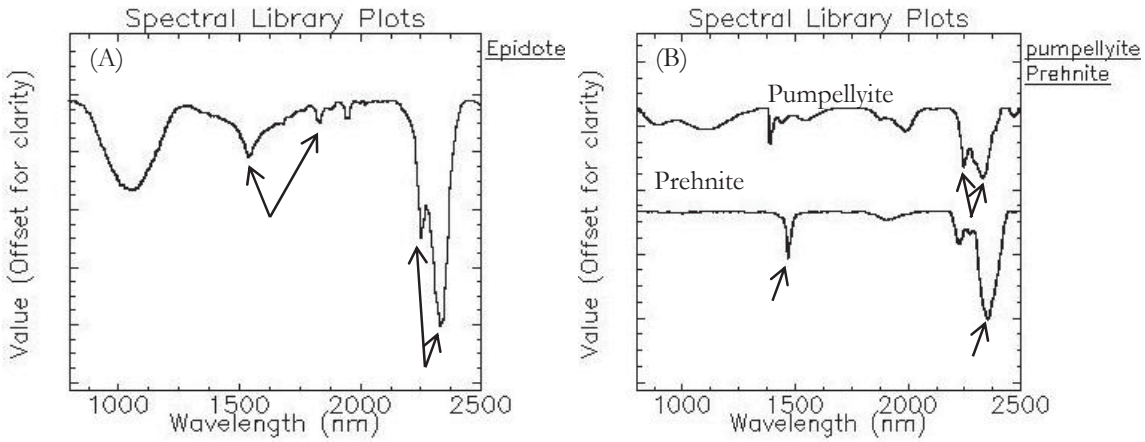

Figure 4.3: (A) Epidote spectrum (epidote1.spc Epidote GDS26.a 75-200um, obtained from the USGS spectral library). (B) Prehnite spectrum (PREHNITE PS-21A, obtained from the ASTER spectral library (Baldridge et al., 2009) and Pumpellyite spectrum (c1ze01, obtained from the NASA RELAB spectral library (*http://www.planetary.brown.edu/relab/*)). Arrows indicate the main diagnostic absorption features that were referred in the text.

Chlorites, epidote, hornblende, actinolite, muscovite and phengite minerals were found abundant in the study area whereas some minerals like paragonite, illite, pyrophyllite and prehnite were found scarce. Sericite and pyrophyllite, only as a main constituent, are restricted to felsic rocks whereas the rest are not constrained to a certain rock type except the Mg-chlorite variety that's related to mafic/ultramafic rocks. Some felsic samples collected from a known intensely hydrothermally altered areas show up pyrophyllite and sericite (mainly muscovitic and less phengitic) minerals.

Some minerals that were seen under the microscope couldn't be spectrally detected such as carbonates (calcite, siderite or ankerite?), feldspars and quartz. Feldspars and quartz can't be detected with the near-infrared spectroscopy at all whereas carbonates cannot be detected due to the overlapping of their spectral features with the others especially chlorite and sericite minerals, nevertheless a slight increase in the depth of the main diagnostic absorption feature close to 2345nm of chlorite and sericite minerals can be noticed in samples containing carbonates. In order to see the effect of the carbonates present, two felsic rocks were studied under the polarized microscope. Both rocks, samples nos. 176757 & 179721, are intensely altered to mainly sericite; and sericite and carbonate (mainly calcite or dolomite) (Figure 4.4 A & B respectively and Appendix 1). From the reflectance spectra, it can be noticed that the absorption feature around 2200nm is deeper in sample no. 176757 because it contains more sericite than sample no. 179721, but the situation is reversed at nearly 2348nm (although it should be as deeper as at 2200nm) due to the effect of the carbonates (Figure 4.4 C).

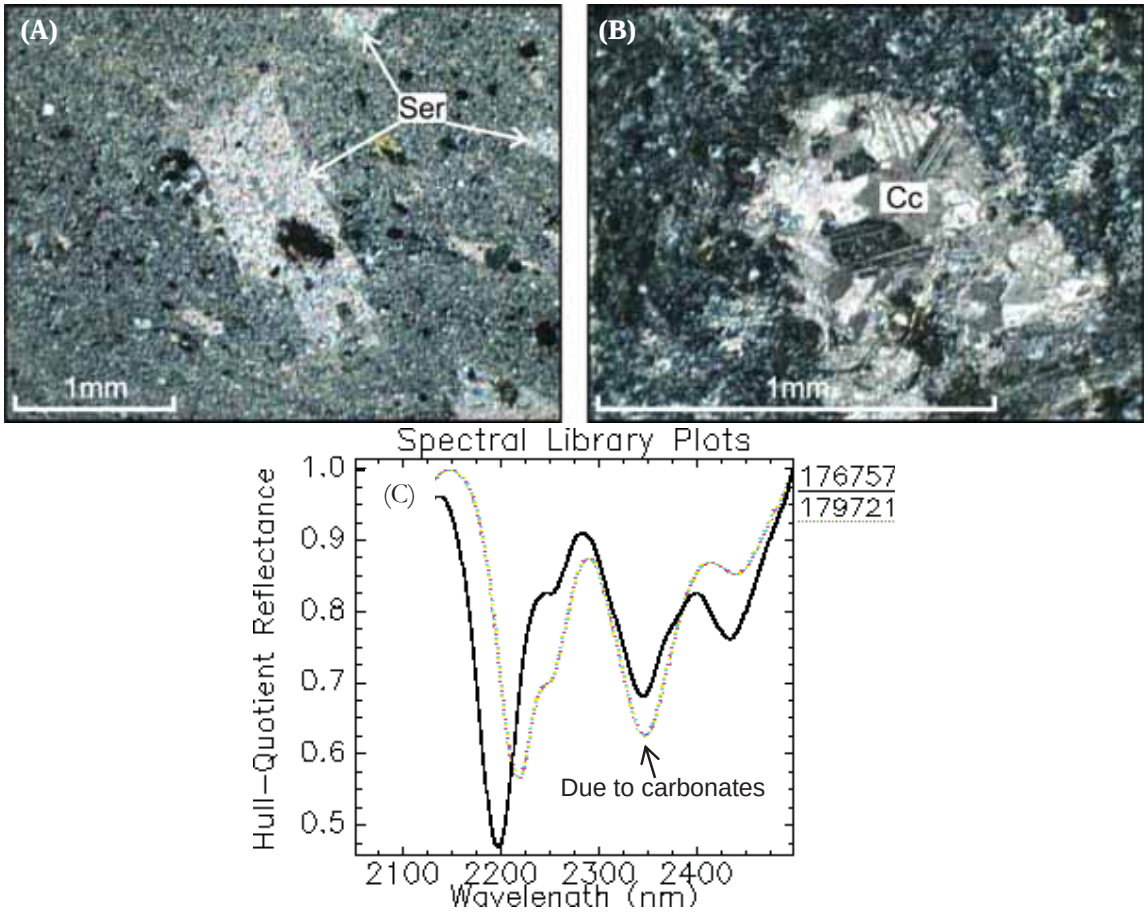

Figure 4.4: (A) Sericite alteration (Ser) mainly after plagioclase phenocrysts and the fine-grained groundmass (sample no. 176757). The field of view is 3.5mm (B) A cavity (may be after plagioclase or mafics) filled by carbonates Cc (calcite or dolomite). The groundmass is amorphous and intensely altered to carbonates (give dark cloudy appearance) and light fine-grained sericite (sample no. 179721). The field of view is 1.4mm. (C) Reflectance spectra of both samples showing the effect of carbonates on the depth of the absorption feature around 2348nm. Sample no. 176757 in solid line and sample no. 179721 in dotted line.

Some minerals, also due to overlapping spectral features, are difficult to distinguish especially actinolite and hornblende. Anyhow, actinolite has a deeper main Mg-OH absorption feature close to 2315nm, shallower secondary Mg-OH absorption feature close to 2385nm, and narrower and deeper absorption features close to 1400nm and 1100nm due to H_2O/OH^-. Also, the wavelengths of the Mg-OH absorption features are shorter for actinolite than hornblende. In the study area, actinolite never comes as pure mineral and is always mixed with other minerals especially chlorite and because of its lower quantity with respect to chlorite its main diagnostic absorption features are overprinted by the chlorite absorption features therefore its secondary absorption features like those close to 1400nm and 1100nm are more helpful and diagnostic for actinolite than hornblende in such a mixture (Figure 4.5 A & B). Epidote mineral is easy to detect as it's the only mineral in this study gives secondary absorption features close to 1540nm and 1835nm (Figure 4.5 C). Prehnite in association with chlorite gives a secondary absorption feature close to 1480nm which is also unique (Figure 4.5 D) (Ehlmann et al. 2009).

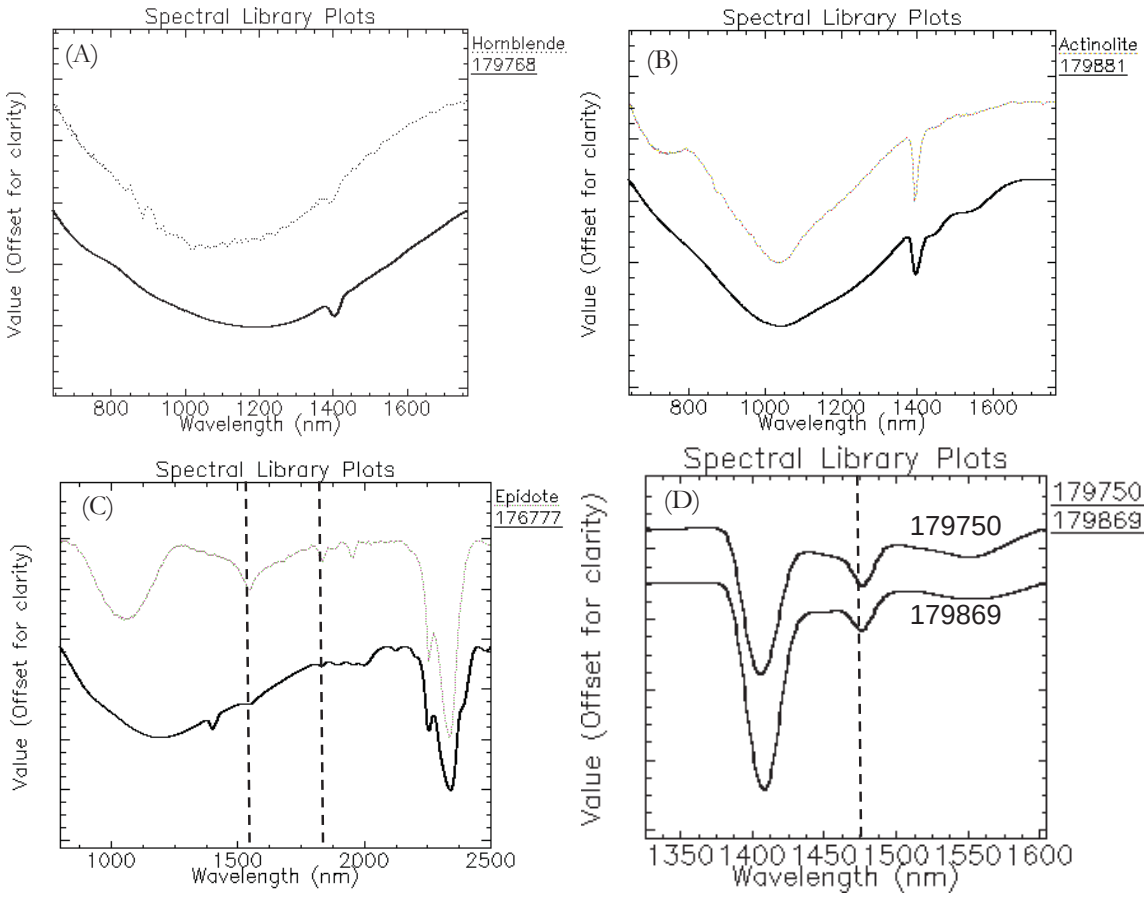

Figure 4.5: Second spectral diagnostic features as a handy tool in case of mixtures. (A) & (B) Hornblende and actinolite mixed with chlorite. Actinolite spectrum is more diagnostic close to 1400nm and 1100nm as it gets sharper and deeper than hornblende spectrum. (C) & (D) Epidote and prehnite are diagnostic at approximately 1540nm & 1835nm, and 1480nm respectively. The two prehnite samples (179869 & 179750) were identified in the same way as the Ehlmann et al., 2009 study.

4.1.2. Spectral Mineral Assemblages

In general, the main greenschist and lower amphibolite facies mineral assemblages in the study area can be summarized as chlorite, actinolite, epidote, quartz, albite and ± sericite; and hornblende respectively (Figure 4.6). According to the literature review and geological maps with the reports, only the two main greenschist and amphibolite metamorphic facies could be identified without any detail information e.g. greenschist subzones and the transition zone. Only one study describing the different metamorphic facies in detail was carried out in the North Pole greenstone but none of the samples were collected from that area. Thus, based on the literature review, the grade of metamorphism was assigned to the samples, either as greenschist or amphibolite facies, and then these samples were spectrally characterized (Appendix 2).

Spectrally, only those minerals have diagnostic features in the short wave infrared can be detected such as chlorite, actinolite, epidote, hornblende and sericite and they represent part of the greenschist and amphibolite facies mineral assemblages, hence the term spectral mineral assemblages has been introduced.

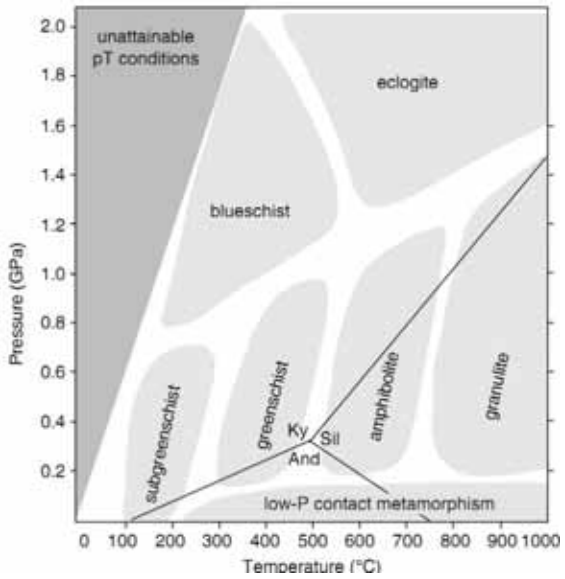

Figure 4.6: Different metamorphic facies P-T diagram (after Bucher & Grapes, 2011).

4.1.3. Mixed Spectra

From the previous sections we note that minerals formed in assemblages, as a consequence, spectra are mixed and difficult to interpret especially if the coexisting minerals have nearly the same spectral features (particularly the main spectral features). In mixed spectra, minerals with stronger absorption features mask or enhance the others and thus leading to misinterpretation. One of the best examples that's common in the greenstone/greenschist rocks is the coexistence of calcite (CO^{2-}_3 bond), sericite and chlorites (OH^- bond) where the sericite and chlorite spectral features overprint the calcite spectral features even if calcite found in considerable quantity (unless it forms more than 20% of the sample, then some secondary diagnostic features become pronounced and then can be identified). In other rocks with coexisting spectral minerals, this problem can be partly handled as the effect of the mixed spectra on each other leads to new reflectance spectra with some modifications. Modifications are mostly developed as little absorption features or inflections and in most cases, they are caused by the main diagnostic absorption features and less by the secondary absorption features e.g. coexistence of dominant chlorite spectrum with less dominant hornblende spectrum leads to a new shallow absorption feature or inflection around 2390nm due to the main hornblende Mg-OH diagnostic feature at that position whereas the coexisting of dominant hornblende spectrum with less dominant chlorite spectrum leads to a new shallow absorption feature or inflection around 2250nm due to the main chlorite Fe-OH diagnostic feature at that position. In other cases where the main diagnostic absorption features in mixtures don't exhibit any diagnostic features because they're strongly overlapping then other secondary spectral features would be helpful e.g. using the main diagnostic features in case of coexisting epidote and chlorite is useless as they're strongly overlapping, instead, little absorption features close to 1540nm and 1830nm are more useful (Figure 4.7). Thus, in case of mixed spectra, one must study both the main and secondary diagnostic absorption features.

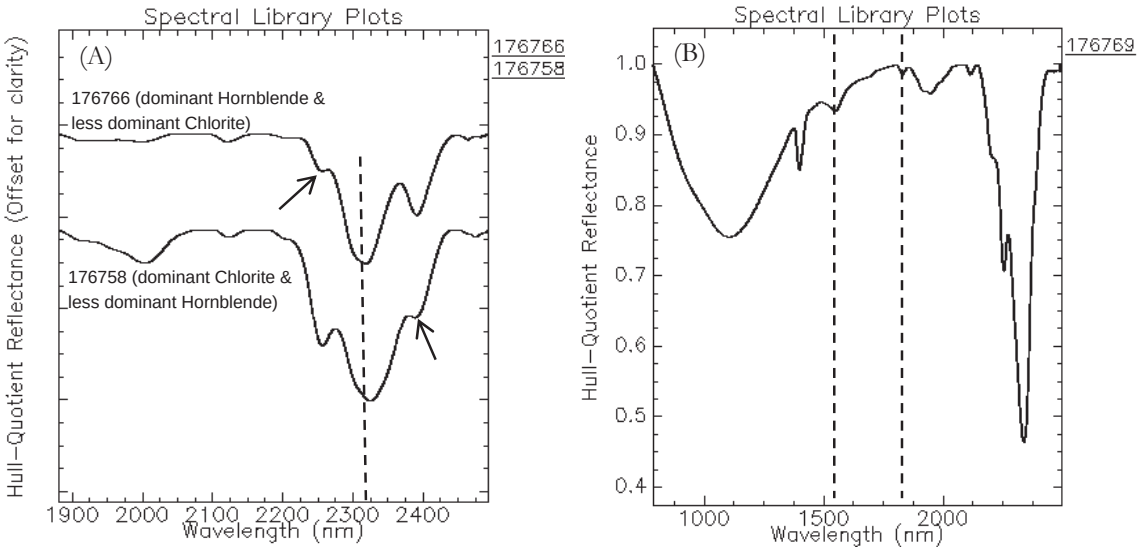

Figure 4.7: Mixed spectral minerals. (A) Spectral mixture of intermediate chlorite and hornblende. Arrows indicate little absorption features that were caused by the main diagnostic absorption features of the less dominant spectral mineral. The dashed straight line refers to the spectral position where both minerals overlap. (B) Spectral mixture of intermediate chlorite and epidote. Epidote can be identified from a little absorption features close to 1540nm and 1830nm.

4.2. Spectral Parameters from Standard Spectral Libraries

Before we start characterizing the different lithological units based on the spectral parameters (absorption feature position and depth) of the different spectral minerals that were identified in the study area, we will look at the same spectral minerals from the USGS and spectral geologist TSG spectral libraries but it must be taken into account that the spectra of the minerals in these libraries are pure to some extent whereas they are mixed in our samples (Figure 4.8 A). The overlapping between the spectral absorption features of the different spectral minerals makes the interpretation more difficult as the absorption feature position, shape and depth are changed. When the absorption features of a spectral mineral mask another spectral mineral's absorption features, or when coexistence spectral minerals overlap the main absorption features, then studying secondary absorption features becomes necessary.

The spectral absorption features (both main and secondary) that were interpreted in this research (according to the detected mineralogy) are Mg-OH, Fe-OH, Al-OH, H_2O/OH and CO_3 but only the Mg-OH (~2335nm) and Al-OH (~2200nm) absorption features were used in terms of mineralogy to characterize the different lithological units (since the abundant spectral minerals for the studied rock units are mafic and rarely felsic). Also the depth parameters for all the absorption features were extracted and interpreted and only those were found useful to this study were used such as the depth parameters of the Mg-OH (~2390nm), Fe-OH (~2250nm), Al-OH (~2200nm) and H_2O/OH (~1400nm) absorption features. The spectral depth parameter, based on the spectral minerals abundances, was used in two ways: to estimate the different metamorphic facies; and to estimate the relative alteration intensity. In terms of metamorphism, the transition from the metamorphic greenschist to amphibolite facies results in the disappearance and appearance of new mineral(s) due to different temperature and pressure. Since this transition occurs gradually thus the spectra vary accordingly and based on this spectral variation the depth of the absorption features can be related to the different metamorphic grades. In case of the alteration intensity, the increase of the relative abundance of certain minerals results in the increase of the depth of the spectral absorption features which in turn can be related to the intensity of the alteration processes.

Although the USGS and spectral geologist TSG spectral libraries don't have mixed spectra similar to that in our samples (different conditions), the depth parameters that were used in this study were extracted to the different spectral minerals from the spectral libraries (Figure 4.8 B & C).

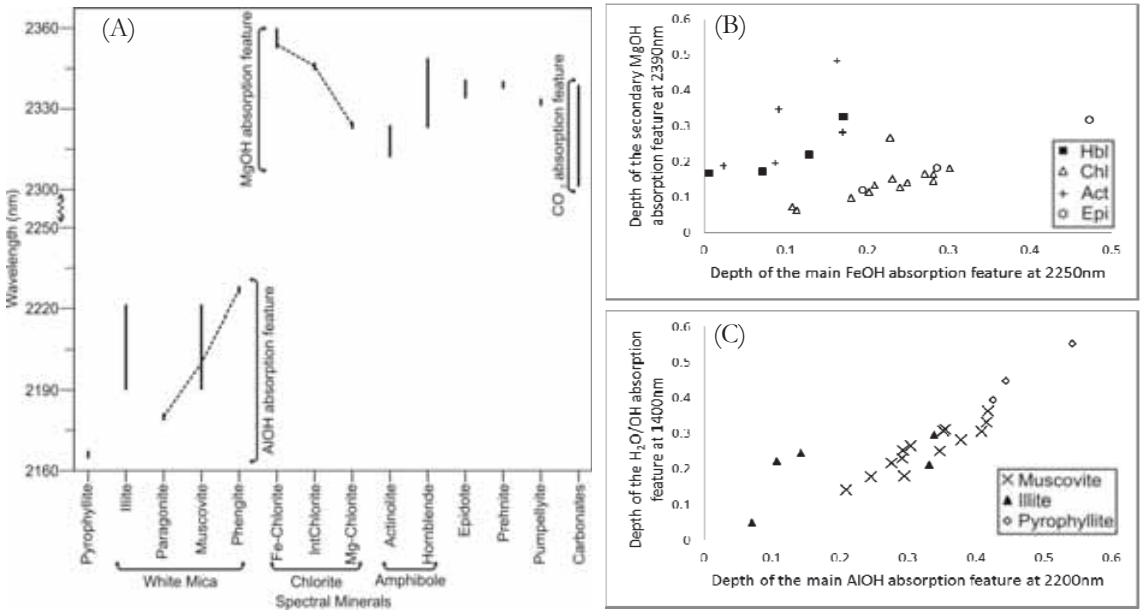

Figure 4.8: The spectral position and depth parameters of the different absorption features of the different spectral mineralogy obtained from the USGS and spectral geologist TSG spectral libraries (A); and (B) & (C) respectively. Dashed lines, as well as solid lines, indicate continuous changes (compositional variations due to elements substitutions).

4.3. Spectroscopy and Lithological Units

Here we relate the results of the spectral analysis to the different lithological units in order to see how spectral minerals vary spatially with respect to the stratigraphic sequence (in other words metamorphic grade) and rock types. In terms of metamorphism, only the main metamorphic facies were determined based on the literature review whereas more details were inferred from the spectroscopy (Appendix 2). For the rock units where mafic minerals dominate, Mg-OH spectral absorption feature was used whereas for those where felsic minerals dominate, Al-OH spectral absorption feature was used. Fe-OH spectral feature wasn't used because it doesn't cover wide spectral range and not common in all mafic minerals like the Mg-OH spectral feature i.e. the maximum ranges that were observed in this study of Fe-OH and Mg-OH were 20nm and 45nm respectively and thus more variations can be detected in case of Mg-OH, on the other hands, some minerals like hornblende and actinolite don't have Fe-OH spectral features. The general lithological description was obtained from the geological maps (100,000 scale) whilst the rock lithology for each sample was obtained from the Smithies et al. (2007) and Thuss (2005).

4.3.1. Mg-OH and Al-OH Spectral Position Parameters

The spectral position parameters of the Mg-OH and Al-OH absorption features were used to characterise the different lithological units in terms of their mineralogy (Table 4.1). Felsic rocks, mainly in the Panorama and Duffer formations, have mainly Al-OH containing minerals whereas the other intermediate-to-ultramafic rocks have mainly Mg-OH containing minerals. Rhyolite rocks show sericite and pyrophyllite as abundant spectral minerals whilst chlorite (mainly Fe-rich to intermediate) is less abundant. Dacite rocks give the same spectral minerals as rhyolite but with the increase in mafic minerals especially intermediate chlorite which can be found as an abundant spectral mineral (only one sample no. 179747 has hornblende as abundant spectral mineral) and less abundant epidote and hornblende spectral

minerals. All the andesitic rocks show chlorite (mainly as intermediate and less Fe-rich) as an abundant spectral mineral with less abundant sericite, epidote and hornblende. Basaltic rocks give the widest variation in spectral mineralogy where chlorite (Fe-rich through intermediate to Mg-rich) and hornblende form the abundant spectral minerals whereas actinolite, epidote, sericite and prehnite form the less abundant spectral minerals. Komatite and peridotite have Mg-chlorite as an abundant spectral mineral, and actinolite as a less abundant spectral mineral. So, it's clear that the spectral mafic minerals increase with the transition from felsic to mafic rocks. The spectral pyrophyllite mineral in the rhyolite rocks (samples nos. 179897 & 179898 in the Panorama Formation) is due to intense (advanced argillic) hydrothermal alteration. Some rocks may give unexpected spectral minerals such as the dacite sample (no. 179747) which contains hornblende as an abundant spectral mineral and this is because of its location in the transition zone to the amphibolite facies in the Coonterunah Subgroup. Under the microscope, the green hornblende mineral can be found as small crystals in the groundmass and as large crystals with plagioclase filling the vesicles (most likely after gas bubbles), so it seems to have been derived from the groundmass suggesting metamorphic fluids and thus metamorphism rather than hydrothermal alteration. (Figures 4.9 A, B & C). As a good example to the mineralogical variation due to the physical (textural) properties, the dacite sample exhibits higher grade than the neighbour samples and this could be because of its high vesicular texture which makes it more permeable and thus more vulnerable to the attack of the different alteration processes. Other rocks, especially basalt, show different abundant spectral minerals based on the composition i.e. high Mg-basalt and komatitic basalt contain Mg-chlorite or hornblende as abundant spectral minerals whereas tholeiitic basalt contains Fe-chlorite. But sometimes, even for the same rock type, abundant spectral minerals vary according to their stratigraphic location. An example is in the Coonterunah Subgroup, where spectral minerals vary from intermediate chlorite + actinolite to hornblende and Mg-chlorite within the AOt unit (fine to medium-grained metabasalt and amphibolite) (Figure 4.9 D & Appendix 4). These variations in spectral mineralogy can be explained as the effect of several factors at the same time i.e. the rock type in terms of bulk composition, the texture of the rocks (massive impermeable or fractured permeable), the metamorphic grade (in the field, it's related to the stratigraphic position) and hydrothermal processes in terms of temperature, pressure and fluids.

All the samples were displayed in terms of their spectral mineralogy and overlain as a layer on top of the geological maps (Appendix 3). In terms of metamorphic grade, two main metamorphic facies could be identified from the spectral mineralogy, the greenschist and amphibolite facies. Even subdivisions could be made to the greenschist facies based on the presence of epidote, actinolite and hornblende in the spectral mineral assemblages. The transition from less abundant spectral epidote through actinolite to hornblende indicates the increase in metamorphic grade within the greenschist facies whilst the appearance of hornblende as an abundant spectral mineral indicates the transition from greenschist to amphibolite facies (Figure 4.9 D). Most of the hornblende spectral mineral was found within the amphibolite facies and it was also found after mafic-ultramafic rocks that are located at higher stratigraphic position which indicates the lithological effect but fortunately they are few samples. Chlorite minerals can be found in the both metamorphic facies where Fe-to Mg-rich chlorite transition indicates the increase in the metamorphic grade but this is just as a relative estimation and based only on this information we can't know the metamorphic facies, thus the existence of other indicator minerals like epidote, actinolite or hornblende is useful. Mg-chlorite is thought to be related to lithology more than metamorphism because it was found associated to ultramafic rocks and some high Mg-basalt regardless their stratigraphic position whether they're located at the bottom of the stratigraphic sequence or at higher levels, in other words, it's difficult to relate Mg-chlorite to either metamorphic or lithological processes.

For estimation of metamorphic grade, sampling should cover the whole stratigraphic sequence and in a proper way e.g. samples must be taken at proper distances and not only based on the lithological variations as more than one metamorphic grade can be found in one lithological unit. And because the different rock units were sampled for geochemical and lithological, and not metamorphic purposes, not all

of them were completely covered. Thus, only those properly sampled rock units such as the Coonterunah Subgroup, the Apex Basalt Formation and the Euro Basalt Formation exhibit the different metamorphic grades (Figure 4.10 and Appendix 5).

Table 4.1: Summary of the spectral mineralogy based on the position parameter of the main Mg-OH (2310-2360nm) and Al-OH (at ~2200nm) absorption features for the different rock units (* less abundant spectral minerals).

Rock Unit	Spectral Mineralogy	Mg-OH position in nm (min, max, range)	Al-OH position in nm (min, max, range)
Coonterunah Subgroup	Fe-chlorite	2350, 2356, 6	
	IntChlorite	2341, 2349, 8	
	IntChlorite + *epidote	2336, 2340, 4	
	IntChlorite + *actinolite	2330, 2335, 7	
	Hornblende	2322, 2329, 11	
	Mg-chlorite	2311, 2316, 5	
	Illite (only one rhyolite sample, no. 179740)		2199, 2199, 0
North Star Basalt Fm.	IntChlorite	2343, 2345, 2	
	IntChlorite + *epidote	2342, 2342, 0	
	IntChlorite + *hornblende	2324	
Mount Ada Basalt Fm.	IntChlorite	2339, 2342, 3	
	IntChlorite + *hornblende	2328, 2330, 2	
	Mg-chlorite	2322, 2326, 4	
Duffer Fm.	Fe-chlorite	2347, 2353, 6	
	IntChlorite + *epidote	2337, 2344, 7	
	Muscovite		2200, 2201, 1
	Phengite		2211, 2218, 7
Apex Basalt Fm.	Fe-chlorite	2348, 2356, 7	
	IntChlorite	2342, 2348, 6	
	IntChlorite + *epidote	2337, 2342, 5	
	IntChlorite + *hornblende	2325, 2335, 10	
	Hornblende + Mg-chlorite	2318, 2323, 5	
Panorama Fm.	Fe-chlorite	2347, 2351, 4	
	IntChlorite ± *epidote	2339, 2347, 8	
	Muscovite		2205, 2209, 4
	Phengite		2214, 2216, 2
	Pyrophyllite		2167, 2167, 0
Euro Basalt Fm.	Fe-chlorite	2347, 2353, 6	
	IntChlorite + *epidote	2338, 2346, 8	
	IntChlorite + *hornblende + *actinolite	2329, 2337, 8	
	Hornblende + Mg-chlorite + *actinolite	2316, 2326, 10	
Charteris Basalt Fm.	IntChlorite	2341, 2342, 1	
	IntChlorite + *epidote	2336, 2339, 3	

According to Table (4.1), the different metamorphic grades in terms of the position parameter of the main Mg-OH (at ~2335nm) spectral feature and spectral mineralogy of the rock units can be summarized as follows:

- Greenschist metamorphic facies and can be subdivided into three subzones (subfacies) from lower to higher grade: Fe-chlorite (2348-2356nm), intermediate chlorite + epidote (2336-2349nm) and intermediate chlorite + actinolite + hornblende (2324-2336nm).
- Transition zone between the greenschist and amphibolite metamorphic facies (2324-2329nm).
- Amphibolite metamorphic facies and characterized by the presence of hornblende as an abundant spectral mineral (2311-2329nm).

The reason behind using the Mg-OH absorption feature as a main parameter to differentiate between the different metamorphic facies is because of the nature of the rocks in the study area since mafic and less intermediate rocks dominate the lithological units where the main alteration minerals are mafics, subsequently, the Mg-OH absorption feature presents along the whole sequence. The Al-OH absorption feature wasn't used for the determination of the metamorphic grades because only few samples have the Al-OH absorption feature as a main diagnostic feature and this is restricted in the felsic rocks.

Prehnite spectral mineral, which represents the subgreenschist prehnite/pumpellyite metamorphic facies, was found distributing all over the spectral position range of the Mg-OH absorption feature and thus it couldn't spectrally be identified as a separate metamorphic facies.

Because prehnite was spectrally identified in few rock samples, mainly basaltic and less intermediate, in addition they are located in different stratigraphic position, sometimes at the top of the stratigraphic sequence like sample no. 180204 from the Charteris Formation and in other areas at the base of the stratigraphic sequence like sample no. 179759 from the Coonterunah Subgroup, as a consequence the explanation might be difficult. Anyhow a simple explanation could be that; because prehnite (and pumpellyite if presents) is formed under very low-grade metamorphic conditions (also known as subgreenschist facies) thus it's sense to be found at higher position in the stratigraphic sequence associated with other low-grade minerals such as intermediate chlorite (and thus longer Mg-OH absorption feature wavelength), at the same time, it can be formed due to retrograde metamorphism (unlike prograde metamorphism where minerals are formed as a result of the increasing of the grade) and this explains the presence of prehnite at the base of the stratigraphic sequence with high-grade minerals like Mg-chlorite and actinolite minerals (and thus shorter Mg-OH absorption feature wavelength). Based on the spectral position parameter, boundaries between different zones within the greenschist facies are sharp and this can be explained by the appearance of new spectral mineral(s) when transition from zone to zone whereas the boundary between the greenschist and amphibolite facies is interference (transition zone) because the same spectral mineral, i.e. hornblende, is found in the both zones. In addition, it's difficult to separate the Mg-chlorite than the hornblende in terms of absorption position and thus they were given the same spectral range which can be for either amphibolite or ultramafic rocks (Figure 4.10).

It should be noted that the different metamorphic facies were compiled from all the collected samples i.e. samples could be collected from a unit in different greenstone belts, thus it's not necessary to find all the metamorphic facies as in Figure (4.10) for a rock unit in one place.

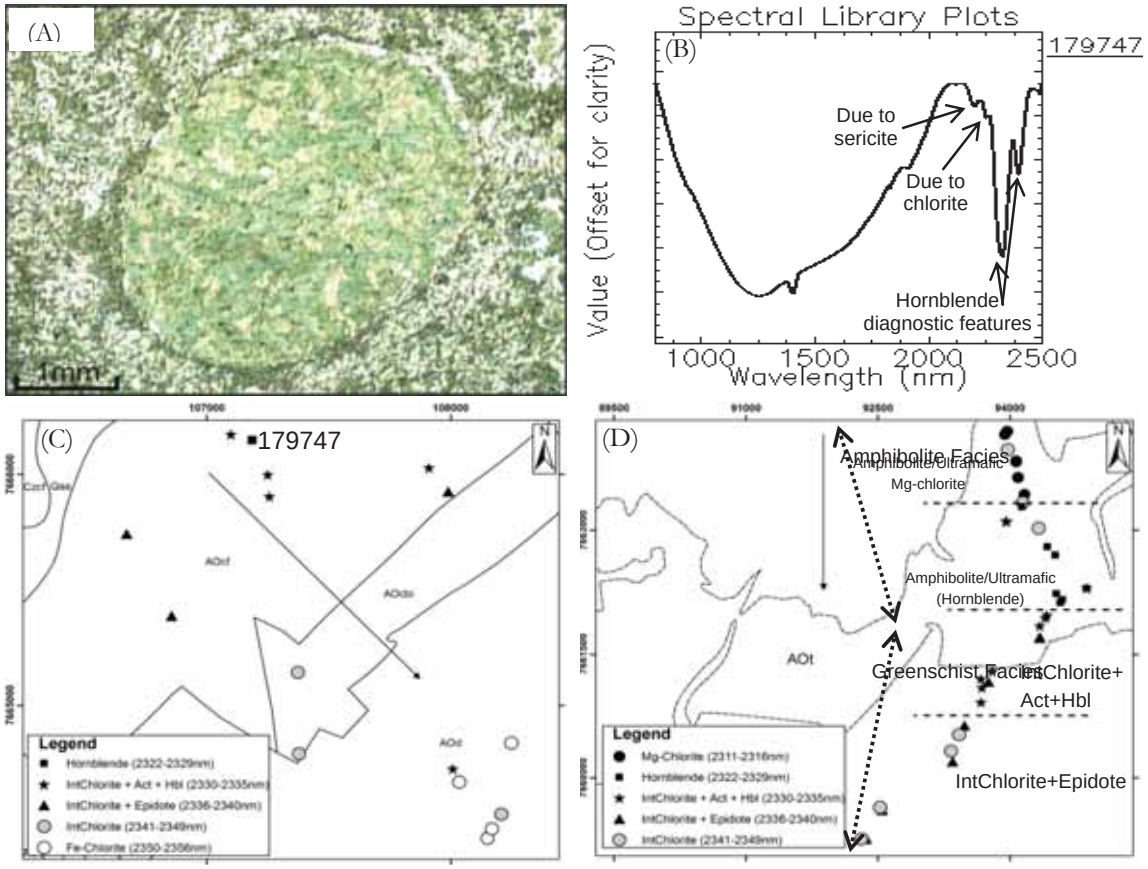

Figure 4.9: (A) Thin section of the dacite sample (no. 179747), studied under the polarized microscope. The field of view is 5.6mm. (B) The spectrum of the same sample indicating abundant hornblende with less abundant chlorite and sericite. (C) The same dacite sample located within the transition zone (collected from the Coonterunah Subgroup-East Strelley greenstone belt). (D) The different metamorphic grades along the Coonterunah Subgroup-East Strelley greenstone belt based on both literature review (dotted lines) and spectroscopy (dashed lines). The area is located to the west of the area in (C). Act. & Hbl.: actinolite and hornblende respectively. Arrows are to younger stratigraphy. For geological maps refer to Appendix 3 and for lithological symbols refer to Appendix 4.

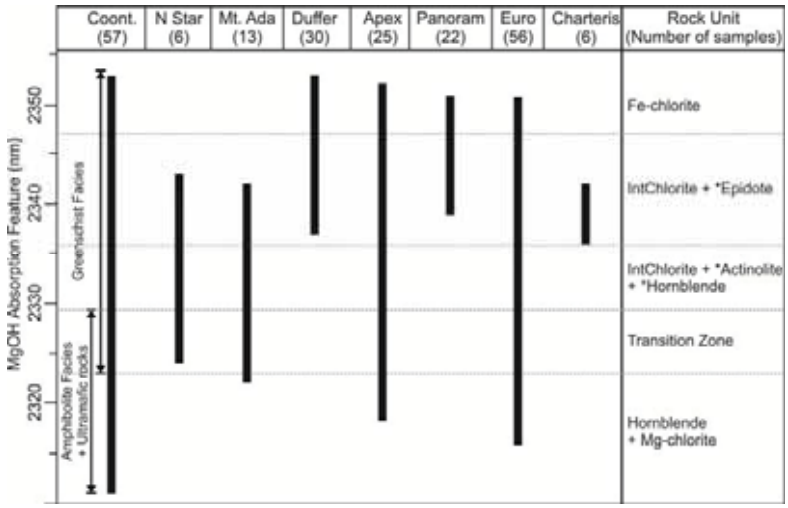

Figure 4.10: The main metamorphic facies for each rock unit based on the literature review (bold lines) and the corresponding spectral position parameter of the Mg-OH absorption feature. Note that based on the spectroscopy, metamorphic subzones can be obtained. Boundaries between spectral minerals were visually outlined at minimum overlap (* less abundant spectral minerals).

4.3.2. Mg-OH and Fe-OH Spectral Depth Parameters for Metamorphic Grade and Relative Alteration Intensity

In this section I will make use of the depth parameters of the secondary Mg-OH (near 2390nm) and main Fe-OH (near 2250nm) absorption features as it was found that this method is useful in the separation between the different spectral minerals (presented in graphs as fields) in terms of the spectral minerals abundance. As a consequence, and because each metamorphic facies is characterised by a certain indicator mineral(s), these spectral mineral fields can be indirectly related to the different metamorphic grades. This method is valid to mafic minerals containing Fe and Mg in their basic structure, although, not all of them show both Mg-OH and Fe-OH absorption features e.g. hornblende and actinolite don't have Fe-OH absorption feature near 2250nm while chlorites and epidote don't have secondary Mg-OH absorption feature near 2390nm. Therefore, and for better comparison, the main and secondary diagnostic Fe-OH (near 2250) and Mg-OH (near 2390nm) absorption features respectively, were used. In other words, if the depth of the Fe-OH absorption feature increases then chlorite abundance increases whereas if the depth of the secondary Mg-OH spectral feature increases then the actinolite and hornblende abundances increase. The advantage of using the depth parameter of these absorption features is the absence of the influence of the sericite and carbonate minerals since they lack the same absorption features in their spectra. Practically, to obtain these depth parameters, one should determine the minimum and maximum wavelengths where the absorption features occur. Simply, intervals can be determined from the histogram provided by the spectral geologist TSG software. The wavelength intervals that were used in this study to extract the depth parameters are summarized in Table (4.2).

Working with the depth parameter needs to be done carefully because mixed spectra strongly affect the depth parameter and can lead to misinterpretation e.g. a spectrum absorption features get shallower if a dark mineral such as magnetite presents even in low quantity whilst an absorption feature depth can get deeper if the coexistence spectral minerals share the same absorption feature.

The depth parameter (which is related to the relative abundance of the spectral minerals) of the main Fe-OH absorption feature near 2250nm versus the secondary Mg-OH absorption feature near 2390nm is useful in the discrimination between the main metamorphic greenschist and amphibolite facies and as described above, this is related to the variation in mineralogy that results in the different spectral mineral fields in scatterplots in Figure (4.11). To explain this, the metamorphic greenschist and amphibolite facies, based on the literature review, were compared with the spectral mineralogy. The results proved that the spectral abundant hornblende is accompanied by the greenschist-amphibolite facies transition (Figure 4.11 A & B). Some rocks, classified according to the previous studies in Figure (4.11 A), overlap the greenschist and amphibolite facies were spectrally found as either Mg-chlorite or as less abundant hornblende and abundant chlorite therefore, they were spectrally assigned to the transition zone which is similar to that in case of the spectral position parameter (Figure 4.10). According to the spectroscopic study, the transition from the greenschist to amphibolite facies was determined by the appearance of hornblende as less abundant mineral with abundant chlorite until it becomes abundant at the expense of the chlorite, epidote and actinolite spectral minerals in the amphibolite facies (Figure 4.11 C). Within the greenschist facies, subzones (abundant intermediate chlorite + less abundant epidote and abundant intermediate chlorite + less abundant actinolite) could be identified based on the presence/absence of epidote that, unlike the actinolite spectral mineral, doesn't have the secondary Mg-OH absorption feature (Figure 4.11 D). As a summary, the transition from abundant chlorite (± epidote spectral mineral) through abundant chlorite + less abundant actinolite and hornblende to abundant hornblende is related to the transition from the metamorphic greenschist, through transition zone to amphibolite facies (Figure 4.11 E). Samples nos. 179707 (metamorphosed at greenschist facies) and 179747 (located within the transition zone) were studied by a polarized microscope. From the petrographic study, the sample no. 179747 was described in Figure (4.9 A) whereas the sample no. 179707 is a lithic tuff and the main alteration minerals are carbonates, chlorite and rare epidote (4.11 F).

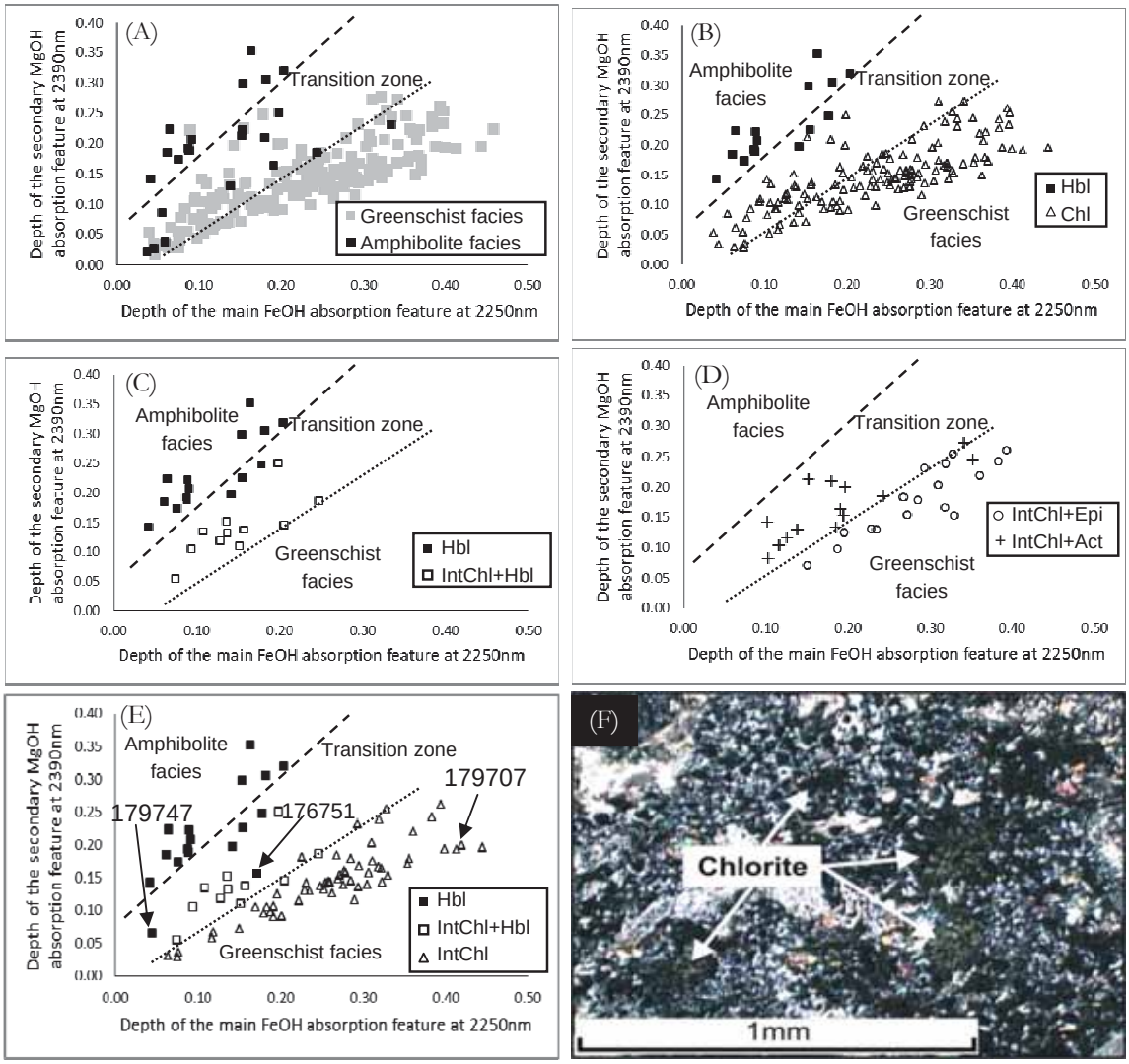

Figure 4.11: The metamorphic facies based on the literature (A) and the corresponding spectral mineralogy (B) based on the depth of the main and secondary Fe-OH and Mg-OH absorption features respectively. (C) Shows the transition zone from the metamorphic greenschist into amphibolite facies. (D) Intermediate chlorite + epidote and intermediate chlorite + actinolite subzones. (E) The transition from the metamorphic greenschist through transition zone to amphibolite facies. (F) Thin section of the intensely altered sample no. 179707 under the polarized microscope (XPL) showing the chlorite mineral in dark colour mainly as cavity filling. The field of view is 1.4mm. (Hbl: hornblende; Chl: chlorite; IntChl: intermediate chlorite; Fe-chl: Fe-chlorite; Epi: epidote; and Act: actinolite).

Regarding the relative alteration intensity, to avoid misestimating we compared between two rocks samples nos. 179747 & 176751 containing nearly the same spectrally detectable alteration minerals, in other words, within the same spectral mineral field (Figure 4.11 E). Sample no. 176751 has deeper absorption features than sample no. 179747 and according to our assumption it must contain higher abundances of alteration minerals which in turn indicate higher degree of alteration. Although sample no. 176751 was collected from a peridotite dyke within an intermediate chlorite + epidote metamorphic zone from the top sequence of the Apex Basalt Formation, it contains higher grade metamorphic minerals (hornblende + intermediate chlorite). Examination by microscope shows that the rock shows high degree of alteration since most of the pyroxene minerals (mainly clinopyroxene) were altered to mainly hornblende and actinolite (as fibrous crystals after pyroxene in a process known as finitization) and less chlorite (Figure 4.12).

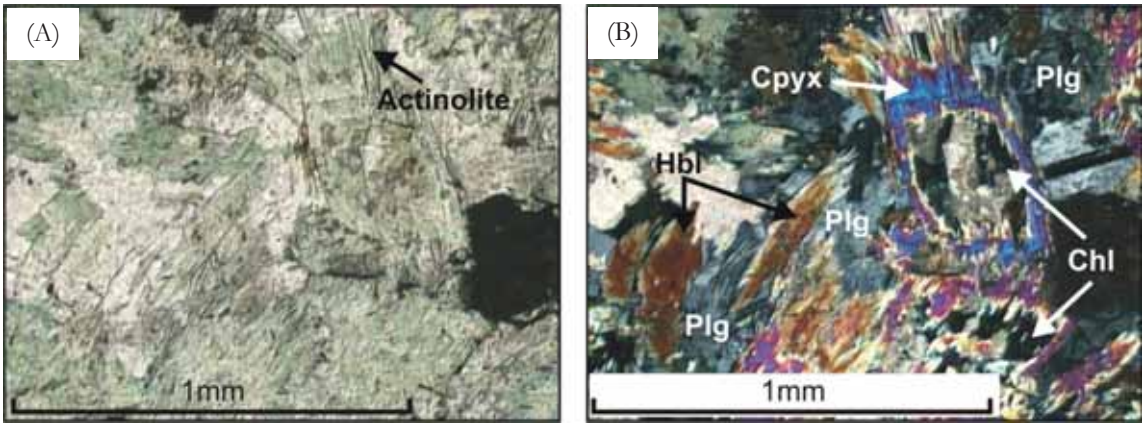

Figure 4.12: Thin section of sample no. 176751 under the polarized microscope. (A) & (B) the same scene taken under the PPL (plane polarized light) and XPL (crossed polarized light) respectively. Cpyx: clinopyroxene; Hbl: hornblende; Chl: chlorite; and Plg: plagioclase.

4.3.3. Al-OH vs. H_2O/OH Spectral Depth Parameter for Relative Alteration Intensity

In this study, the relationship between the depth parameters of the main Al-OH (near 2200nm) and H_2O/OH (near 1400nm) absorption features was found convenient in the discrimination between the intensely altered and the less altered felsic rocks because they both contain mainly felsic alteration minerals which are characterized by the diagnostic Al-OH and H_2O/OH absorption features. It was found that the increase of depths of both absorption features can be related to the abundance of the spectral minerals (proved by the petrographic study). The wavelength intervals of the Al-OH and H_2O/OH that were used to extract the depth parameters are summarized in Table (4.2). The rock samples (six) that were used for this purpose are felsic (rhyolite) in composition and were collected from intensely hydrothermally altered zones from the Panorama Formation. From the geological maps in Appendix 3 and based on the literature review, the Panorama Formation can be found in different greenstone belts and thus different alteration conditions i.e. the Panorama Formation underwent intense hydrothermal alteration in the Panorama and Marble Bar Greenstone belts whereas the formation underwent mainly low-grade metamorphism in the McPhee Greenstone belt. According to this information, a comparison between the intensely altered and the less altered felsic rocks was made (Figure 4.13 A).

Table 4.2: The wavelength (λ) intervals that were used to extract the depth of the different absorption features.

Absorption Feature	Min. λ (nm)	Max. λ (nm)
H_2O/OH (~1400nm)	1380	1420
main Al-OH (~2200nm)	2160	2230
main FgOH (~2250nm)	2238	2262
secondary Mg-OH (~2390nm)	2382	2404

From the Figure (4.13 A), it is clear that the alteration minerals are located and clustered into two groups where the six felsic rock samples that underwent intense hydrothermal alteration could be distinguished from the less altered felsic rocks. The gap between these clusters is thought to be due to the insufficient number of the felsic samples of intermediate alteration intensities. Samples nos. 176757 and 179721 were studied by a polarized microscope and showed intense alteration where most of the primary minerals were altered to secondary minerals (for explanation see Figure 4.4 A & B; and Appendix 1). Sample no. 179713 was compared with the sample no. 176757 in order to explain the usefulness of the depth parameter in the semi quantitative estimation of the spectral mineral abundance (Figure 4.13 B, C & D). The petrographic study of the sample no. 179713 showed that the chlorite is mainly formed along fractures and as cavity filling whereas the sericite (spectrally identified as phengite) was formed after plagioclase phenocrysts (slightly altered) and the groundmass. The comparison between the both samples emphasised the

relationship between the abundance of minerals and their absorption features depth i.e. the absorption features (especially the Al-OH and H_2O/OH absorption features near 1400nm and 2200nm respectively) in sample no. 176757 are deeper than that in sample no. 179713 and this is can be directly related to the sericite minerals abundance which is higher in the sample no. 176757.

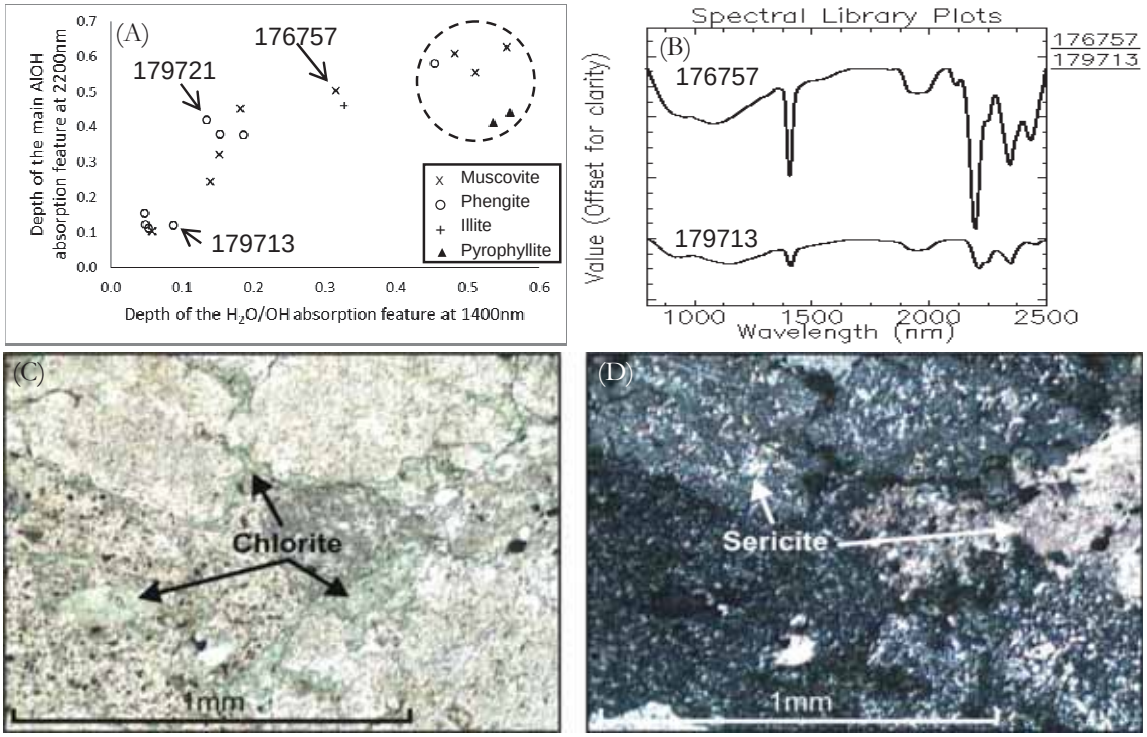

Figure 4.13: (A) The discrimination between intensely altered (inside the dashed circle) and less altered felsic rocks based on the main Al-OH and H_2O/OH absorption features depth parameter. (B) The spectra of two samples, referred in (A), differ in sericite abundance. (C) & (D) The same view of the petrographic study of sample no. 179713 under the polarized microscope showing chlorite and sericite minerals under the PPL (plane polarized light) and XPL (crossed polarized light) respectively. The field of view is 1.4mm.

4.4. Major Elements Lithogeochemistry

4.4.1. Exploratory Data Analysis (EDA)

The major elements geochemical dataset was inspected before it was used for lithological and alteration interpretations (Appendix 6). The average, mode median and geometric mean are very similar for most elements indicating normal distributions and therefore didn't need to be transformed (Table 4.3). Since the major elements are compositional (closed) data they were opened using the centered log-ratio transformation (clr) method (Filzmoser et al., 2010). The results showed no significant differences before and after applying the centered log-ratio transformtion thus the raw major elements data was adopted for this study.

Table 4.3: Summary statistics for the major elements expressed as oxides (* total iron).

	SiO_2	TiO_2	Al_2O_3	FeO	Fe_2O_3*	MnO	MgO	CaO	Na_2O	K_2O	P_2O_5
Max.	71.25	2.81	18.94	15.30	19.51	0.44	31.99	14.26	6.10	3.38	0.56
Min.	41.49	0.19	4.41	1.09	1.78	0.05	0.85	1.57	0.01	0.01	0.02
Average	51.45	0.97	13.56	7.11	11.33	0.19	6.87	8.54	2.59	0.48	0.12
Mode	52.60	1.06	13.71	9.37	15.37	0.19	3.17	6.86	3.98	0.02	0.08
Median	50.50	0.94	14.07	6.60	11.49	0.19	6.04	8.73	2.57	0.28	0.11
Mean	51.19	0.87	13.25	6.58	10.75	0.18	5.70	7.98	2.00	0.22	0.10

4.4.2. Major Elements for Lithology Discrimination

The major elements were used to differentiate between the different rock types after excluding the intensely altered rocks (determined by the alteration indices method in section 4.4.3). The intensely altered rock samples are felsic rocks (six rhyolitic and one dacitic rocks) and only one of intermediate andesitic composition where the spectral minerals are sericite and pyrophyllite, and intermediate chlorite + epidote respectively.

Mole proportions for the major elements expressed as oxides were found to better separate the different rock types than the original weight percentages. The correlation between the major oxides (as mole proportions) was calculated (Table 4.4). The positively correlated major oxides against the negatively correlated major oxides were used to interpret the different rock lithologies. Different elements combinations were made in order to find the best elements combination until the final best-describing combination of the correlated TiO_2, MgO, FeO and CaO major oxides (as mole proportions) and the correlated SiO_2 and K_2O major oxides (as mole proportions) was set. This combination of the major elements mole proportions was named "lithological index" and is the proportion of the summation of the mole proportions of TiO_2, MgO, FeO and CaO represented in the numerator to the same major elements plus the summation of the mole proportions of SiO_2 and K_2O major oxides represented in the denominator.

In order to study the relationship between the spectral mineralogy and the different volcanic rock types, the spectral mineralogy was compared with the lithological index (Figure 4.14). Based on the main Mg-OH absorption feature near 2335nm, the results showed that the spectral minerals are not controlled by volcanic lithological composition (but rather reflect the different metamorphic grades) as some spectral minerals (especially the intermediate chlorite and epidote spectral minerals that dominate the study area) overlap the different lithologies (Figure 4.15). In case of felsic rhyolitic and ultramafic rocks, the spectral minerals reflect strongly the lithology whereas in other rock types the spectral minerals reflect strongly the metamorphic grade.

Table 4.4: Correlation matrix of the major oxides (as mole proportion).

	SiO_2	TiO_2	Al_2O_3	FeO	Fe_2O_3t	MnO	MgO	CaO	Na_2O	K_2O	P_2O_5
SiO_2	1.00										
TiO_2	-0.37	1.00									
Al_2O_3	0.39	0.11	1.00								
FeO	-0.70	0.71	-0.22	1.00							
Fe_2O_3t	-0.80	0.68	-0.33	0.91	1.00						
MnO	-0.67	0.44	-0.29	0.67	0.76	1.00					
MgO	-0.53	-0.29	-0.74	0.15	0.28	0.21	1.00				
CaO	-0.58	0.04	-0.21	0.32	0.45	0.63	0.21	1.00			
Na_2O	0.51	0.02	0.53	-0.31	-0.44	-0.39	-0.59	-0.44	1.00		
K_2O	0.71	-0.20	0.32	-0.53	-0.62	-0.51	-0.47	-0.50	0.27	1.00	
P_2O_5	0.19	0.58	0.41	0.17	0.03	-0.01	-0.51	-0.34	0.39	0.23	1.00

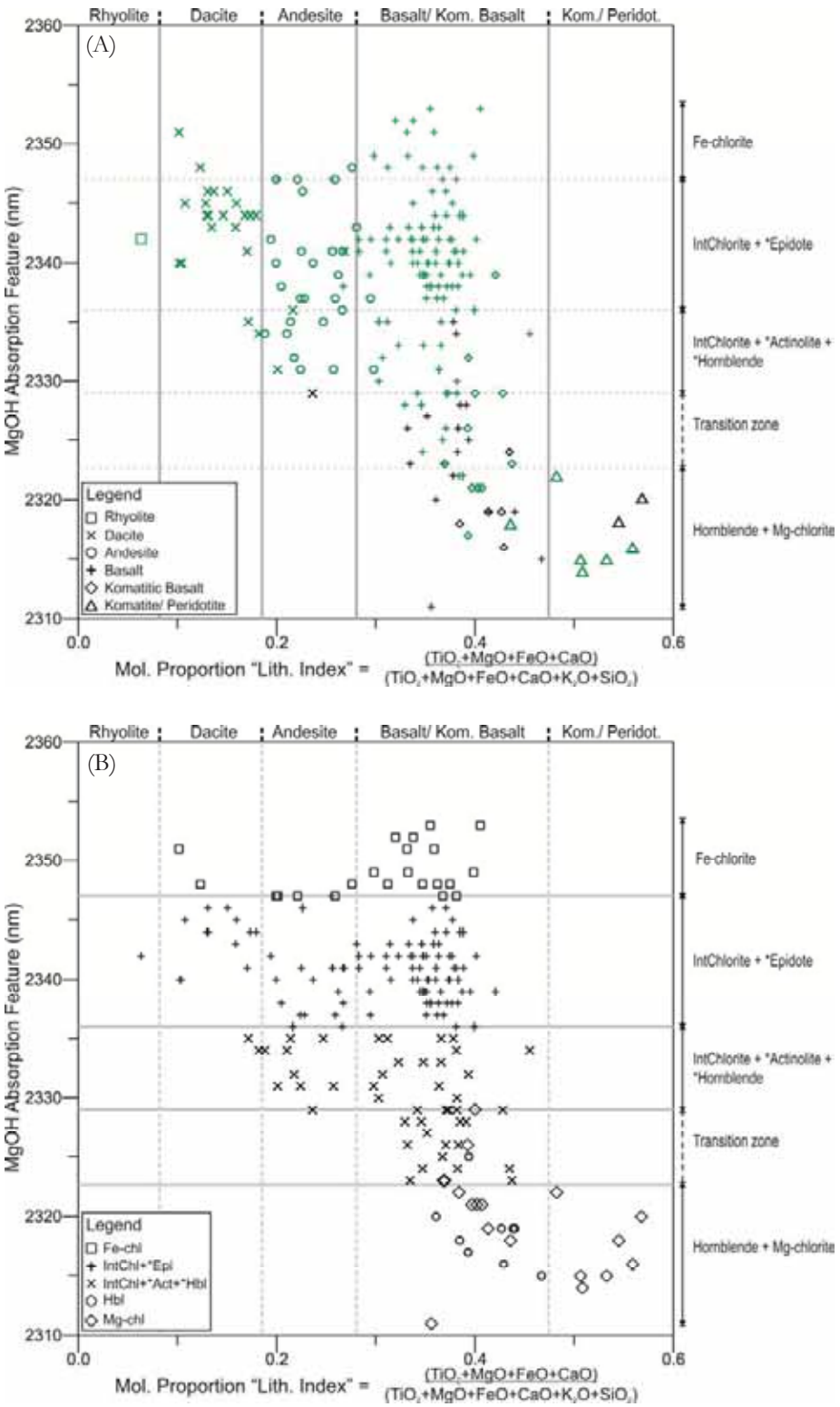

Figure 4.14: Scatter plot of the samples showing the lithological index (Lith. Index) and the spectral minerals (in terms of the main Mg-OH absorption feature near 2335nm) of the samples represented as reported-classification lithology (A) and spectral minerals (B). The green and black samples are at greenschist and amphibolite metamorphism based on the literature review. (*less abundant spectral minerals)

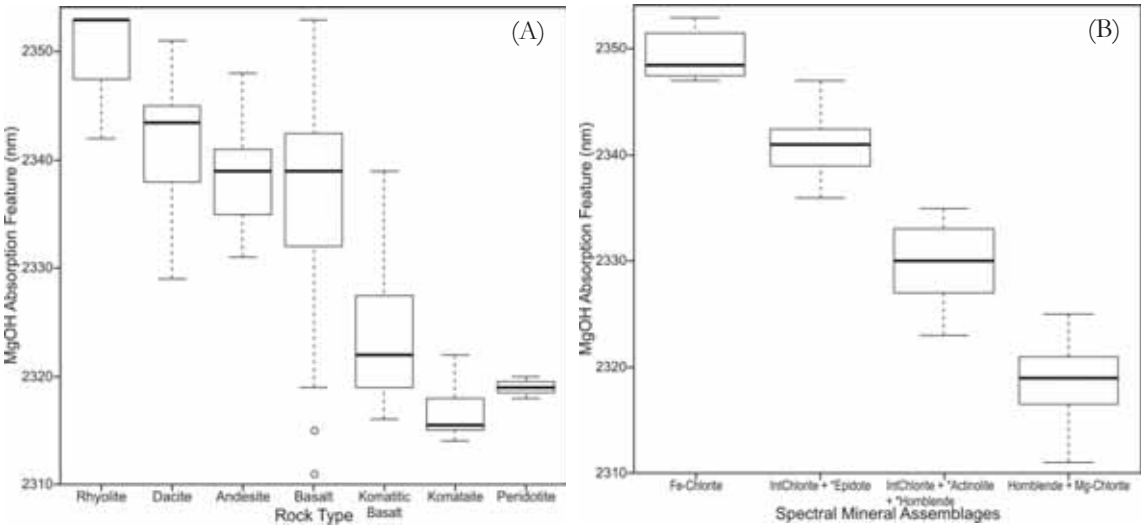

Figure 4.15: Univariate box plots showing the samples in terms of lithology (A) and metamorphic grades (B) based on the main Mg-OH absorption feature near 2335nm.

4.4.3. Alteration Box Plots

In this section alteration box plots were used to identify the intensely altered rocks. The relative alteration intensity was compared with the spectroscopic depth parameter method. As mentioned in the literature review, alteration in the study area was either isochemical due to the low-grade metamorphism which is considered as a background alteration in this study, or metasomatic due to hydrothermal alteration. Both processes can result in the same alteration minerals e.g. in case of felsic rocks the sericite minerals are resulted by either processes. Based on the spectral position parameter method, both processes can be detected (since both processes result in detectable spectral minerals) but cannot be differentiated (as isochemical or metasomatic) whereas in case of the spectral depth parameter method (since the relative alteration intensity can be estimated) if the background alteration is determined then it becomes easy to distinguish it from the intensely hydrothermal alteration process. This separation might not be possible in case of lower degree of hydrothermal alteration because we need a contrast between the alteration intensities. The whole-rock major elements geochemistry (represented by the alteration box plot) can detect metasomatic alteration even in low intensities as long as chemistry changes but it can't detect the isochemical alteration since the chemistry of the rocks doesn't change. As a summary, the spectroscopic method has the advantage in detecting both processes in addition to the possibility of estimation the relative alteration intensity which can be used to locate the mineralization whereas the whole-rock major elements lithogeochemistry has the advantage of determining the lower degree metasomatic alteration.

From the alteration box plot in Figure (4.16), eight rock samples were interpreted as metasomatically altered (by hydrothermal alteration process) whereas the remaining samples were considered as least altered even the mafic and ultramafic rocks that are located outside the least altered box due to the typical composition of these rocks where chlorite is the main alteration mineral (Figure 4.16 A & B). Unfortunately and unlike felsic rocks, the sample set doesn't contain any known hydrothermally altered mafic rocks in order to test the usability of the alteration box plot. As a consequence and unlike the spectroscopic method, it's difficult to determine the metamorphic grade based on the alteration box plot. On the other hand, this method was found useful in determining the metasomatic alteration of felsic and intermediate rocks where the general alteration styles (based on the trend of the samples and according to the standard alteration minerals at the boundary) are sericitization and potassic alteration (K-feldspar). The six felsic rhyolitic rocks could be separated by both the alteration box plot and the spectral depth parameter of the main Al-OH (near 2200nm) and H_2O/OH (near 1400nm) absorption features and based on this comparison the boundary between the metamorphosed and hydrothermally altered rocks was

roughly made (Figure 4.16 C). The dacitic sample (no. 179872) wasn't recognized as hydrothermally altered rocks by the spectral depth parameter method and the reason could be due to low degree of metasomatic alteration, or due to chlorite presence, or due to the style of K-alteration where the main alteration mineral is K-feldspar, which is undetectable by the near-infrared spectroscopy (Figure 4.16 C). Since the differentiation between the metasomatic and metamorphic processes has not been studied yet in case of the spectral depth parameter of the main and secondary Fe-OH (near 2250nm) and Mg-OH (near 2390nm) absorption features, no further discussion was made on the andesitic sample no. 179719. Nevertheless its relative alteration intensity is considered as high based on the depth parameter (Figure 4.16 D).

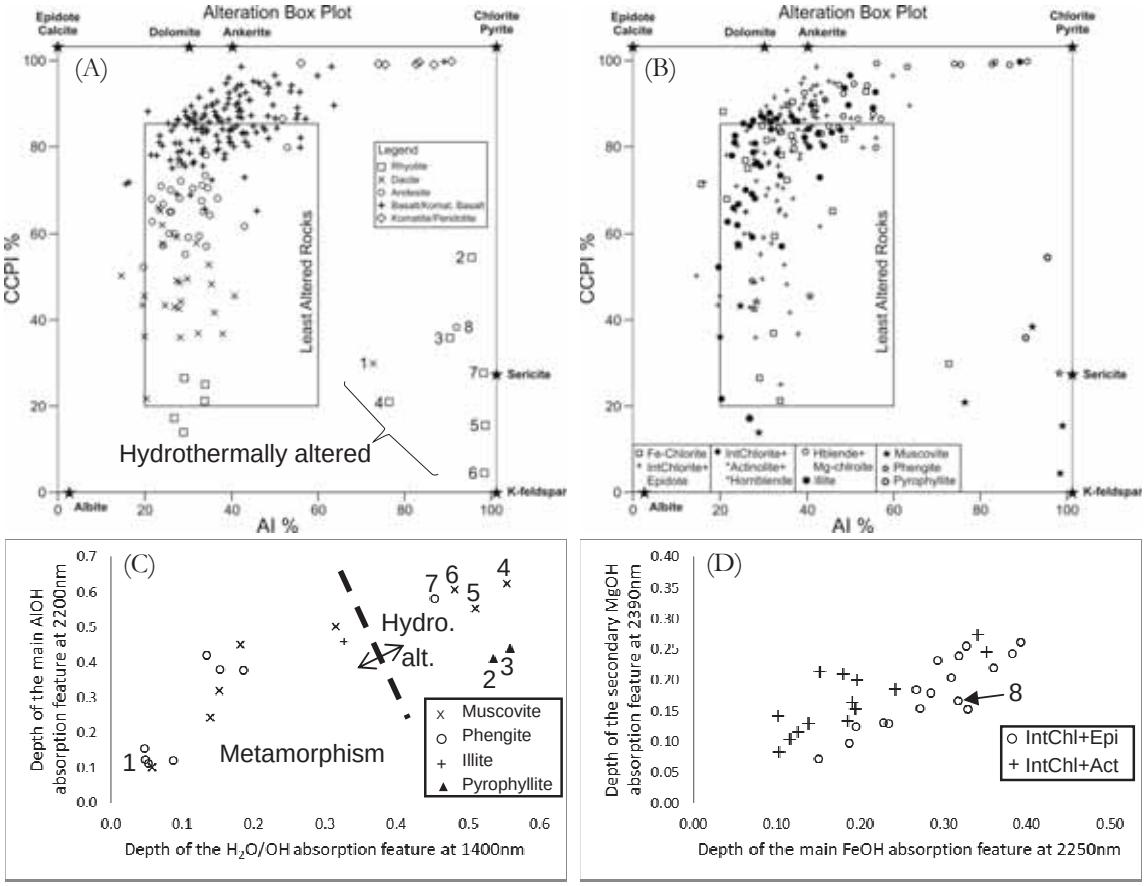

Figure 4.16: The alteration box plot of the samples represented as lithology (A)and spectral mineralogy (B) comparing to the depth parameter of the main Al-OH (near 2200nm) and H_2O/OH (near 1400nm) absorption features (C) and the secondary Fe-OH (near 2250nm) and Mg-OH (near 2390nm) absorption features (D). 1: 179872; 2: 179897; 3: 179898; 4: 179899; 5: 180223; 6: 180224; 7: 180225; 8: 179719.

5. SUMMARY AND CONCLUSIONS

Near-infrared reflectance spectra (350-2500nm) of the different volcanic rocks ranging in composition from ultramafic to felsic rocks from the East Pilbara Granite-Greenstone Terrane were measured, by an ASD Fieldspec Pro spectrometer, and interpreted. These rocks are metamorphosed at low-grade greenschist to amphibolite facies. Some samples (seven felsic rocks and one of andesitic composition) are intensely hydrothermally altered. Detectable abundant spectral minerals that were identified from the different volcanic rocks are chlorite (Fe-chlorite, intermediate and Mg-chlorite), amphiboles (hornblende and actinolite), white mica (illite, paragonite, muscovite and phengite), prehnite and pyrophyllite. The study shows that the spectral characteristics of the different low-grade metamorphosed volcanic rocks represent metamorphic grade rather than lithology. Hornblende can be related to either metamorphism or lithology. Abundant Mg-chlorite, and sericite and pyrophyllite are related to lithological composition i.e. ultramafic and high Mg-content basalt, and felsic rocks respectively.

The spectral position parameter of the main Mg-OH absorption feature (2310-2360nm) was used to characterize the different volcanic rocks in terms of metamorphic grade. Three metamorphic subfacies within the greenschist facies could be determined based on the detectable spectral minerals assemblages such as Fe-chlorite; intermediate chlorite + epidote; and intermediate chlorite + actinolite and hornblende, in addition to the amphibolite facies. In comparison with the previous studies, only greenschist and amphibolite facies were determined based on the conventional methods. Boundaries between the greenschist subfacies are sharp due to appearance of new spectral minerals such as epidote and actinolite whereas the boundary between greenschist and amphibolite facies is transitional due to the increase of hornblende spectral mineral abundance. Prehnite-pumpellyite metamorphic facies, as well as the carbonates, couldn't be detected based on the main Mg-OH (2310-2360nm) absorption feature. Basaltic rocks were found containing any of these spectral minerals therefore they are the most suitable in the characterization of the different metamorphic grades. The spatial distribution of the spectral minerals is conformable with the stratigraphic sequence i.e. the spectral minerals grade increases with depth in the volcanic sequence, in other words, with proximity to granitoid complexes.

The spectral position parameter of the main Al-OH absorption feature (near 2200nm) was used to characterize the intensely altered rocks where sericite and pyrophyllite are the abundant spectral minerals.

The spectral depth parameters of the main and secondary Fe-OH (near 2250nm) and Mg-OH (near 2390nm) absorption features, respectively, were used to estimate the relative abundance of the alteration minerals and thus the relative alteration intensity of the different low-grade metamorphosed volcanic rocks, as well as the different metamorphic grades.

The spectral depth parameter of the main Al-OH (near 2200nm) and H_2O/OH (near 1400nm) absorption features, in the absence of any Mg-OH spectral minerals influence, was found useful in the separation between metamorphic and hydrothermal alteration processes in case of rhyolitic rocks.

Major elements lithogeochemistry was used to determine lithology, relative alteration intensity and metasomatism but not the metamorphic grade. In addition, it can discriminate between the background (diagenetic and metamorphic isochemical alteration) and hydrothermal (metasomatic) alteration processes in case of rhyolitic rocks.

As a conclusion, the integration between the near-infrared spectroscopy and major elements lithogeochemistry is useful to characterise the low-grade metamorphosed volcanic rocks in the East Pilbara Granite-Greenstone Terrane (EP) in terms of lithology, relative alteration intensity and metamorphic grade in addition to the type of alteration in case of rhyolitic rocks.

5.1. Recommendations

Based on the results of this study, the following recommendations are made:

- Spectroscopy was found useful in determination different metamorphic grades and major elements lithogeochemistry was found useful in discriminating different volcanic lithologies therefore it's recommended to integrate both methods to study low-grade metamorphosed volcanic rocks.
- Prehnite-pumpellyite metamorphosed volcanic rocks are recommended to be studied by the near-infrared method to test its applicability.
- Intensely altered volcanic rocks (i.e. metasomatically altered rocks from the VMS footwalls and discharge zones) must be collected to test the usability of the spectral depth parameter of the main and secondary Fe-OH (near 2250nm) and Mg-OH (near 2390nm) absorption features in the separation between background (diagenetic and metamorphic) and hydrothermal (metasomatic) alteration processes.
- Hyperspectral imaging of rock slabs together with the petrographic study of thin sections is recommended to further study quantification of the estimated mineralogy.
- Near-infrared method is recommended to be applied on a spaceborne/airborne imagery scale as long as the different metamorphic facies have distinct spectral mineral assemblages and considerable dimensions and this requires a preliminary study of weathering surfaces since this study was done on fresh surfaces.

APPENDICES

Appendix 1: Petrographic study of nine samples collected from different lithological units.

Sample No.	Lithology	Petrographic Description		Spectral Minerals
		Primary Minerals	Secondary Minerals	
176751	Peridotite	Plagioclase: partly altered to calcite, epidote and chlorite. Pyroxene: mostly clinopyroxene with fibrous amphibole (?) at the edges due to fenitization; moderately altered to chlorite and carbonates.	Amphibole (mainly hornblende and less actinolite?): mainly as acicular and fibrous (after the alteration of pyroxenes especially at the edges of the minerals), and difficult to distinguish. Chlorite, carbonates and epidote: mainly after clinopyroxene and plagioclase.	Abundant hornblende and less abundant IntChlorite
176757	Rhyolite	Plagioclase: phenocrysts were completely altered to sericite. Quartz: distributed mainly as individuals and less as clusters. Biotite: moderately altered to chlorite. Groundmass: intensely altered to sericite; contains rock fragments (pyroclastics); cross-cut by veinlets filled by sericite.	Sericite: mainly after plagioclase. Chlorite: after biotite. Quartz: rounded filling cavities.	Abundant muscovite and less abundant IntChlorite
179707	Andesite (lithic tuff)	Plagioclase: moderately altered to carbonate (calcite?) and epidote; tiny crystals exhibit flow texture. Groundmass: very fine-grained and seems to be slightly altered due to dark and dirty look material (carbonates?). Rock fragments and pyroclastics: mainly pyroclastics; vesicular or amygdaloidal due to quartz, carbonates and chlorite; porphyritic or amorphous; moderately altered.	Carbonates: mainly after plagioclase; also as cavity and veinlets filling. Chlorite: mostly as cavity and veinlets filling. Epidote: very rare in some cavities and veinlets and within some plagioclase. Sericite: very rare in some cavities and veinlets.	Abundant IntChlorite
179721	Dacite	Plagioclase: phenocrysts were intensely altered to sericite and less carbonates. Quartz: mainly as groundmass and less as phenocrysts. Biotite: completely altered to brownish iron-oxides and less epidote.	Sericite: ranges from fine- to coarse-grained; mostly after plagioclase. Carbonates: found as common after plagioclase and filling cavities. Chlorite: rare mainly around some plagioclase crystals and rock fragments, and less in cavities. Epidote: very rare in cavities and after biotite.	Abundant phengite and less abundant IntChlorite (v. rare)

Continue

179713	Dacite	Plagioclase: large phenocrysts are partly altered to sericite and less carbonates whereas smaller phenocrysts (as laths) were completely altered to sericite and less carbonates. Quartz: mainly as groundmass and less as phenocrysts. Groundmass: very fine-grained and seems to be slightly altered to sericite and carbonates; tiny plagioclase crystals show flow texture.	Sericite: dominant after plagioclase. Chlorite: mainly in cavities and cracks. Carbonates: after plagioclase. Quartz: small crystals as cavity filling.	Abundant phengite and less abundant IntChlorite
179736	Kom. Bas	Pyroxene: mostly spinifex orthopyroxene and less clinopyroxene minerals (they show clear twinning due to intergrowth); slightly altered to chlorite. Plagioclase: small laths partly altered to chlorite. Olivine: completely replaced by pseudomorphs quartz in the middle and chlorite at the rims.	Quartz: as cavity fillings and after olivine. Chlorite: mainly as cavity filling and after olivine and pyroxenes.	Abundant Mg-chlorite and less abundant IntChlorite
179719	Andesite	Plagioclase; large phenocrysts; moderately altered to chlorite, dark fine-grained material (carbonates?) and less epidote. Mafics: difficult to distinguish as they completely altered to chlorite, carbonates and epidote. Quartz: small crystals distributed all over the scene. Groundmass: very fine-grained; altered to chlorite; rich in epidote.	Chlorite: mainly after plagioclase. Epidote: mostly in the groundmass after plagioclase and mafics and in cavities. Carbonates: rare mostly after mafics and less plagioclase.	Abundant IntChlorite and less abundant epidote
179747	Dacite	Plagioclase: phenocrysts were partly altered to carbonates, less epidote and chlorite. Hornblende: mainly fine-grained and less altered phenocrysts (mostly after devitrification of the groundmass); some shows brownish staining of iron-oxides indicating the Fe content. Quartz: fine-grained crystals (due to devitrification?). Groundmass: mostly devitrified.	Hornblende: large crystals mainly as cavity filling. Chlorite: found in the groundmass and less in cavities. Epidote: sparse within plagioclase. Carbonates: found either as naked crystals or dirty look that cover (mainly plagioclase) surfaces. Sericite: mainly in cavities. Quartz: mainly in cavities.	Abundant Mg-chlorite and less abundant hornblende, IntChlorite, epidote, and muscovite
176800	Basalt	Plagioclase: phenocrysts were partly altered to very fine-grained material (carbonates?), chlorite and rare epidote. Mafics: completely altered to carbonates and chlorite; most likely pyroxenes and some hornblende (remains).	Carbonates: abundant after mainly mafics and less plagioclase. Chlorite: mainly after mafics and less after plagioclase. Epidote: very rare after plagioclase.	Abundant IntChlorite and less abundant epidote

Appendix 2: The database including the samples and their attributes were provided in an Excel spread sheet and copied in a CD attached to this thesis report.

Appendix 3: Geological maps of the different rock units in different greenstone belts showing the collected samples in terms of spectral mineralogy and position parameter. Mafic and felsic minerals were represented based on the Mg-OH and Al-OH spectral features respectively. Numbers of samples that used for petrographic study were shown on the maps and thus can be referred to Appendix 1. The arrows direction is towards the younger stratigraphy.

- **Coonterunah Subgroup**

East Strelley Greenstone Belt

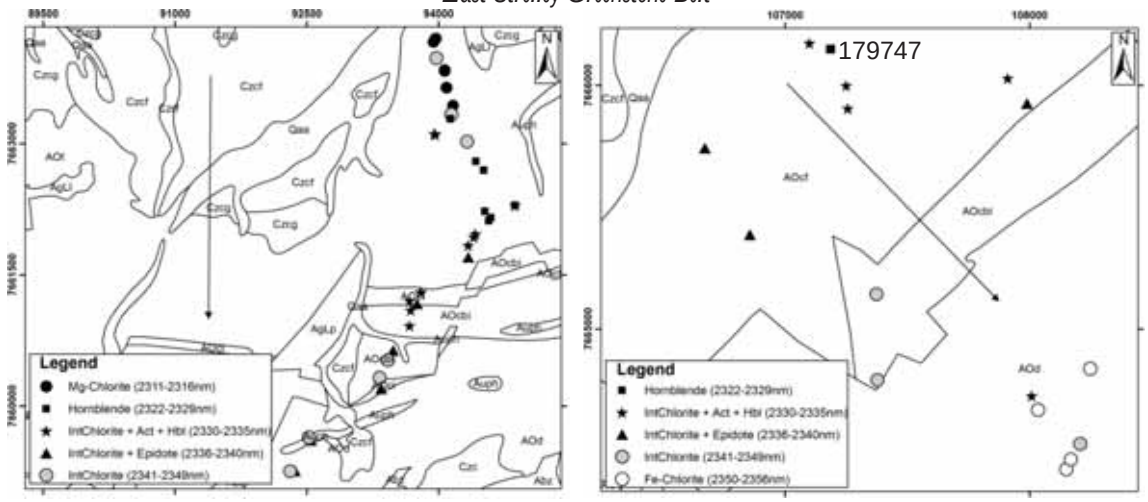

AOcbi (meta. andesitic to basaltic pillowed and massive, associated with intrusive sills); AOcf (meta. felsic volcanic rocks, local felsic agglomerate); AOd (meta. massive tholeiitic basalt, locally pillowed and schistose); AOci (meta. cherty banded iron-formation, black and white, and rarely red layered); AOt (fine to medium-grained metabasalt and amphibolite); and Auph (meta. harzburgite, medium to coarse-grained).

- **North Star Basalt Formation**

Marble Bar Greenstone Belt

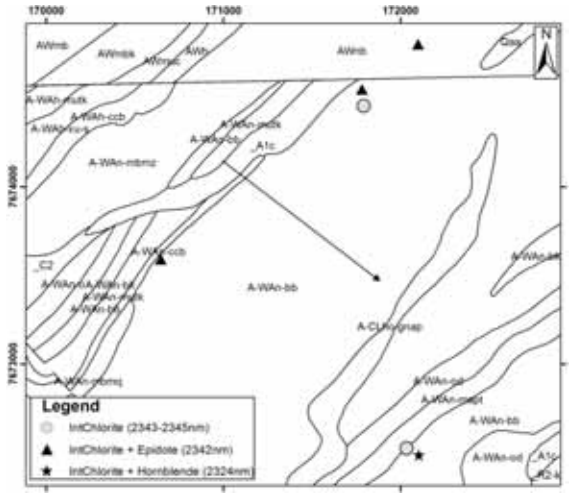

AWnb and A-Wan-bb (meta. basalt, generally massive, includes syn-volcanic dolerite intrusions, locally schistose).

- **Mount Ada Basalt Formation**

Marble Bar Greenstone Belt *Warralong Greenstone Belt*

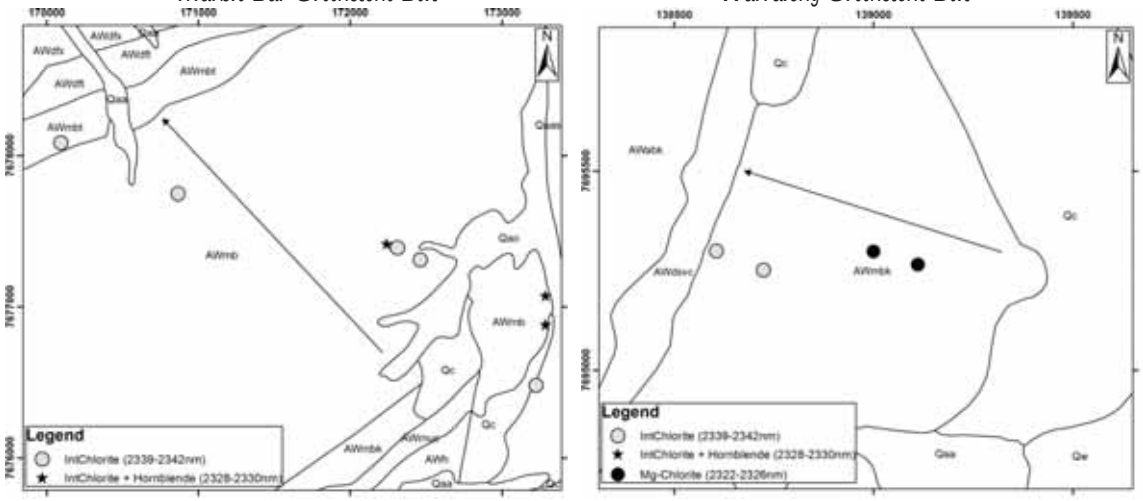

Qc (colluvium sand, silt and gracvel); AWmb (meta. basalt, includes local syn-volcanic dolerite intrusions); AWmbt (weakly metamorphosed mafic to felsic tuff, medium to fine-grained); and AWmbk (weakly metamorphosed komatitic basalt, commonly pillowed, with pyroxene spinifex texture).

- **Duffer Formation**

Marble Bar Greenstone Belt

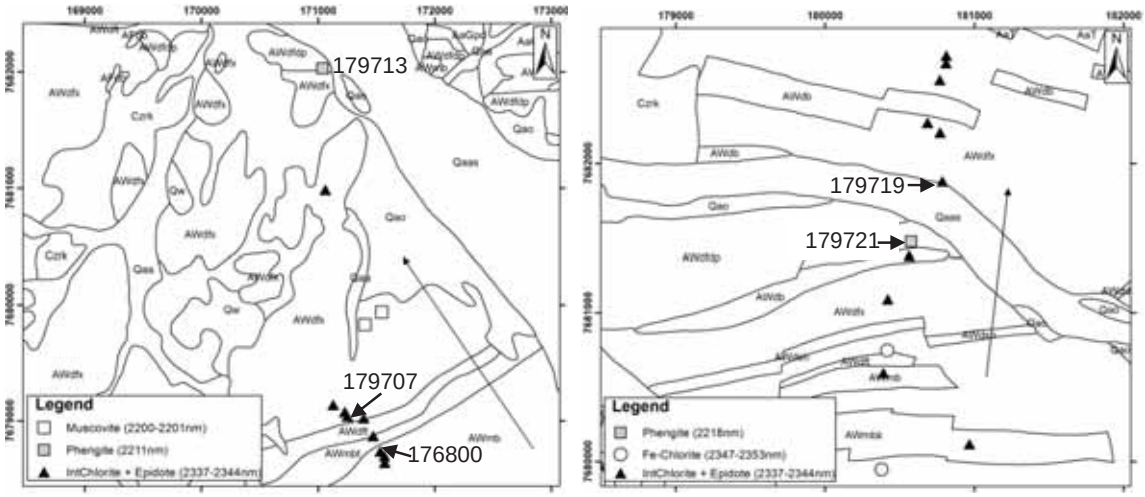

AWdfdp (weakly metamorphosed massive medium-grained feldspar porphyritic andesite to dacite); AWdfx (weakly metamorphosed coarse to fine-grained dacitic to andesitic, lithic volcaniclastic breccia and conglomerate); AWdb (weakly metamorphosed pillowed basalt); AWmb (meta. basalt, undivided, includes local syn-volcanic dolerite intrusions); AWmbk (weakly metamorphosed komatitic basalt, commonly pillowed, with pyroxene spinifex texture); and AWmbt (weakly metamorphosed mafic to felsic tuff, medium to fine-grained).

- **Apex Basalt Formation**

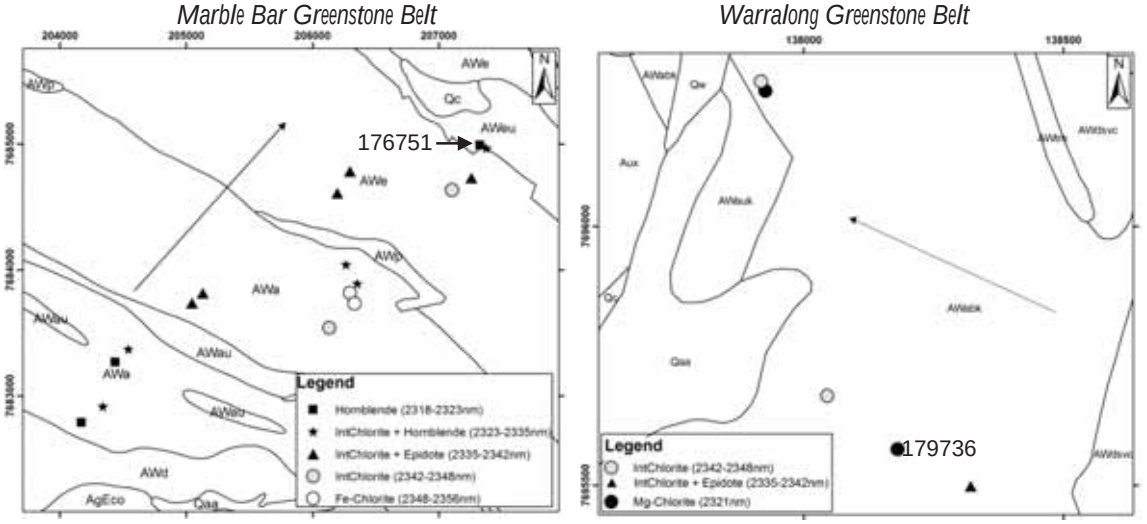

AWa (meta. massive and pillowed basalt, high Mg-basalt, and thin intercalated chert); AWe (meta. basalt, pillowed basalt, high Mg-basalt, and intercalated thin thin-bedded chert); and AWeu (talc-chlorite schist (mylonitic fabric), pods of altered komatitic basalt).

- **Panorama Formation**

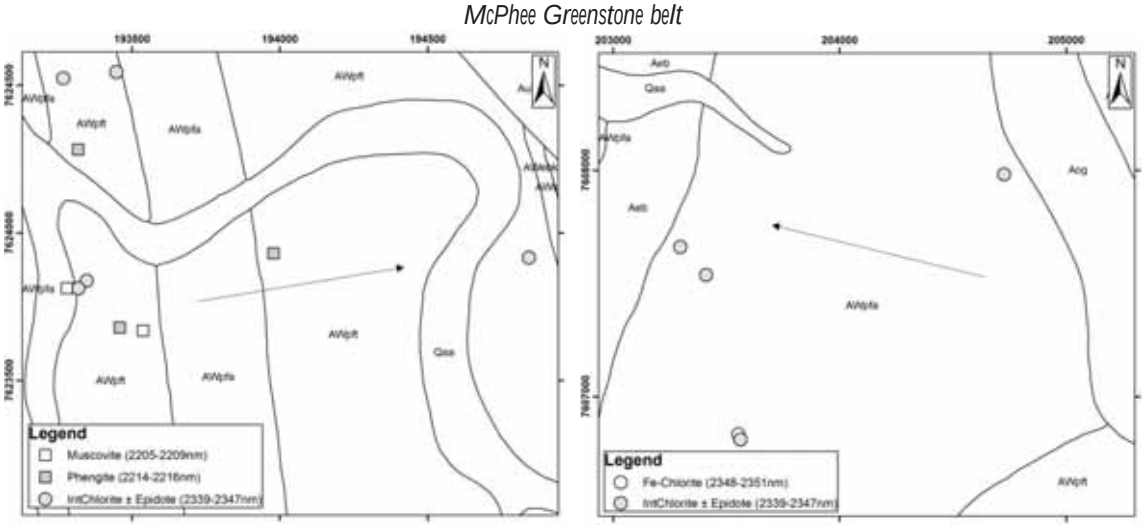

Qaa (alluvial sand and gravel in rivers and creeks, clay, silt and sand in channels on floodplains); AWpft (weakly metamorphosed felsic tuff and minor felsic agglomerate and andesitic basalt, locally silicified); and AWpfa (weakly metamorphosed felsic agglomerate and minor felsic tuff and andesitic basalt, locally silicified).

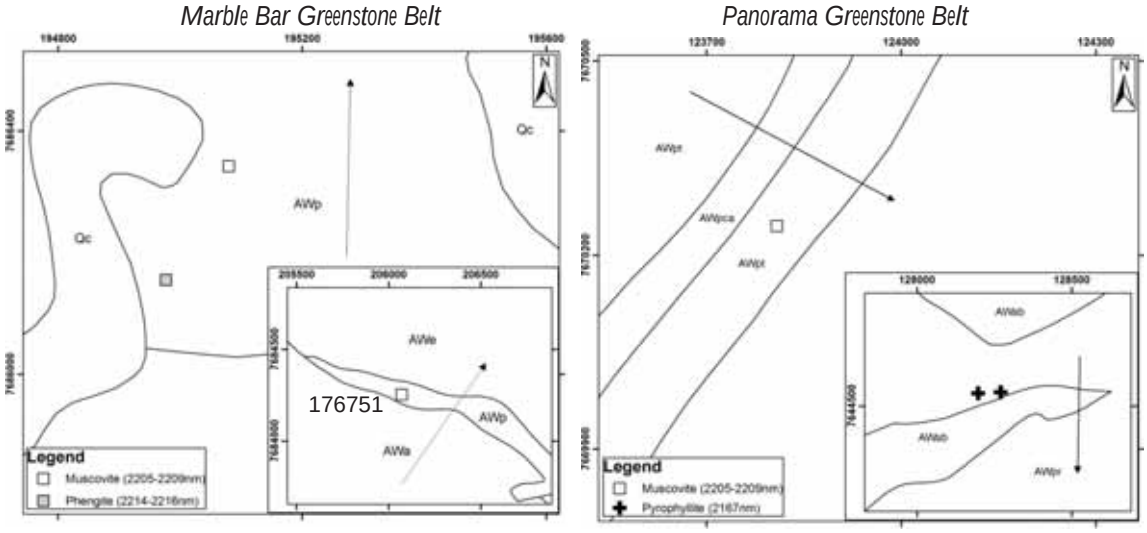

AWp (meta. felsic volcanic rocks, mainly rhyolitic, quartz-feldspar porphyry and felsic tuff); and AWpt (meta. fine-grained felsic tuff and local coarse agglomerate, locally silicified); and AWpr (meta. rhyolite and felsic schist).

- **Euro Basalt Formation**

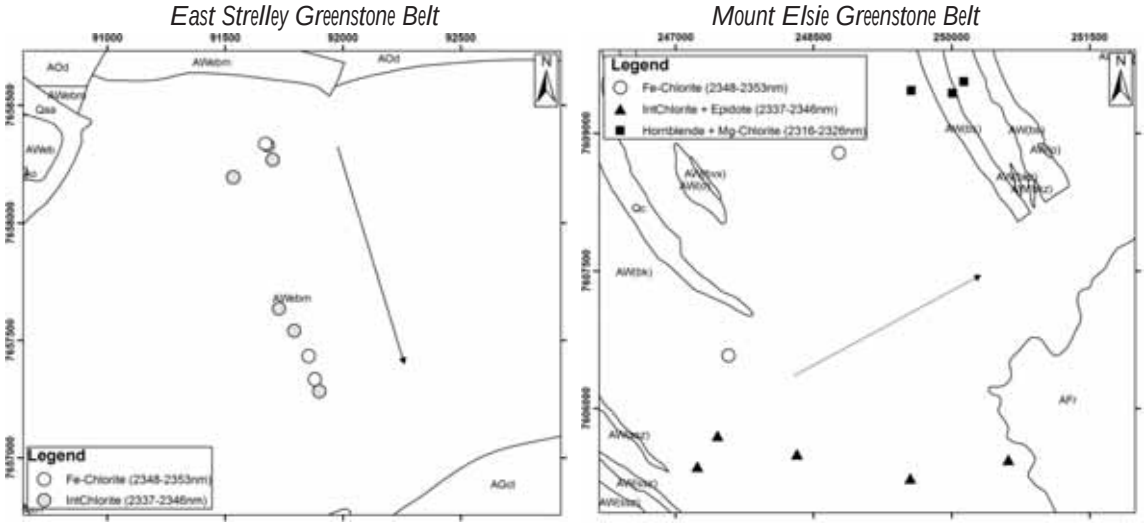

AWebm (meta. high Mg-basalt, commonly pillowed); AW(bk) (meta. komatitic basalt, local pyroxene spinifex texture and zones of carbonate alteration includes some mafic schist); and AW(bs) (mafic schist, slate and strongly foliated metamorphosed komatitic basalt).

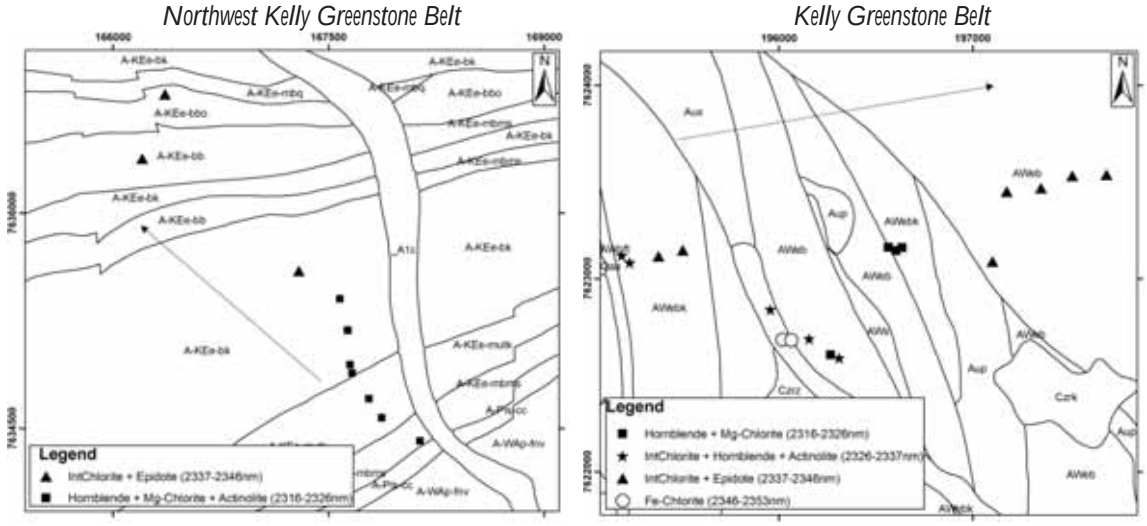

Qaa (alluvial sand and gravel in rivers and creeks, clay, silt and sand in channels and floodplains); A-KEe-bk (meta. komatitic basalt, local pyroxene spinifex texture); A-KEe-mbq (silicified meta-mafic volcanic rocks); A-KEe-bbo/bb (meta. pillowed basalt, with dolerite and komatitic basalt); A-KEe-mutk (talc-carbonate rocks derived from metamorphosed peridotite, includes volcanic protoliths); A-KEe-mbms (mafic schist derived from komatitic basalt); AWebk (meta. komatitic basalt, as lavas and subvolcanic intrusions); and AWeb (meta. tholeiitic and high Mg-basalt and dolerite sills).

- **Charteris Basalt Formation**

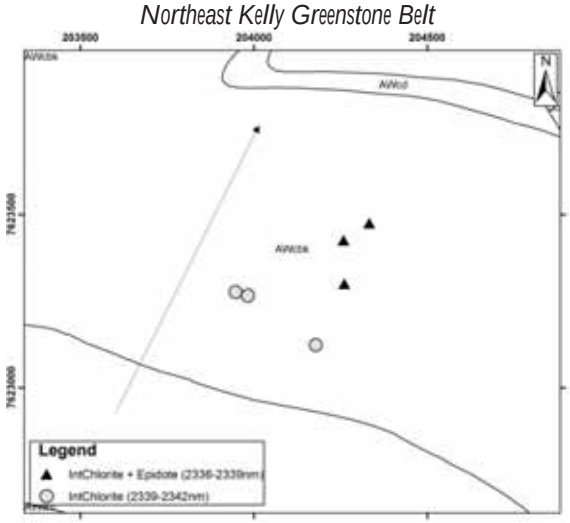

AWcbk (meta. komatitic basalt and minor tholeiitic basalt, numerous pillows).

Appendix 4: Lithological symbols abbreviations.

Lithological Symbols	Description
A-KEe-bbo/bb	Meta. pillowed basalt, with dolerite and komatitic basalt
A-KEe-bk	Meta. komatitic basalt, local pyroxene spinifex texture
A-KEe-mbms	Mafic schist derived from komatitic basalt
A-KEe-mbq	Silicified meta-mafic volcanic rocks
A-KEe-mutk	Talc-carbonate rocks derived from metamorphosed peridotite, includes volcanic protoliths
AOcbi	Meta. andesitic to basaltic pillowed and massive, associated with intrusive sills
AOcf	Meta. felsic volcanic rocks, local felsic agglomerate
AOci	Meta. cherty banded iron-formation, black and white, and rarely red layered
AOd	Meta. massive tholeiitic basalt, locally pillowed and schistose
AOt	Fine to medium-grained metabasalt and amphibolite
Auph	Meta. harzburgite, medium to coarse-grained
AWa	Meta. massive and pillowed basalt, high Mg-basalt, and thin intercalated chert
AW(bk)	Meta. komatitic basalt, local pyroxene spinifex texture and zones of carbonate alteration includes some mafic schist
AW(bs)	Mafic schist, slate and strongly foliated metamorphosed komatitic basalt
AWcbk	Meta. komatitic basalt and minor tholeiitic basalt, numerous pillows
AWdb	Weakly metamorphosed pillowed basalt
AWdfdp	Weakly metamorphosed massive medium-grained feldspar porphyritic andesite to dacite
AWdfx	Weakly metamorphosed coarse to fine-grained dacitic to andesitic, lithic volcaniclastic breccia and conglomerate
AWe	Meta. basalt, pillowed basalt, high Mg-basalt, and intercalated thin thin-bedded chert
AWeb	Meta. tholeiitic and high Mg-basalt and dolerite sills
AWebk	Meta. komatitic basalt, as lavas and subvolcanic intrusions
AWebm	Meta. high Mg-basalt, commonly pillowed
AWeu	Talc-chlorite schist (mylonitic fabric), pods of altered komatitic basalt
AWmb	Meta. basalt, undivided, includes local syn-volcanic dolerite intrusions
AWmbk	Weakly metamorphosed komatitic basalt, commonly pillowed, with pyroxene spinifex texture
AWmbt	Weakly metamorphosed mafic to felsic tuff, medium to fine-grained
AWnb (A-Wan-bb)	Meta. basalt, generally massive, includes syn-volcanic dolerite intrusions, locally schistose
AWp	Meta. felsic volcanic rocks, mainly rhyolitic, quartz-feldspar porphyry and felsic tuff
AWpfa	Weakly metamorphosed felsic agglomerate and minor felsic tuff and andesitic basalt, locally silicified
AWpft	Weakly metamorphosed felsic tuff and minor felsic agglomerate and andesitic basalt, locally silicified
AWpr	Meta. rhyolite and felsic schist
AWpt	Meta. fine-grained felsic tuff and local coarse agglomerate, locally silicified
Qaa	Alluvial sand and gravel in rivers and creeks, clay, silt and sand in channels on floodplains
Qc	Colluvium sand, silt and gracvel

Appendix 5: Lithology and spectral mineralogy of the different rock units.

Coonterunah Supergroup

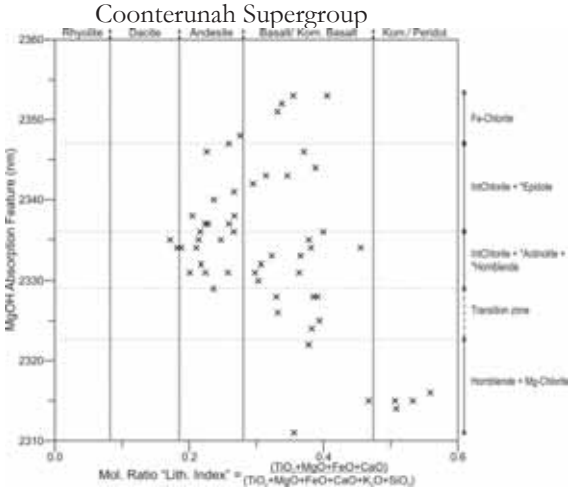

North Star Basalt Formation

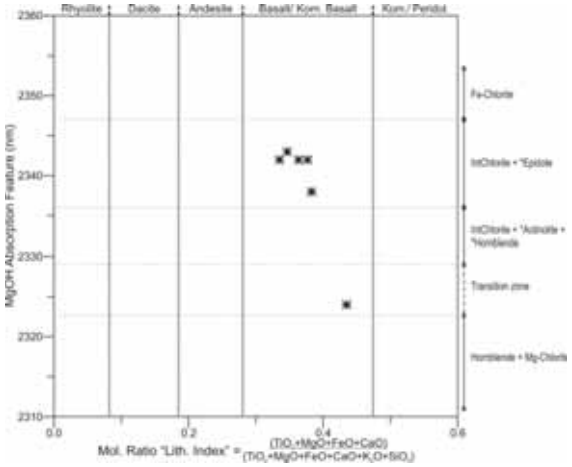

Mt. Ada Basalt Formation

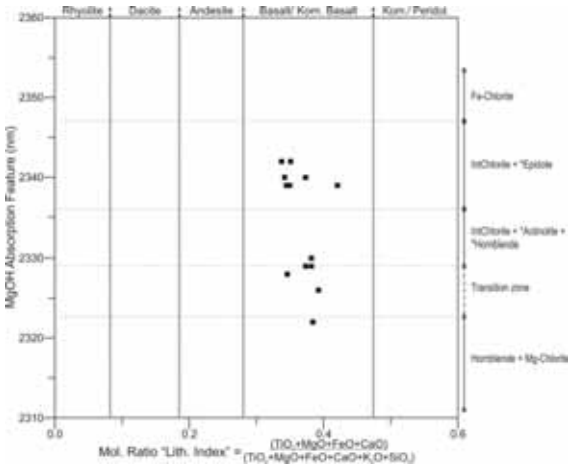

Duffer Formation

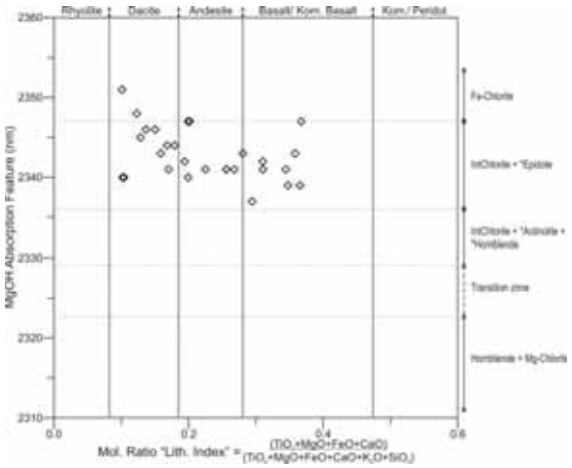

Apex Basalt Formation

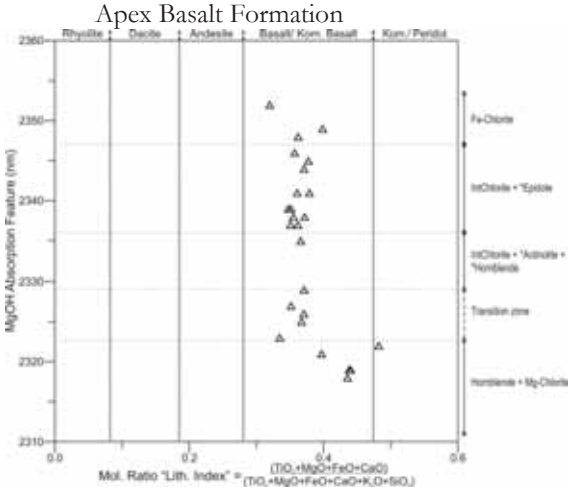

Panorama Formation

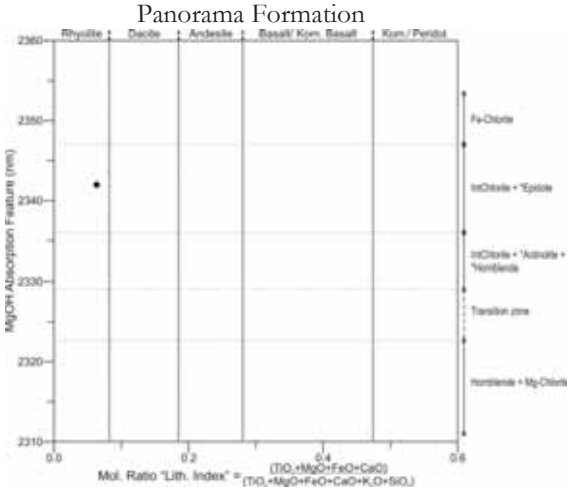

Euro Basalt Formation

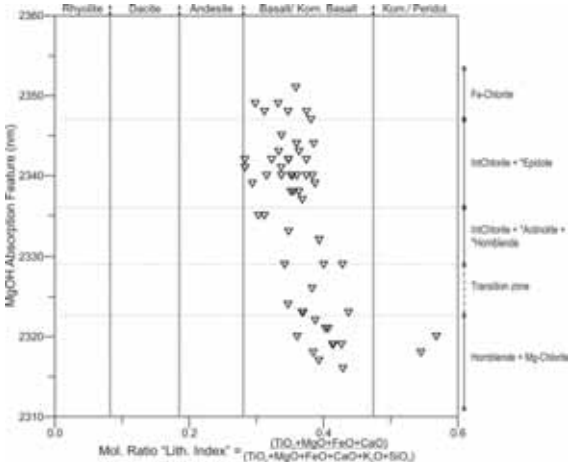

Charteris Basalt Formation

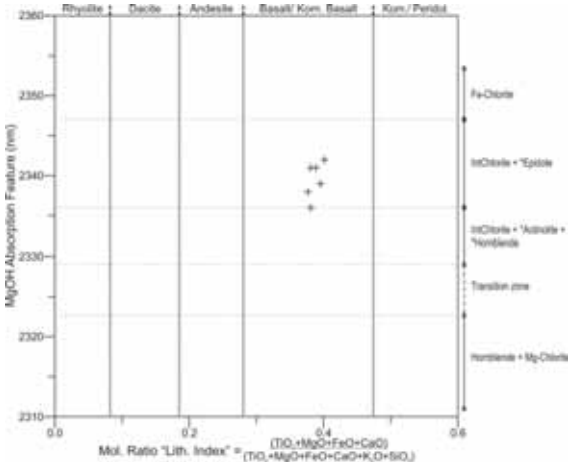

Appendix 6: Histograms and boxplots of the normal and log-transformed major elements (expressed as oxides).

Histograms

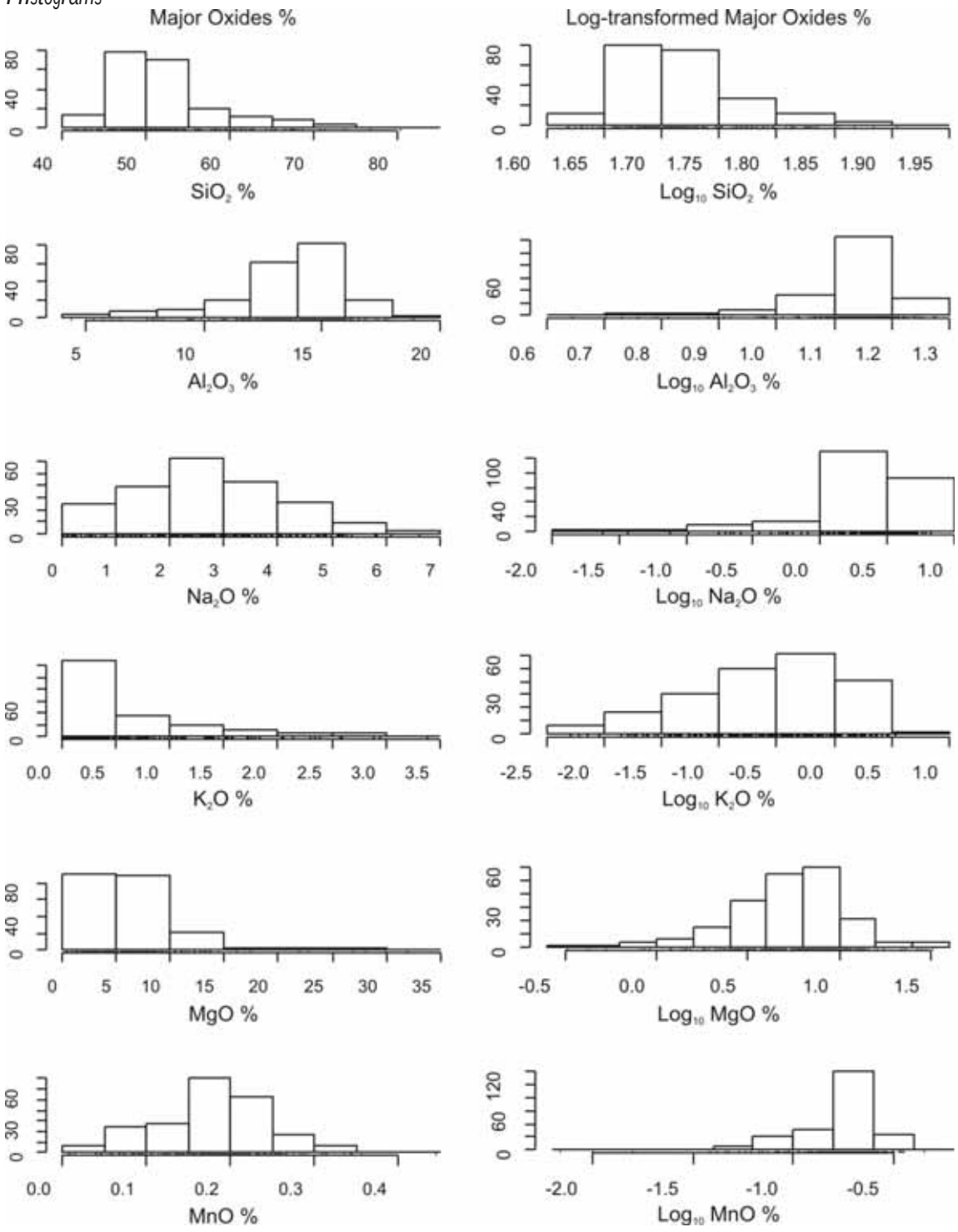

continue

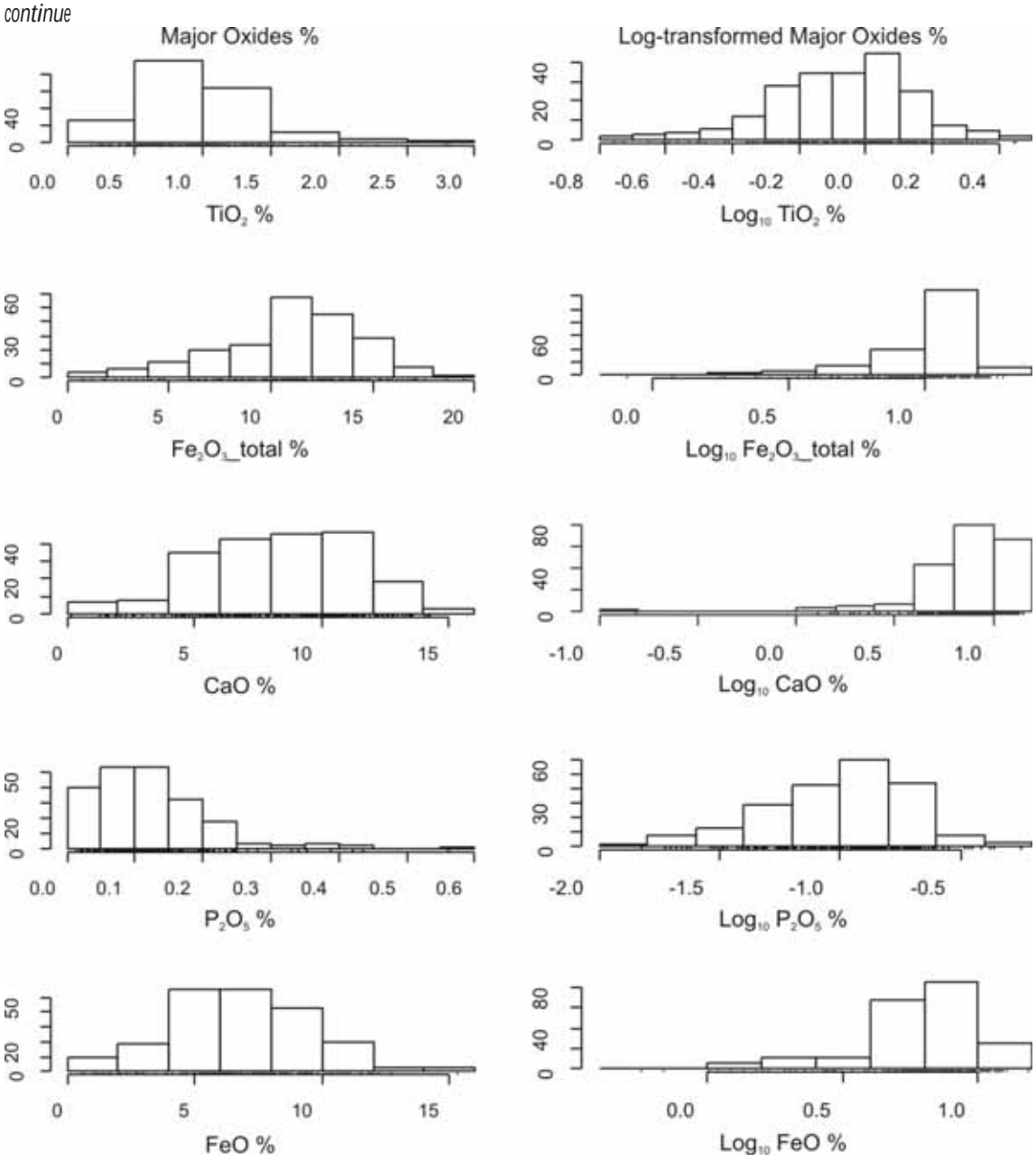
Major Oxides %
Log-transformed Major Oxides %
TiO2 %
Log10 TiO2 %
Fe2O3_total %
Log10 Fe2O3_total %
CaO %
Log10 CaO %
P2O5 %
Log10 P2O5 %
FeO %
Log10 FeO %

Boxplots

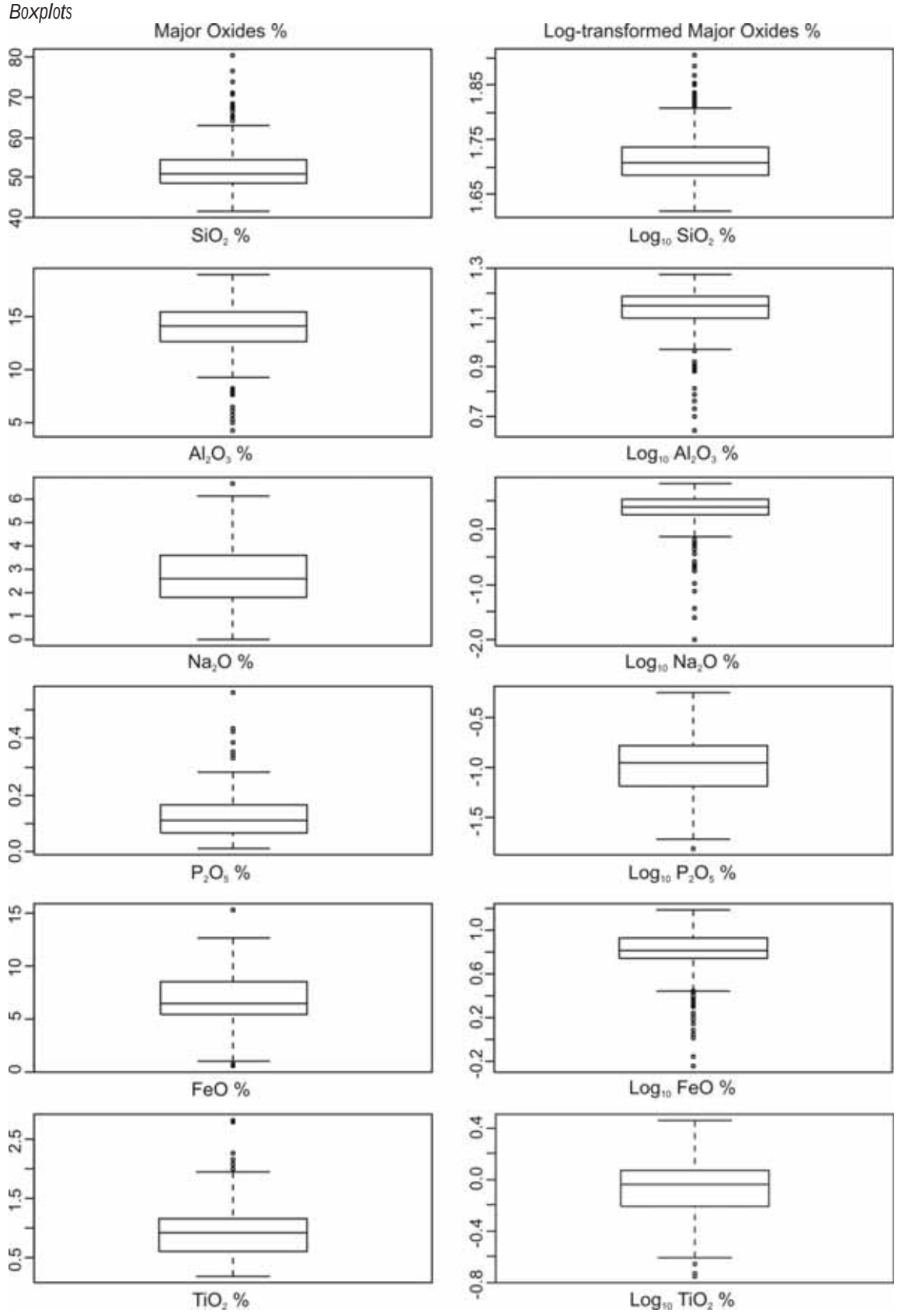
Major Oxides %
Log-transformed Major Oxides %
SiO2 %
Log10 SiO2 %
Al2O3 %
Log10 Al2O3 %
Na2O %
Log10 Na2O %
P2O5 %
Log10 P2O5 %
FeO %
Log10 FeO %
TiO2 %
Log10 TiO2 %

continue

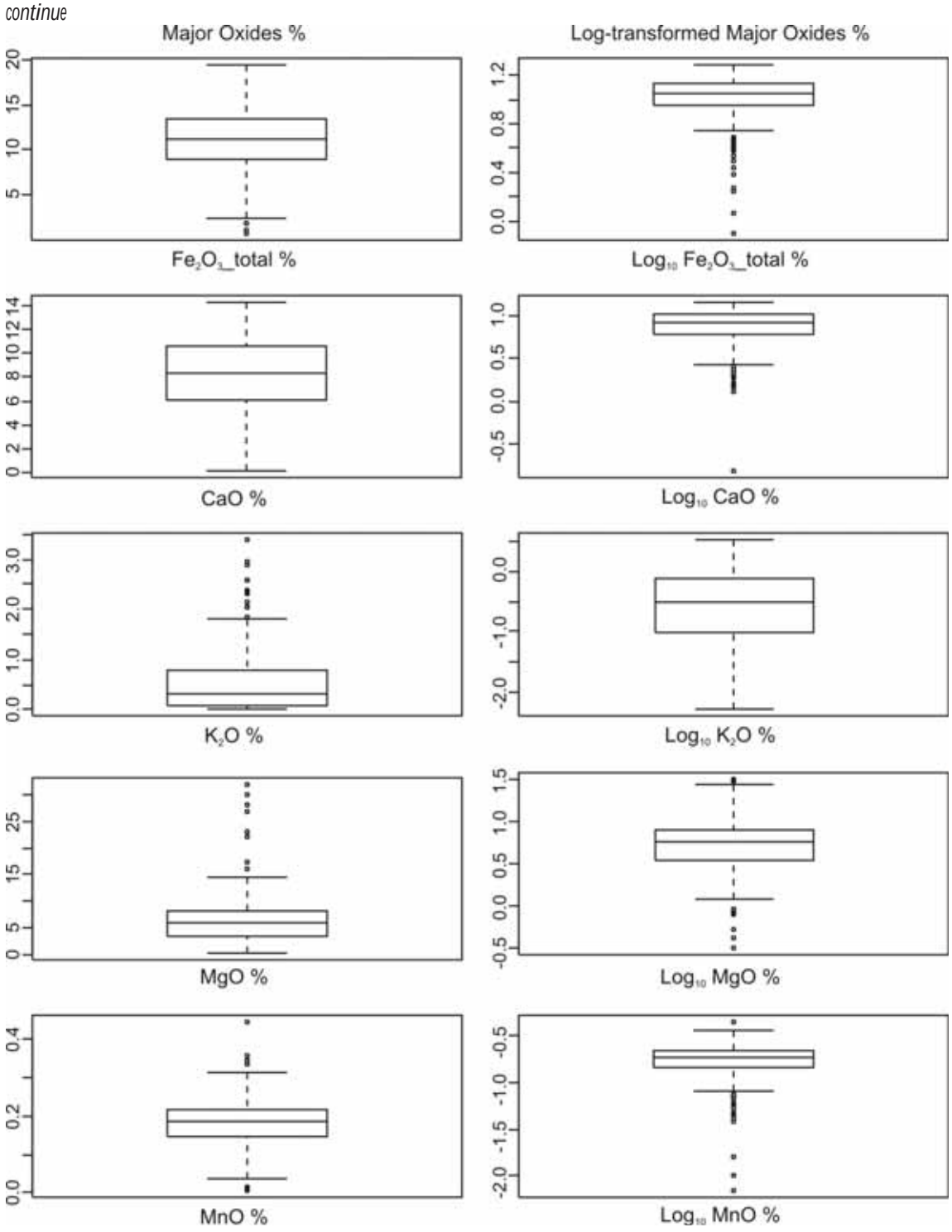
Major Oxides %
Log-transformed Major Oxides %
Fe2O3_total %
Log10 Fe2O3_total %
CaO %
Log10 CaO %
K2O %
Log10 K2O %
MgO %
Log10 MgO %
MnO %
Log10 MnO %

LIST OF REFERENCES

Bagas, L. (2005). Geology of the Nullagine 1:100 000 sheet. *Western Australia Geological Survey*, 1:100 000. Geological Series Explanatory Notes, 33p.

Baldridge, A. M., Hook, S.J., Grove, C.I. & Rivera, G. (2009). The ASTER spectral library version 2.0. *Remote Sensing of Environment*, *v*113, 711-715.

Barley, M. E. (1998). Archean volcanic-hosted massive sulphides. *AGSO Journal of Australian Geology & Geophysics*. *17*(4), 69-73.

Bierwirth, P., Huston, D & Blewett, R. (2002). Hyperspectral Mapping of Mineral Assemblages Associated with Gold Mineralization in the Central Pilbara, Western Australia. *Economic Geology*, *v*97, 819-826.

Bozkaya, O., Yalcin, H., Basibuyuk, Z., & Bozkaya, G. (2007). Metamorphic-hosted pyrophyllite and dickite occurrences from the hydrous Al-silicate deposits of the Malatya-Puturge region, Central Eastern Anatolia, Turkey. *Clays and Clay Minerals*, *55*(4), 423-442.

Brauhart, C. W., Groves, D. I., & Morant, P. (1998). Regional alteration systems associated with volcanogenic massive sulfide mineralization at Panorama, Pilbara, Western Australia. *Economic Geology and the Bulletin of the Society of Economic Geologists*, *93*(3), 292-302.

Brown, A. J., Cudahy, T. J., & Walter, M. R. (2006). Hydrothermal alteration at the Panorama Formation, North Pole Dome, Pilbara Craton, *Western Australia. Precambrian Research*, *151*(3-4), 211-223.

Bucher, K., & Grapes, R. H. (2011). Petrogenesis of metamorphic rocks. New York, *Springer*, 8th edithion, 428p.

Clark, R. N. (1999). Chapter 1: Spectroscopy of rocks and minerals, and principles of spectroscopy, in manual of remote sensing. *Remote Sensing for the Earth Sciences*, *v*3, 3- 58.

Coad, P.R. (1985). Rhyolite geology at Kidd Creek-a progress report. *Cim Bulletin*, *v*78, 70-83.

Condie, K.C. (1981). Archean Greenstone belts. *Developments in Precambrian Geology, v*3, ISBN 0-444-41854-7.

Doublier, M. P., Roache, T., & Potel, S. (2010). Short-wavelength infrared spectroscopy: A new petrological tool in low-grade to very low-grade pelites. *Geology*, *38*(11), 1031-1034.

Duke, E. F. (1994). Near infrared spectra of muscovite, Tschermak substitution, and metamorphic reaction progress: Implications for remote sensing. *Geology*, *22*(7), 621-624.

Ehlmann, B. L., Mustard, J. F., Swayze, G. A., Clark, R. N., Bishop, J. L., Poulet, F., Des Marais, D. J., Roach, L. H., Milliken, R. E., Wray, J. J., Barnouin-Jha, O., & Murchie, S. L. (2009). Identification of hydrated silicate minerals on Mars using MRO-CRISM: Geologic context near Nili Fossae and implications for aqueous alteration. *Journal of Geophysical Research*, *v*114, E00D08, doi:10.1029/2009JE003339.

Fairén, A. G., Chevrier, V., Abramov, O., Marzo, G. A., Gavin, P., Davila, A. F., et al. (2010). Noachian and more recent phyllosilicates in impact craters on Mars. *Proceedings of the National Academy of Sciences*, *107*(27), 12095-12100.

Farrell, T. R. (2006).Geology of the Eastern Creek 1:100 000 sheet. *Western Australia Geological Survey*, 1:100 000. Geological Series Explanatory Notes, 33p.

Filzmoser, F., Hron, K., & Reimann, C. (2010). The bivariate statistical analysis of environmental (compositional) data. *Science of the Total Environment*, *408*(19), 4230-4238.

Franklin, J. M. (1997). Lithogeochemical and Mineralogical Methods for Base Metal and Gold Exploration. *Exploration Geochemistry*, Paper 28, 191–208.

Freek, v. d. M. (2004). Analysis of spectral absorption features in hyperspectral imagery. *International Journal of Applied Earth Observation and Geoinformation*, *5*(1), 55-68.

Frey, M., & Robinson, D. (1999). Low-grade metamorphism. *Blackwell Science*, ISBN 0-632-04756-9, 313p.

Ghataka, A., Basua, A. R., & Wakabayashi, J. (2011). Elemental mobility in subduction metamorphism: insight from metamorphic rocks of the Franciscan Complex and the Feather River ultramafic belt, California. *International Geology Review,* 1–32.

Gifkins, C.C., & Herrmann, W and Large, RR (2005) Altered volcanic rocks: a guide to description and interpretation. *Centre for Ore Deposit Research*, 296p.

Grapes, R. H., & Graham, C. M. (1978). The actinolite-hornblende series in metabasites and the so-called miscibility gap: A review. *Lithos*, *11*(2), 85-92.

Grapes, R. H., & Hoskin, P. W. O. (2004). Epidote Group Minerals in Low–Medium Pressure Metamorphic Terranes. *Reviews in Mineralogy and Geochemistry*, *56*(1), 301-345.

Green, A. A., & Graig, M. D. (1985). Analysis of aircraft spectrometer data with logarithmic residuals. *NASA-JPL Publ., 85-41*, 111–119.

Guidotti, C. V. (1984). Micas in metamorphic rocks. *Reviews in Mineralogy*, *v*13, 357-467.

Hashiguchi, H., & Usui, H. (1975). Delineation of prospecting targets for Kuroko deposits based on modes of volcanism of underlying dacite and alteration haloes. *Mining Geology*, *v*25, 293-301. (in Japanese with English abstract).

Herrmann, W., Blake, M., Doyle, M., Huston, D., Kamprad, J., Merry, N., & Pontual, S. (2001). Short wavelength infrared (SWIR) spectral analysis of hydrothermal alteration zones associated with base metal sulfide deposits at Rosebery and Western Tharsis, Tasmania, and Highway-Reward, *Queensland. Economic Geology*, *v*96, 939-955.

Hickman, A. H. (2004). Two contrasting granite-greenstone terranes in the Pilbara Craton, Australia: evidence for vertical and horizontal tectonic regimes prior to 2900 Ma. *Precambrian Research*, *131*(3-4), 153-172.

Inoue, A., & Utada, M. (1991). Smectite-to-chlorite transformation in thermally metamorphosed volcanoclastic rocks in the Kamikita area, northern Honshu, *Japan. American Mineralogist*, *76*(3-4), 628-640.

Ishikawa Y, Sawaguchi T, Iwaya S, Horiuchi M. (1976). Delineation of prospecting targets for Kuroko deposits based on modes of volcanism of underlying dacite and alteration haloes. *Min Geol.*, *v*26, 105-117.

Large, R. R., Gemmell, J. B., Paulick, H., & Huston, D. L. (2001). The alteration box plot: A simple approach to understanding the relationship between alteration mineralogy and lithogeochemistry associated with volcanic-hosted massive sulfide deposits. *Economic Geology and the Bulletin of the Society of Economic Geologists*, *96*(5), 957-971.

Lister, C.R.B., (1982). "Active" and "passive" hydrothermal systems in the ocean crust. Predicted physical conditions. *The Dynamic Environment of the Ocean Floor*, 441 – 470.

Meunier, A. (2005). Clays. *Springer*, ISBN 3-540-21667-7, 476p.

Morris, P.A., & Pirajno, F. (2005). Mesoproterozoic sill complexes in the Bangemall Supergroup, Western Australia: geology, geochemistry and mineralization potential. *Western Australia Geological Survey Report, 99* , 75p.

Nieto, F., Velilla, N., Peacor, D. R., & Huertas, M. O. (1994). Regional retrograde alteration of sub-greenschist facies chlorite to smectite. *Contributions to Mineralogy and Petrology, 115*(3), 243-252.

Norris, K., & Chappell, B.W. (1977). X-ray fluorescence spectrometry, in Zussman, J. (Ed.), *Physical Methods in Determinative Mineralogy*. Academic Press, 201–272.

Norris, K., & Hutton, J.T. (1969). An accurate X-Ray spectrographic method for the analysis of a wide range of geological samples. *Geochimica et Cosmochimica Acta, 33*, 431-453.

Okada, K., & Iwashita, A. (1992). Hyper-multispectral image analysis based on waveform characteristics of spectral curve. *Advances in Space Research*, *12*(7), 433-442.

Piché, M., & Jébrak, M. (2004). Normative minerals and alteration indices developed for mineral exploration. *Journal of Geochemical Exploration*, *82*(1-3), 59-77.

Pyke, J. (2000). Minerals laboratory staff develops new ICP-MS preparation method. *AGSO Research Newsletter*, December, 12-14.

Rowan, L. C., & Mars, J. C. (2003). Lithologic mapping in the Mountain Pass, California area using AdVanced Spaceborne Thermal Emission and Reflection Radiometer (ASTER) data. *Remote Sensing of Environment*, *84*(3), 350-366.

Sabine, P.A., Harrison, R.K., & Lawson, R.I. (1985). Classification of volcanic rocks of the British isles on the total alkali oxide-silica diagram, and the significance of alteration. *British Geological Survey Report*, *17*(4), 1-9.

Saeki, Y., & Date, J. (1980). Computer applications to the alteration data of the footwall dacite lava at the Ezuri kuroko deposits, Akita Prefecture. *Mining Geology*, *30*(4), 241-250.

Shapiro, L., & Brannock, W. W. (1962). Rapid analysis of silicate, carbonate, and phosphate rocks. *U.S. Geol. Survey Bull. 1144-A*, p.56.

Shikazono, N., & Kawahata, H. (1987). Compositional differences in chlorite from hydrothermally altered rocks and hydrothermal ore deposits. *Canadian Mineralogist*, *v*25, 465-474.

Smithies, R. H., Champion, D. C., Van Kranendonk, M. J., & Hickman, A. H. (2007). Geochemistry of volcanic rocks of the northern Pilbara Craton, Western Australia. *Western Australia Geological Survey*, Report 104, 47pp.

Spitz, G., & Darling, R. (1978). Major and minor element lithogeochemical anomalies surrounding the Louvem copper deposit, Val D'Or, Québec. *Canadian Journal of Earth Sciences*, *15*(7), 1161-1169.

Sykes, M. L., & Moody, J. B. (1978). Pyrophyllite and metamorphism in the Carolina slate belt. *American Mineralogist*, *v*63, 96-108.

Terabayashi, M., Masada, Y., and Ozawa, H. (2003). Archean ocean-floor metamorphism in the North Pole area, Pilbara Craton, Western Australia, *Precambrian Research*, *v*127 (1-3), 167-180.

Theart, H. F. J., Ghavami-Riabi, R., Mouri, H., & Gräser, P. (2011). Applying the box plot to the recognition of footwall alteration zones related to VMS deposits in a high-grade metamorphic terrain, South Africa, a lithogeochemical exploration application. *Chemie der Erde - Geochemistry*, *71*(2), 143-154.

Thuss, B. (2005). Spectroscopic study of Early Archean volcanic rocks in the Pilbara Craton (Western Australia). Bachelor Thesis for Applied Earth Sciences, TU Delft. *Unpuplished report*.

Van der Meer, F. (2004). Analysis of spectral absorption features in hyperspectral imagery. *International Journal of Applied Earth Observation and Geoinformation*, *5*(1), 55-68.

Van der Meer, F. D., & Jong, S. M. d. (2006). Imaging Spectrometry : Basic principles and prospective Applications. *Springer*, *v*4.

Van Kranendonk, M. J. (2000). Geology of the North Shaw 1:100 000 sheet. *Western Australia Geological Survey*, 1:100 000. Geological Series Explanatory Notes, 86p.

Van Kranendonk, M. J. (2010). Geology of the Coongan 1:100 000 sheet. *Geological Survey of Western Australia*. 1:100 000 Geological Series Explanatory Notes, 67p.

Van Kranendonk, M. J., Hickman, A. H., Smithies, R. H., Nelson, D. R., & Pike, G. (2002). Geology and tectonic evolution of the Archaean North Pilbara terrain, Pilbara Craton, *Western Australia. Economic Geology*, *v* 97, p. 695–732.

Van Kranendonk, M. J., & Pirajno, F. (2004). Geological setting and geochemistry of metabasalts and alteration zones associated with hydrothermal chert ± barite deposits in the ca. 3.45 Ga Warrawoona Group, Pilbara Craton, Australia. *Geochemistry, Exploration, Environment, Analysis*, *v*4, 253–278.

Van Kranendonk, M. J., Hickman, A. H., Smithies, R. H., Williams, I. R., Bagas, L., & Farrell T. R. (2006). Revised lithostratigraphy of Archean supracrustal and intrusive rocks in the northern Pilbara Craton, Western Australia: *Western Australia Geological Survey*, *v*15, 57p.

Van Kranendonk, M. J., Hugh Smithies, R., Hickman, A. H. and Champion, D. (2007). Review: secular tectonic evolution of Archean continental crust: interplay between horizontal and vertical processes in the formation of the Pilbara Craton, Australia. *Terra Nova*, *v*19, 1–38.

Van Ruitenbeek, F. J. A., Cudahy, T., Hale, M., & Van der Meer, F. D. (2005). Tracing fluid pathways in fossil hydrothermal systems with near-infrared spectroscopy. *Geology*, *33*(7), 597-600.

Van Ruitenbeek, F. J. A., Debba P., Van der Meer, F. D., Cudahy, T., Van der Meijde, M., & Hale, M. (2006). Mapping white micas and their absorption wavelengths using hyperspectral band ratios. *Remote Sensing of Environment*, *102*(3-4), 211–222.

Velde, B., & Meunier, A. (2008). The origin of clay minerals in soils and weathered Rocks. *Springer*, ISBN: 978-3-540-75633-0, 426p.

Williams, I. R.. (1999). Geology of the Muccan 1:l00,000 sheet. *Western Australia Geological Survey*, 1:100,000 Geological Series Explanatory Notes, 39p.

Williams, I. R., & Bagas, L. (2007). Geology of the Mount Edgar 1:100 000 sheet. *Geological Survey of Western Australia*. 1:100 000 Geological Series Explanatory Notes, 62p.

Winchester, J. A., & Floyd, P. A. (1977). Geochemical discrimination of different magma series and their differentiation products using immobile elements. *Chemical Geology*, *v*20, 325-343.

Yuasa, M., Watanabe, T., Kuwajima,T., Hirama,T., & Fujioka, K. (1992). Prehnite-pumpellyite facies metamorphism in oceanic arc basement from site 791 in the Sumisu Rift, Western Pacific. Proceedings of the Ocean Drilling Program, *Scientific Earth Drilling Information Service-SEDIS*, *v*126, 185-193.

Zane, A., & Sassi, R. (1998). New data on metamorphic chlorites as a petrogenetic indicator mineral, with special regard to greenschist-facies rocks. *The Canadian Mineralogist*, *v*36, 713-726.